

Functional Selectivity at the Dopamine D2 Receptor

by

Sean Michael Peterson

Department of Cell Biology
Duke University

Date: _____

Approved:

Marc G. Caron, Supervisor

Scott H. Soderling, Chair

Vadim Y. Arshavsky

Terrence Peter Kenakin

Sudha Shenoy

Dissertation submitted in partial fulfillment of
the requirements for the degree of Doctor
of Philosophy, Master of Science in the Department of
Cell Biology in the Graduate School
of Duke University

2015

ABSTRACT

Functional Selectivity at the Dopamine D2 Receptor

by

Sean M Peterson

Department of Cell Biology
Duke University

Date: _____

Approved:

Marc G. Caron, Supervisor

Scott H. Soderling, Chair

Vadim Y. Arshavsky

Terrence Peter Kenakin

Sudha Shenoy

An abstract of a dissertation submitted in partial
fulfillment of the requirements for the degree
of Doctor of Philosophy in the Department of
Cell Biology in the Graduate School of
Duke University

2015

Copyright by
Sean Michael Peterson
2015

Abstract

The neuromodulator dopamine signals through the dopamine D₂ receptor (D₂R) to modulate central nervous system functions through diverse signal transduction pathways. D₂R is a prominent target for drug treatments in disorders where dopamine function is aberrant, such as schizophrenia. D₂R signals through distinct G protein and β -arrestin pathways and drugs that are functionally selective for these pathways could have improved therapeutic potential. How D₂R signals through the two pathways is still not well defined, and efforts to elucidate these pathways have been hampered by the lack of adequate tools for assessing the contribution of each pathway independently. To address this, *Evolutionary Trace* was used to produce D₂R mutants with strongly biased interactions for either G protein or β -arrestin. Additionally, various permutations of these mutants were used to identify critical determinants of D₂R functional selectivity. D₂R interactions with the two major downstream signal transducers were effectively dissociated and G protein signaling accounts for D₂R canonical MAP kinase signaling cascade activation. Nevertheless, when expressed in mice, the β -arrestin biased D₂R caused a significant potentiation of amphetamine-induced locomotion, while the G protein biased D₂R had minimal effects. The mutant receptors generated here provide a new molecular tool set that enable a better definition of the individual roles of G protein and β -arrestin signaling in D₂R pharmacology, neurobiology and associated pathologies.

Contents

Abstract	iv
List of Tables	viii
List of Figures	ix
Acknowledgements	xiv
1. Introduction	1
1.1 The conformational theory of functional selectivity.....	2
1.2 A molecular and mechanistic basis for functional selectivity at D ₂ R.....	5
1.2.1 The physical properties of dopamine	5
1.2.2 Lipid membrane domains and interactions with other receptors modulate D ₂ R function	6
1.2.3 D ₂ R interacting proteins	10
1.2.4 Non-canonical D ₂ R interacting proteins.....	18
1.2.5 D ₂ R possesses a common allosteric modulator binding site, the extracellular vestibule.....	20
1.2.6 Unexpected sites of allosteric modulation.....	22
1.3 D ₂ R functional selectivity is a function of cellular organization.....	24
1.3.1 Dopamine and D ₂ R genetic mouse models reveal functional selectivity <i>in vivo</i>	27
1.3.2 Functional selectivity in D ₂ R circuitry	29
1.4 The therapeutic implications of D ₂ R functional selectivity	31
2. Functional separation of D ₂ R using Evolutionary Trace	33
2.1 Evolutionary Trace guided mutagenesis of D ₂ R.....	33

2.2 Evolutionary Action at D ₂ R yields a robust landscape of functional selectivity ...	35
3. Ligand, receptor and transducer contributions to D ₂ R functional selectivity	42
3.1 ^[G_{protl}] D ₂ R and ^[β_{arr}] D ₂ R display distinct but expected properties.....	42
3.2 Operationally defined, receptor dictated functional selectivity	45
3.3 Agonist texture reveals novel modes of functional selectivity	49
3.4 The status of receptor interacting partners in extremely biased mutant D ₂ Rs	53
4. The physiological relevance of D ₂ R functional selectivity	56
4.1 MAP kinase signaling in ^[G_{protl}] D ₂ R and ^[β_{arr}] D ₂ R	56
4.2 ^[G_{protl}] D ₂ R and ^[β_{arr}] D ₂ R are biologically active and display functional differences ..	58
5. Application of functional selectivity principles to diverse receptor systems.....	62
5.1 Evolutionary Action at related but diverse GPCRs.....	62
5.2 A roadmap to universal functional separation	64
5.3 D ₂ R neuronal subtype expression dictates functional selectivity.....	68
6. Discussion	71
6.1 Future Directions.....	77
6.2 Outlook and Impact	82
7. Materials and Methods.....	84
7.1 Evolutionary Trace	84
7.2 Molecular Pharmacology	85
7.2.1 Mutagenesis PCR.....	85
7.2.2 Cell culture and transfections.....	86
7.2.3 G protein activity.....	86

7.2.4 Bioluminescent Resonance Energy Transfer	86
7.2.5 Radioligand binding	86
7.2.6 Confocal microscopy.....	87
7.2.7 Receptor internalization assay.....	87
7.2.8 MAP kinase transcriptional activity reporter.....	87
7.2.9 ERK phosphorylation by western blot	87
7.2.10 Alternative G protein signaling.....	88
7.3 Neuropsychopharmacology	88
7.3.1 Adeno-associated viral expression vectors.....	88
7.3.2 Adeno-associated virus production.....	88
7.3.3 Mouse lines.....	89
7.3.4 Mouse stereotaxic injection for viral delivery	89
7.3.5 Locomotor activity	89
7.3.6 Motor coordination	89
7.3.7 HA-staining of virally transduced brains	90
7.4 Data Analysis	90
References	95
Biography.....	115

List of Tables

Table I: Evolutionary Action guided mutagenesis. Each residue predicted from ET is color coded the same in Figure 3 and Figure 4 in the first column. The second column shows the predicted residues in increasing ET harshness (amino acid conservation and side chain chemistry) from left to right. Each single point mutation was generated and tested for G protein and β -arrestin activity. Note that A135 was found to be a critical residue for G protein activation, but not β -arrestin activation and all 19 mutations were made in order to titrate the most β -arrestin biased mutant.....	36
Table II: Evolutionary Action predicted functional selectivity phenotype mutations in diverse GPCRs. Receptors presented in Figure 14 are predicted for mutations at the $^{[G_{\text{prot}}]}$ D ₂ R (L3.42 and Y3.51) and $^{[\beta_{\text{arr}}]}$ D ₂ R (A3.53 and M3.58) residues. Predicted harshness on phenotype is displayed from left to right.	64
Table III: Calculated values from Figure 6 and 12.....	91
Table IV: Receptor manipulations yield operationally defined functional selectivity. Values derived from Figures 7 and 8 to demonstrate the receptor's contributions to functional selectivity. * $p < 0.05$ when compared to $^{[WT]}$ D ₂ R for efficacy and potency as determined by Bonferroni post-hoc test after $p < 0.05$ for one-way ANOVA. B_{INF} and $\Delta\Delta\log(\tau/\text{KA})$ were calculated according to references in the table.....	92
Table V: Ligand contributions to functional selectivity. Calculated from Figures 9 and 10. * $p < 0.05$ when compared to $^{[WT]}$ D ₂ R for efficacy and potency at each ligand as determined by Bonferroni post-hoc test after $p < 0.05$ by one-way ANOVA.....	92
Table VI: Transducer contributions to functional selectivity. Calculated from Figure 11. * $p < 0.05$ when compared to $^{[WT]}$ D ₂ R or control receptors ($\beta_{2A}R$ for $G_{\alpha s}$ or $AT_{1A}R$ for $G_{\alpha q}$) for efficacy and potency as determined by Bonferroni post-hoc test after $p < 0.05$ for one-way ANOVA.....	94

List of Figures

Figure 1: The functional selectivity of D₂R. (A) Interaction with dopamine stimulates G proteins (G_α in green, G_β in cyan and G_γ in magenta), recruitment of GPCR kinases (GRKs) which phosphorylate the receptor (red spheres) and β-arrestins (yellow) at D₂R. Subunit variations that are known to interact with D₂R are labelled (seven G_α, three G_β, and ten G_γ subunits, five major serine/threonine kinases, and two β-arrestins). (B) Aripiprazole is a potent antagonist at the β-arrestin recruitment assay as determined by Bioluminescent Resonance Energy Transfer (BRET) but a weak partial agonist when the same assay is performed with high levels of GRK2 (C). 4

Figure 2: D₂R functional selectivity is dependent upon context. (A) D₂R interactions and downstream effectors leading to signaling events. (B) D₂R physical states are dynamic and determine extent of functional selectivity. (C) Central nervous system architecture of D₂R expression and connectivity. Dopaminergic projections (blue arrows) to cortex and striatum modulate excitatory (green arrows) and inhibitory (red arrows) neural circuits. D₂R is prominently expressed in dopaminergic, striatal and cortical cells. VTA: ventral tegmental area; SN: substantia nigra; GPi/SNr: internal globus pallidus/substantia nigra reticulate; STN: subthalamic nucleus; GPe: external globus pallidus. 25

Figure 3: Evolutionary Trace of D₂R facilitated by advances in crystallography and algorithm design. (A) TYY mapped onto D₃R (159) (PDB ID: 3PBL in red). (B) Four rounds of ET predicted residues for mutagenesis mapped onto D₃R. (C) piET (green residues depicted as spheres). (D) G_α-CT proximity (160) (PDB ID: 3DQB residues in yellow, G_α-CT is represented as a green α-helix cartoon), and (E) G_{αβγ} (161) (PDB ID: 3SN6 α is green and β is blue) interaction with IC2 of D₃R (grey spheres). 34

Figure 4: G protein and β-arrestin activity of ET predicted mutants. Dose response curves for each mutant were normalized to a WT control that was performed the same day and the log(τ/K_A) was calculated. Since all values were 38

Figure 5: Generation of functionally selective D₂R mutants. (A) Snake-like plot of D₂R with each round of mutagenesis color-coded according to Table I and Figure 3. Red spheres: residues derived from TYY, green spheres: predicted from piET algorithm, yellow spheres: predicted from proximity to rhodopsin/transducin α subunit C-terminal fragment co-crystal; grey spheres: identified residues from β₂AR/G_{αβγ} co-crystal in intracellular loop two. Ballesteros-Weinstein numbering identified for each transmembrane domain. The same color scheme was used to highlight the residues on the structure of D₃R (159) because D₃R is the most closely related GPCR to D₂R with an

available crystal structure (81% sequence identity for transmembrane domains). (B), D₃R structure represented as a blue ribbon, and ET-identified residues are spheres. (C) The biased mutants all occur within 20 amino acids of the DRY motif on transmembrane domain three (TM3). (D) D₃R aligned to β2AR in complex with G_{αβγ}, green cylinder PDB ID: 3SN6) (161) as well as rhodopsin in complex with the finger-loop domain of visual arrestin (167) (purple cylinder PDB ID: 4PXF). D₃R to β2AR alignment yielded an RMSD = 1.8 and D₃R alignment to rhodopsin RMSD = 2.7 using pymol MatchAlign command.

..... 40

Figure 6: Biased D₂R mutants derived from Evolutionary Trace. (A) Inhibition of cAMP as determined by GloSensor compared to [W^{TI}]D₂R positive control and [D^{80A}]D₂R negative control. (B) β-arrestin 2 recruitment determined by BRET for the same receptors as in (A). All points are SEM of n=3-7 done in duplicate. Confocal images of (C) [W^{TI}]D₂R, (D) [G^{prot}]D₂R, (E) [β^{arr}]D₂R, and (F) [D^{80A}]D₂R expressed in live cells. (G) B_{MAX} (with SEM) determined from n=3 radioligand binding experiments. (H) K_D from B_{MAX} determination experiments. (I) DA competition binding experiments to determine K_I. (J) D₂R internalization assessed by live cell HA antibody staining of D₂R (SEM, n=5 done in triplicate).

43

Figure 7: Functional selectivity is operationally defined. (A) β-arrestin 2 recruitment comparing [W^{TI}]D₂R and [Y^{IV}]D₂R as determined by bioluminescent resonance energy transfer (BRET). (B) GRK2 overexpression enhances β-arrestin 2 recruitment by BRET for [Y^{IV}]D₂R and [W^{TI}]D₂R, but only slightly for [G^{prot}]D₂R, [β^{arr}]D₂R, and [D^{80A}]D₂R when compared to Figure 6B. All data are presented with SEM from n=3-4 independent experiments, with statistical significance calculated in Table IV. Quantification of bias between G protein activity and β-arrestin 2 recruitment using (C) a statistical formalism (171) or (D) bias plot mapping under normal (solid lines) and GRK2 overexpression enhanced (broken lines) conditions.....

46

Figure 8: Receptor control of partial agonism at D₂R. (A) G protein activity as determined by inhibition of isoproterenol-induced cAMP accumulation of basic and acidic residue substitutions at A135 (A3.53) and (B) β-arrestin 2 recruitment. (C) G protein activity of bulky polar substitution (tyrosine) is roughly 75% (τ/1.5) of [W^{TI}]D₂R (dotted line) and (D) β-arrestin 2 recruitment is similarly reduced. When combined with one residue from [G^{prot}]D₂R (L125N) or [β^{arr}]D₂R (M140D) these mutants display partial biased agonism for their respective retained pathways. (E) G protein and (F) β-arrestin 2 recruitment of an even more reduced (50%; τ/2) partial agonism induced by substitution of A135 for a bulky nonpolar residue (phenylalanine). Similarly combined with L125N

or M140D to generate weak partial biased agonism in response to full agonists. All data presented with SEM from n=3-5 independent experiments. 48

Figure 9: A unique G protein biased mutant demonstrates agonist texture. (A) Dopamine (DA) and quinpirole equivalently inhibit cAMP production, which is equivalent to ^[WT]D₂R for ^[Gprot4PM]D₂R (T69F Y133L Y209N A372S). (B) ^[Gprot4PM]D₂R has roughly 50% efficacy in response to DA but not quinpirole for β -arrestin 2 recruitment. (C) GRK2 overexpression rescues both DA and quinpirole β -arrestin 2 recruitment activity nearly to ^[WT]D₂R levels (dotted line, from Figure 7B). (D) GRK2 recruitment as determined by BRET (where GRK2 is tagged with YFP) shows the same ligand discrepancy as β -arrestin 2. All data are presented with SEM from n=3 independent experiments, with statistical significance calculated in Table V. 50

Figure 10: Agonists and antagonists with diverse pharmacophores elicit predictable responses at ^[Gprot]D₂R and ^[β arr]D₂R. The D₂R agonists quinpirole, apomorphine, and NPA were tested for G protein activity (A,C,E, respectively) and β -arrestin 2 recruitment (B,D,F, respectively). For each agonist, ^[Gprot]D₂R showed a response similar to ^[WT]D₂R at G protein activation and more similar to ^[D80A]D₂R for β -arrestin recruitment, while ^[β arr]D₂R was not active at the G protein pathway but retained activity at the β -arrestin pathway. The antagonists raclopride (G,H) haloperidol (I,J) and partial antagonist aripiprazole (K,L) were able to block DA elicited D₂R activation at the G protein pathway (G,I,K, respectively) for ^[Gprot]D₂R and ^[WT]D₂R to the same extent, while ^[D80A]D₂R and ^[β arr]D₂R had no effect to inhibit. In contrast, these antagonists block DA elicited β -arrestin 2 recruitment (H,J,L, respectively) for ^[β arr]D₂R and ^[WT]D₂R. All data are presented with SEM from n=3-4 independent experiments, with statistical significance calculated in Table V. 53

Figure 11: Interacting partners and allosteric D₂R determinants of functional selectivity. (A) GRK2 and (B) β -arrestin 1 recruitment as assessed by BRET show a similar profile as β -arrestin 2: ^[β arr]D₂R recruits normally, while ^[Gprot]D₂R is severely deficient. (C) Each D₂R construct was expressed in HEK 293T cells and assessed for its ability to stimulate cAMP in response to DA. Stimulation of endogenous receptor by isoproterenol was used as a control response. (D) G _{α q} mediated Ca²⁺ flux, as measured by the aequorin luminescence assay, is not stimulated by ^[WT]D₂R, ^[Gprot]D₂R, ^[β arr]D₂R or ^[D80A]D₂R, compared to AngII induced Ca²⁺ flux induced by transient expression of AT_{1A}R. (E) B_{MAX} was determined by binding, while luciferase-tagged receptors provided a B_{MAX}-independent measure of receptor number. In this assay, the responsiveness to salt is retained for all mutants (except ^[D80A]D₂R). All data are presented with SEM from n=3-4 independent experiments, with statistical significance calculated in Table VI. 54

Figure 12: Assessment of MAP Kinase activity at D₂R. (A) SRF and (B) SRE MAP kinase transcriptional promoter mediated expression of luciferase (SEM, n=5-6 done in triplicate). (C) Traditional western blot analysis of ERK (*p<0.05 Newman-Keuls posthoc when compared to ^[D80A]D₂R or untransfected after one-way ANOVA p<0.05, SEM, n=3-6) with and without β-arrestin 2 overexpression. (D) Representative blot for the data presented in (C). 57

Figure 13: The physiological relevance of D₂R functional selectivity. (A) Viral transgene packaged into AAV, which allowed for Cre-dependent expression of D₂R through a double-floxed inverted open reading frame (DIO). (B) 0.75 μL of virus was injected bilaterally into the dorsal and ventral striatum with each injection site indicated by the red dots, and a total of 3 μL was injected into the striatum of each mouse. CPu: caudate putamen; AcbC: nucleus accumbens, core; AcbSh: nucleus accumbens, shell. (C) Representative staining pattern of the N-terminal HA tagged D₂R shows transduction of a majority of the dorsal striatum and at least 50% of the ventral striatum with variable transduction in the olfactory tubercle. Radioligand binding revealed a two- to four-fold overexpression of each receptor as determined from membranes prepared from striatal dissections from Adora2a-Cre (D) and Adora2a-Cre::β-arrestin 2^{FLOX/FLOX} (E) mice (*p<0.05 Newman-Keuls posthoc when compared to Cre (-) controls after one-way ANOVA p<0.05, SEM, n=4-6). (F) Potentiation of amphetamine-induced locomotion in mice when D₂R is overexpressed (*p<0.05 bonferroni posthoc when compared to ^[D80A]D₂R after repeated measures two-way ANOVA p<0.05 for receptor expression type SEM, n=11-12, color coded for receptor type). (G) The amphetamine response potentiation of ^[WT]D₂R and ^[βarr]D₂R is abolished when β-arrestin 2 is genetically deleted from D₂R-expressing medium spiny neurons (*p<0.05 bonferroni posthoc when compared to ^[D80A]D₂R after repeated measures two-way ANOVA p<0.05 for receptor expression type SEM, n=8-13). 61

Figure 14: Evolutionary Trace at pharmacologically and genetically diverse GPCRs for the generation of functionally selective mutants. hAGTR1 (human angiotensin receptor), hAPLNR (human apelin receptor), hM3 (human muscarinic type 3 receptor), hADRB2 (human β-adrenergic receptor, type 2A), hDRD1 (human dopamine D1 receptor), hHTR1A (human serotonin type 1A receptor), and mDRD2 (mouse D₂R) GPCRs were chosen based on genetic diversity (Tree calculated from % identity), as well as G protein (Gαq, Gαi or Gαs) and β-arrestin coupling (Class A: transient β-arrestin interaction, Class B: robust β-arrestin interaction) profiles. The alignment of the twenty residues surrounding the DRY motif was the basis of the tree presented, and ^[Cprot]D₂R is color coded as green residues while ^[βarr]D₂R is red. 63

Figure 15: Achieving functional selectivity in GPCRs with diverse pharmacological and genetic profiles. (A) Cytosolic influx of Ca^{2+} as determined by the aequorin assay shows AT1AR M3.53G mutation completely abolishes G protein activity, while (B) β -arrestin 2 recruitment as determined by BRET remains intact. For the apelin receptor (APLNR), $G_{\alpha i}$ activation as determined by inhibition of isoproterenol induced cAMP increase (C) is intact for Y3.51S but slightly decreased for A3.53S. In contrast, β -arrestin 2 recruitment (D) is intact for A3.53S but not Y3.51S. Finally, for D_1R , Y3.51S showed partial agonist activity at $G_{\alpha s}$ mediated cAMP accumulation as measured by GloSensor (E) and A3.53S showed full activity. While at β -arrestin 2 recruitment (B), Y3.51S had no activity while A3.53S showed partial activity, which means that both mutations display bias for the G protein pathway..... 65

Figure 16: Dissection of diverse D_2R -expressing neuronal subpopulations. $D_2R^{FLOX/FLOX}::Adora2A-Cre$ induces genetic deletion of D_2R and reexpression (using the same injection scheme in Figure 13) of each mutant D_2R . Assessment of (A) basal locomotor activity at the beginning of the night cycle (lights off) and (B) motor coordination with the beam walking assay. (C) $D_2R^{FLOX/FLOX}::ChAT-Cre$ has D_2R deleted only from cholinergic interneurons which causes a major deficiency in the amphetamine locomotor response but not the basal/habituation locomotor phase..... 68

Figure 17: Potential inducible mouse knock-in construct design. This design relies upon expression of the DOX inducible tTA transcription factor and Flp recombinase from the introns of the endogenous $DRD2$ gene (polyadenylation and promoters abridged for simplicity). (A) tTA and the $^{[WT]}D_2R$ exon are expressed in normal cells (restricted by the endogenous $DRD2$ expression pattern). (B) Mouse crossed to Cre expressing lines orients Flp recombinase Cerulean expression cassette that is not active until (B) addition of DOX drives Flp::P2A::GFP (cerulean or citrine), and Flp recombines $^{[WT]}D_2R$ exon to $^{[\beta arr]}D_2R$ exon (with cerulean or citrine serving as reporters of recombination). 82

Acknowledgements

I would like to thank my advisor, Dr. Marc Caron, for guidance and inspiration throughout this project. This work was made possible by my collaborators. Drs. Olivier Licharge and Angela Dawn Wilkins at Baylor who developed the Evolutionary Trace approach. Dr. Caroline Bass at SUNY-Buffalo who generated adeno-associated viruses. My coworkers in the laboratory: Tom Pack who generated pERK and $^{[17/2]}D_2R$ data, Kathryn Walder who worked on applying the mutations to other GPCRs, Dr. Daniel Urban who trained me in stereotactic injections and animal behavior, Dr. PJ Nicholls who designed the inducible knock-in construct, and Dr. Nikhil Urs who provided valuable experimental design insight throughout the project.

1. Introduction

The dopamine D₂ receptor (D₂R) is an inhibitory G protein-coupled receptor (GPCR) that is a common target of all antipsychotics. D₂R responds to the binding of a single ligand, dopamine (DA), to transduce pleiotropic signaling patterns. Synthetic D₂R ligands have been shown to elicit or blunt a subset of these responses, a property referred to as *functional selectivity*. The literature describing these phenomena is reviewed and a mechanistic understanding of D₂R functional selectivity is proposed based on the receptor's physical environment in the plasma membrane as well as its interactions with canonical signaling molecules (heterotrimeric G proteins) and non-canonical signaling molecules (β -arrestins and other proteins). This mechanistic understanding of functional selectivity will then be used to explore the role of functional selectivity of D₂R in the central nervous system at the cellular and circuitry levels. The therapeutic potential of D₂R functional selectivity requires a mechanistic understanding of D₂R in physiologically relevant systems in order to be leveraged for the development of improved drugs targeting D₂R. This review of the current state of the literature places context for the work presented in Chapters 2-5 and provides a clear rationale for elucidating D₂R functional selectivity.

1.1 The conformational theory of functional selectivity

Functional selectivity is a term that describes the phenomenon of ligands eliciting multiple downstream signaling events through one GPCR (1). Functional selectivity was originally observed when the administration of a drug to a system resulted in pleiotropic responses (2-4) and D₂R functional selectivity was observed when studying the effects of the atypical antipsychotic aripiprazole (5, 6). The concept has evolved and the molecular details have been elucidated for many prototypical GPCRs, culminating in the structural determination of the serotonin type 2B receptor in complex with different functionally selective ligands (7). The dopamine system is one of the earliest examples of functional selectivity observed and the therapeutic implications are manifold.

Functional selectivity has been theorized to arise from the ability of a protein to adopt multiple heterogeneous conformations. The functional significance of conformational heterogeneity is that each conformation allows for distinct interactions with ligands, G proteins, kinases, and β -arrestins (Figure 1A). The conformational theory was proposed in 1995 and described ligands that would interact preferentially with a specific conformation as a *protean agonist* (8) because the character of the ligand (agonist or antagonist) would change depending on how the receptor was observed. For example, a cell that expresses a high concentration of GPCR kinases (GRKs) will make

an antagonist (such as aripiprazole, Figure 1B) seem to act as an agonist (Figure 1C) in a β -arrestin recruitment assay. The term *biased agonism* describes a similar phenomenon: an agonist that is able to preferentially signal through a specific pathway (9) such as β -arrestin rather than G proteins.

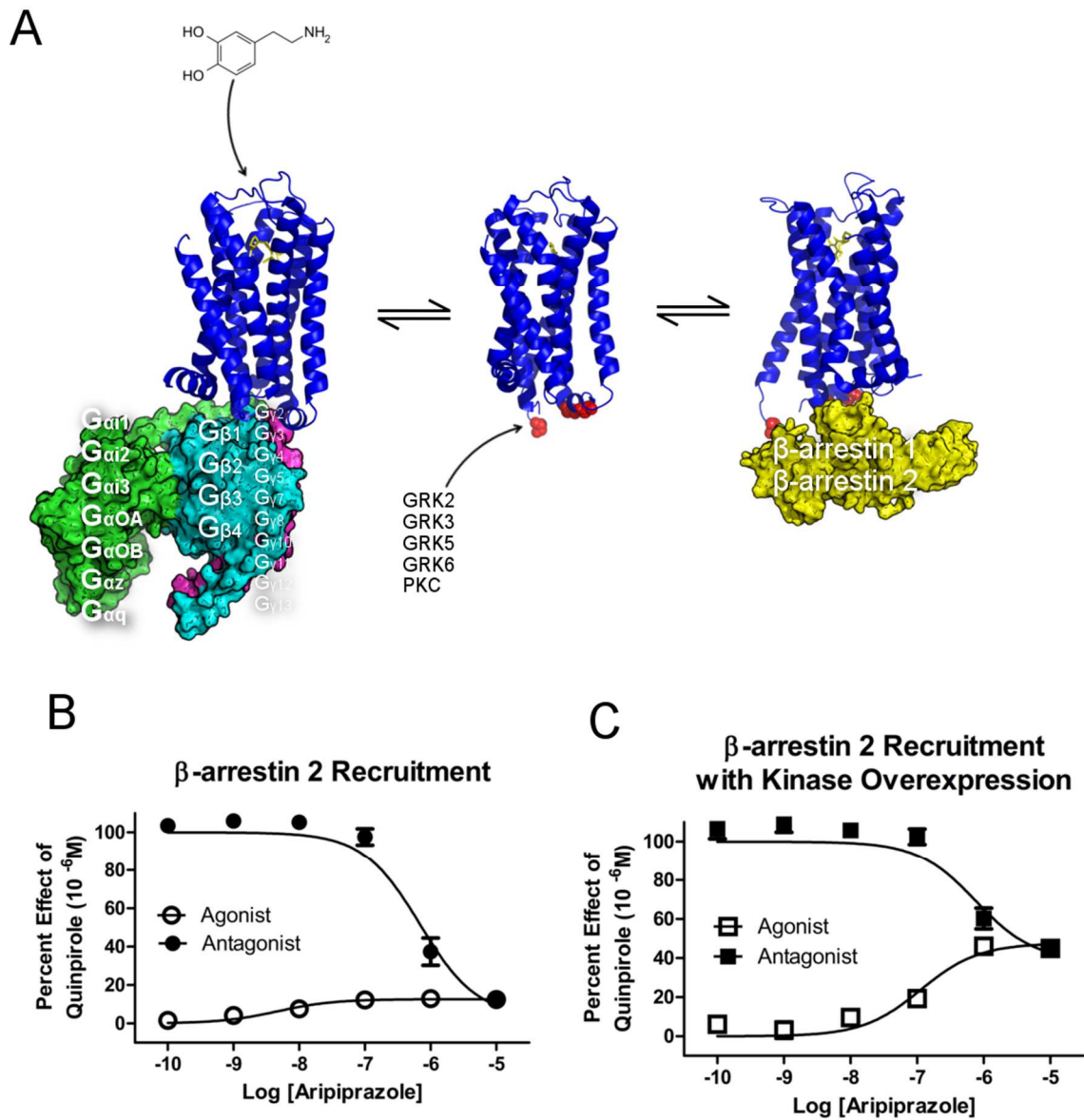


Figure 1: The functional selectivity of D₂R. (A) Interaction with dopamine stimulates G proteins (G_α in green, G_β in cyan and G_γ in magenta), recruitment of GPCR kinases (GRKs) which phosphorylate the receptor (red spheres) and β-arrestins (yellow) at D₂R. Subunit variations that are known to interact with D₂R are labelled (seven G_α, three G_β, and ten G_γ subunits, five major serine/threonine kinases, and two β-arrestins). (B) Aripiprazole is a potent antagonist at the β-arrestin recruitment assay as determined by

Bioluminescent Resonance Energy Transfer (BRET) but a weak partial agonist when the same assay is performed with high levels of GRK2 (C).

While the distinctions between functional selectivity, protean agonism, and biased agonism are not always clear, the term functional selectivity is a broad definition that encompasses phenomenon observed in crystallography all the way to intact neural circuits. D₂R functional selectivity can arise from predicted mechanisms (such as GRK expression and ligand structure) as well as novel mechanisms (such as receptor dimerization and ligand allostery). Furthermore, the therapeutic implications of D₂R functional selectivity are apparent in preclinical models of D₂R related diseases such as schizophrenia, Parkinson's disease, bipolar disorder, attention deficit-hyperactivity disorder, and addiction.

1.2 A molecular and mechanistic basis for functional selectivity at D₂R

A bare-bones model of D₂R signal transduction is presented in Figure 1A. The functional selectivity of D₂R is based on the interaction between D₂R, ligand, and interacting proteins. Described below is a thorough (though not exhaustive) examination of each of these elements as they relate to D₂R.

1.2.1 The physical properties of dopamine

Dopamine (DA) is the endogenous ligand for D₂R and is considered the *reference agonist* (meaning that the bias of agonists at D₂R are relative to the ability of DA to elicit

that response). DA is synthesized from the amino acid tyrosine and is only one step in the biosynthesis of many small molecule ligands for other GPCRs. Tyrosine is hydroxylated by tyrosine hydroxylase to L-DOPA, which is decarboxylated by aromatic L-amino acid decarboxylase to form DA. DA is further metabolized into norepinephrine and epinephrine, as well as trace amines (all of which are the endogenous ligands for other GPCRs) (10, 11). DA is toxic to cells, as it is a catechol and can be oxidized to release free radicals (12). However, D₂R appears to modulate L-DOPA (and DA) free radical cytotoxicity (13) in a pleiotropic manner. DA itself may also have an effect on the plasma membrane and lipid environment of D₂R by binding directly to membranes (14).

1.2.2 Lipid membrane domains and interactions with other receptors modulate D₂R function

D₂R is embedded into the plasma membrane, thus functional selectivity and conformational heterogeneity is dependent on the lipid environment. D₂R has been shown to exist in both detergent soluble and insoluble fractions of the plasma membrane and the insoluble fraction was shown to interact with G proteins and β -arrestin (15). Additionally, the N-terminus of D₂R has been shown to regulate compartmentalization through lipid microdomains into intracellular vesicles (16). D₂R has been shown to preferentially internalize in nonsynaptic membranes of dendrites *in vivo* (17). Recently, GPCRs have been shown to signal from intracellular vesicles (18) which is another means by which D₂R can achieve functional selectivity. The lipid environment

fundamentally affects D₂R conformational heterogeneity, however, the other GPCRs present in these membrane domains also affect D₂R signaling.

There is considerable evidence for GPCR dimerization as a substrate for D₂R functional selectivity (19). D₂R can interact with many other GPCRs, which results in diverse functional consequences. There are five DA receptors that belong to two pharmacologically and genetically homologous families: the D₁-like family (D₁R and D₅R) and the D₂-like family (D₂R, D₃R, and D₄R). All D₂-like family receptors have a large third intracellular (IC₃) loop and no C-terminus (the protein ends with the lipidated cysteine of helix 8). There is evidence that D₂R can heterodimerize with all of the members of the DA receptor family. Functional selectivity can be a direct consequence of GPCR dimerization. The unique aspect of dimerization mediated functional selectivity is that it is dependent upon which specific GPCRs are interacting with D₂R. However, it should be noted that the functional and physiological relevance of the concept of GPCR dimerization is still highly debated (20, 21), with D₂R at the center of the physiological relevance debate (22).

D₂R homodimers have been shown using cross-linking and mutagenesis (23). The functional consequences of D₂R homodimerization was shown using a novel, albeit artificial, system of D₂R fused to a G_α subunit (24). This system showed that D₂R homodimers are more efficient than monomers at transducing their signal. This

principle may have therapeutic significance, as D₂R homodimers were shown to be increased in post-mortem tissue from schizophrenia patients (25). Functional selectivity could be achieved by ligands that specifically manipulate the balance of D₂R dimers and monomers. For instance, SB269652 was recently described as functioning as a D₂R allosteric modulator for the D₂R homodimer, but a competitive antagonist for the monomer (26). Functional selectivity was shown for the agonist NPA at D₁R/D₂R heterodimers when compared to D₂R homodimers (27) when G_{αi} activation was used as the readout.

D₂R has been shown to heterodimerize with many receptors, including the dopamine D₁ receptor (D₁R). D₁R, unlike D₂R, is intronless in its coding sequence, coupled to G_{αs}, and possess a traditional GPCR C-terminal tail. *In vitro* and *in vivo* it was shown that D₁R and D₂R heterodimerize but instead of signaling through inhibitory or stimulatory G proteins, the heterodimer signals through G_{αq} and activates calcium release when both D₁R and D₂R are activated (28). D₂R is thus functionally selective in this regard, depending on the dimerization state with D₁R. It has been suggested that GRK2 regulates aspects of this signaling paradigm (29) and that the G protein signal is mediated through G_{βγ} subunits (30). This adds another layer of functional selectivity to D₂R: functional selectivity through D₂R monomers (i.e. G protein versus β-arrestin) and D₂R functional selectivity through D₁R heterodimers (i.e. G_α versus G_{βγ}).

While D₁R was shown to heterodimerize with D₂R to generate a new G protein coupling, for the closely related D₅R it was shown that D₅R signals through G_{αq} as a monomer and that this signal is inhibited by heterodimerization with D₂R (31). However, this inhibition is disinhibited when D₂R is activated. D₂R also has been shown to heterodimerize with its closely related D₂-like family members, D₃R and D₄R. The significance of the D₂R/D₃R heterodimer is that each receptor is able to transactivate G proteins, which was shown by G protein-receptor fusions (32). The D₂R/D₄R dimerization state seems to be sensitive to the alternative splicing that the IC3 of D₂R undergoes and the variable number of tandem repeats of the IC3 of D₄R (33). This D₂R/D₄R heterodimer was shown to signal through MAP kinases and modulate glutamate release *in vivo*.

D₂R has also been shown to dimerize with many diverse GPCRs. The adenosine 2A receptor (A_{2A}R) is coexpressed with D₂R in the striatal medium spiny neurons (MSNs) and has been shown to be in a complex with D₂R and calmodulin (34). *In vitro* the functional consequence of the D₂R/A_{2A}R heterodimer is that D₂R acts as a negative allosteric modulator of A_{2A}R ligand binding (35). *In vivo*, the D₂R/A_{2A}R dimer works in an antagonistic fashion when the depolarized membrane potential is measured by patch-clamp recordings (36). A small molecule was discovered that modulates the D₂R/A_{2A}R dimer by inducing cointernalization of the receptors (37). Thus, a functionally

selective ligand has been developed that targets the dimerization state of D₂R. Finally, D₂R has also been shown to dimerize with neurotensin receptors (38) as well as the ghrelin receptor (39). Both of these receptors have high therapeutic potential as small molecule targets, and D₂R dimerization with them adds a more specific potential to develop effective therapeutic small molecules.

1.2.3 D₂R interacting proteins

Just as D₂R functional selectivity is dependent on the lipid environment and other receptors present, it is also dependent on the presence and abundance of signaling molecules. Figure 1A depicts the *possible* interacting partners (including different complements of G protein subunits, kinases and β -arrestins). D₂R's interaction partners are perhaps the most important determinant of functional selectivity, as Figure 1B and 1C demonstrate, the level of kinase determines the efficacy of aripiprazole and its classification as an antagonist or partial agonist.

D₂R is a cell surface, ligand activated guanine nucleotide exchange factor (GEF) for heterotrimeric G proteins. Heterotrimeric G proteins are comprised of a G α subunit and G $\beta\gamma$ subunits (referred to as G $\beta\gamma$ because the G β and G γ subunits are always bound to each other) (40). The G α subunit contains a GTPase domain (that shares homology to small GTPases and is referred to as a ras-like domain) as well as an alpha-helical domain. The GTPase domain hydrolyzes GTP into GDP to go from an active to inactive

conformation (41), and D₂R catalyzes the exchange of GDP for GTP. D₂R binds to the pertussis toxin sensitive family of inhibitory G_α subunits referred to as the G_{αi/o} family (G_{αi1}, G_{αi2}, G_{αi3}, and G_{αo}) as well as the pertussis toxin insensitive inhibitory G protein G_{αz}. The specificity of G protein/D₂R interactions is regulated by the G_α C-terminal tail, as well as the complement of G_{βγ} subunits. D₂R could possibly be queried with 280 different G_{αβγ} combinations and D₂R binds to the GDP-bound state of the heterotrimer under basal conditions (42). D₂R functional selectivity is largely dependent upon the complement and specificity of G proteins present and the significance of functional selectivity is largely dependent on the functional diversity of the different G proteins.

The three related inhibitory G proteins (G_{αi1}, G_{αi2}, and G_{αi3}) are all able to inhibit cAMP production by binding to adenylyl cyclase (AC). The N-terminus is alternatively spliced into two isoforms for G_{αi1}, and six for G_{αi2}, while G_{αi3} is not alternatively spliced which may dictate specificity between AC subtypes and other effectors. There is also a short C-terminal splice variant of G_{αi2} (sG_{αi2}) that regulates intracellular D₂R functions (43). cAMP is a diverse second messenger and inhibition of cAMP production by D₂R activation has long been regarded as D₂R's canonical signaling paradigm. However, cAMP functions as a pleiotropic second messenger in its own right, thus D₂R can exhibit functional selectivity even within its canonical signaling paradigm. For instance, cAMP is known to activate protein kinase A (PKA) and DARPP-32 in D₂R expressing medium

spiny neurons (MSNs) and this has been shown to regulate a diverse set of functional outputs such as epigenetic changes (44). Furthermore, the role of cAMP was tested directly in D₂R expressing MSNs using pharmacogenetics. The G_{αs} coupled DREADD was expressed in the D₂R MSNs and activated to cause an increase in cAMP and this activated DARPP-32 and blunted amphetamine sensitization (45). D₂R and its regulation of cAMP encompass a vast body of literature and the history of some of the groundbreaking work by John Kebabian and Paul Greengard is reflected upon by one of the luminaries of DA research, Solomon Snyder in (46). D₂R can modulate cAMP in functionally selective ways, and cAMP can signal in a functionally diverse manner. However, functional selectivity at D₂R also encompasses the ability of D₂R to engage novel interacting signaling partners and generate unexpected responses that can be leveraged for clinically effective pharmaceuticals.

The “other” inhibitory G protein, G_{αo}, is alternatively spliced in its C-terminus to generate two distinct C-termini (47). These alternative splice variants are referred to as G_{αoA} and G_{αoB} and most likely affect specificity between G_α and GPCRs (48) as well as G_{βγ}. G_{αo} is largely regarded to have unknown effector binding in its GTP-activated state. Despite this mysterious function, G_{αo} is the most highly expressed G_α subunit, comprising up to 2% of all membrane proteins in the brain (49). Furthermore, it has been asserted that G_{αo} is responsible for most of the signal transduction downstream of D₂R

(50). These results are hard to reconcile with the substantial body of work regarding the actions of cAMP, PKA and DARPP-32 in D₂R expressing MSNs. Nevertheless it is hard to deny the evidence presented: GTP γ S binding in G α_o versus G α_{i1} /G α_{i2} or G α_{i1} /G α_{i3} knockout mice, as well as earlier work that showed G α_o knockout mice showed neurological abnormalities in many DA related phenotypes (51) and a recent study that showed G α_o mutations cause epileptic encephalopathy (52). It is clear that D₂R is able to engage both G α_i and G α_o subunits and this yields diverse functional outcomes, however targeting D₂R activation of one subunit (i.e. creating a biased agonist for G α_o) has not been successfully done, partly because of the difficulty in assessing G α_o activation and separating it from G α_i signaling as the proteins are closely related.

G α_o 's primary function may be as a molecular clock (via its intrinsic GTPase activity) for G $\beta\gamma$ signaling, a functional relationship that has been well characterized in yeast (53). G $\beta\gamma$ is an important transducer for D₂R signaling in the brain that has been shown to couple to diverse signaling pathways. The most well characterized effector for G $\beta\gamma$ is G protein-gated inward rectifier K⁺ (GIRK) channels because this provides a direct link from D₂R activation to plasma membrane excitability. Interestingly, a crystal structure of GIRK/G $\beta\gamma$ was recently solved that showed that there are minimal conformational changes that occur in G $\beta\gamma$ when bound to GDP bound G α versus GIRK (54). This illustrates a unique principle of D₂R/G $\beta\gamma$ functional selectivity: unlike the

receptor, which exists in a conformationally heterogeneous population, $G_{\beta\gamma}$ needs to simply be liberated from G_{α} to be activated. $G_{\beta\gamma}$ binds to G_{α} GTPase-activating proteins (GAPs) and regulators of G protein signaling (RGSs) to inhibit GTPase activity thus extending their active time as well as the G_{α} effector PLC (the normal effector for $G_{\alpha q}$) (55). Although the details of $G_{\beta\gamma}$ have long been elucidated, new signaling paradigms, such as $G_{\alpha i}$ binding two $G_{\beta\gamma}$ subunits (56) and inhibition of DA transporters (57) continue to emerge. Functionally selective ligands at D₂R could selectively activate a particular $G_{\alpha\beta\gamma}$ heterotrimer, the consequence of which could be long-term depression (LTD) through GIRK, but not cAMP inhibition through $G_{\alpha i}$. Such structure-activity ligand relationships would require significant technical achievement in screening platforms and even more advances in the molecular details of D₂R activation of G proteins before they could be feasible.

Like $G_{\beta\gamma}$'s ability to slow down the GTPase activity of G_{α} , $G_{\beta\gamma}$ participates in another crucial point in D₂R signal transduction, it binds to GPCR kinase (GRK) 2 and 3, which recruits the kinases to the activated receptor (58). Conversely, GRK 5 and 6 are lipidated which localizes them to the plasma membrane independent of G protein activation (59). D₂R can interact with all four of these proteins and is coexpressed with them (albeit at different ratios, depending on the cell). GRKs phosphorylate the intracellular loops of D₂R which mediates the desensitization and internalization of D₂R

(60). The significance of multiple GRKs is that different patterns of phosphorylation (most likely on D₂R's long third intracellular loop) would yield different functional outcomes, such as intracellular trafficking to different compartments or recruitment of different intracellular signaling molecules. This is the *barcode hypothesis*, which means different phosphorylation barcodes would be scanned by intracellular proteins (61). This is a theory that has been validated in D₂R: GRK 2/3 phosphorylation sites were mutated which resulted in no deficiency in β -arrestin recruitment or desensitization but rather a deficiency in receptor recycling (62). Additionally, D₂R is also phosphorylated by PKC (63) the consequences of which yield distinct signaling paradigms from GRK2: $G_{\beta\gamma}$ activated GIRK channels are more rapidly desensitized. GRK2 may play a role in D₂R signaling in its own right, as it (along with GRK3) possesses an RGS domain and has been shown to regulate D₂R independently of its kinase activity (64).

Another significant consequence of D₂R phosphorylation is increased affinity for β -arrestins. β -arrestins are multifunctional adaptor proteins that bind to clathrin-coated pits to mediate GPCR internalization (65). Furthermore, β -arrestins have been shown to cause changes in up to 1,500 phosphorylation sites *in vitro*, and these interactions are mediated by the active state of the receptor (66). β -arrestins are the major transducer of G protein-independent signaling from GPCRs. β -arrestins are phosphosensors encoded by two different genes, named β -arrestin 1 and 2. The β -

arrestin 2 global knock out mouse was used to discover the existence of a D₂R/ β -arrestin 2/PP2A/Akt signaling complex that results in the inhibition of Akt, which relieves Akt-mediated inhibition of GSK3 β signaling (67). This pathway was validated with GSK3 β heterozygous mice and mice with GSK3 β knocked out specifically in D₂R expressing MSNs (68). This D₂R mediated inhibition of Akt has also been shown to be crucial in the developing zebrafish brain (69) and implicated in DA related feeding behavior (70). D₂R/ β -arrestin has also been implicated in MAP kinase (ERK) signaling *in vitro* (71), and has been shown to significantly be increased *in vivo* when mice are given amphetamine and methylphenidate (72). Finally, an intronic single nucleotide polymorphism (SNP) in D₂R, as well as a synonymous SNP in Akt1 were shown to be associated with schizophrenia phenotypes as well as olanzapine treatment efficacy in patients (73). Antipsychotics, which have long been known to bind to D₂R (74) also all function as β -arrestin 2 antagonists (75). Taken together, these data suggest a clear impetus for functionally selective biased ligands between β -arrestin and G protein signaling pathways.

Antipsychotics, because of their therapeutic relevance, have undergone extensive molecular characterization. The first principle of antipsychotic efficacy is D₂R binding (74), and typical antipsychotics are potent D₂R antagonists. However, atypical antipsychotics have yielded a more complex pharmacology: two of the best studied

atypical antipsychotics are aripiprazole and clozapine. Clozapine binds D₂R weakly, while aripiprazole is a partial agonist. The selectivity of its partial agonism is debatable, as it could be considered a biased partial agonist or a balanced partial agonist, depending on the kinase expression, see Figure 1B and 1C. The study of antipsychotics is where the concept of functional selectivity at D₂R originated, and as more advanced techniques have developed, more data has been made available to elucidate the robust and complex activation of D₂R. For instance, the phosphorylation pattern downstream of D₂R was originally shown to involve Thr 308 of Akt and not Ser 473 (67). However, a recent study showed that haloperidol increased Ser 473 phosphorylation in cultured MSNs (76) and a study in HEK cells showed that D₂R activation caused an increase in both Akt phosphorylation sites (77). In another *in vivo* study, the phosphorylation status of Akt is shown to be decreased 90 minutes after methamphetamine injection, however, in another panel of the same study, Akt is shown to be increased with methamphetamine injection (78). In addition, different brain regions have been shown to have increased Akt phosphorylation in response to amphetamine and methyphenidate. The cortex is increased, while the striatum is decreased in this study (79). The picture gets even more out of focus when targets of Akt are considered. GSK3 β heterozygous (80) and D₂R-cell type specific knock-out mice (68) show a decreased response to amphetamine (just as β -arrestin 2 knock-out mice do) and a well characterized GSK3 β

target, β -catenin was shown to be stabilized in β -arrestin 2 knock-out mice (80) and activated by haloperidol and clozapine (81). However, genetic stabilization of β -catenin did not phenocopy GSK3 β heterozygous knock-outs (GSK3 β causes the destabilization of β -catenin) (68). These discrepancies illustrate the incredible complexity of pleiotropic signaling at one single GPCR but also demonstrate the utility of understanding functional selectivity in more detail.

1.2.4 Non-canonical D₂R interacting proteins

Akt/GSK3 β is an integrator of cellular signaling and while functional selectivity at D₂R (e.g. G $\beta\gamma$ activation of PI3K and Akt versus β -arrestin 2 inactivation of Akt via PP2A recruitment) contributes to the contradictory findings, it is also because of non-canonical D₂R interacting proteins. For example, D₂R has been shown to interact directly with β -catenin (82) and a small GTPase expressed in the striatum called Rhes was shown to interact with β -arrestins, PP2A, and be crucial for Akt dephosphorylation in Rhes knockout animals (83).

D₂R has been shown to interact with many other non-canonical signaling proteins, which increases the possibilities for functional selectivity exponentially (a ligand could activate β -arrestin/Rhes/PP2A signaling but block β -arrestin/clathrin internalization). D₂R directly interacts with and increases the expression of the transient receptor potential channel canonical (TRPC) 1 (84). TRPC channels are expressed in the

brain and are known to modulate intracellular calcium concentration. The D₂R/ β -arrestin interaction may also play a role in this function, as β -arrestins have been shown to ubiquitinate (85) and desensitize (86) transient receptor potential channel vanilloid (TRPV). This is yet another possibility for D₂R functional selectivity, as D₂R could both increase TRP function by directly binding and decrease its function through β -arrestin. Another physiologically important channel, the NMDA receptor, was shown to interact directly with D₂R through the NR2B subunit *in vivo* and D₂R modulated NMDA receptor activity, which controls neuronal firing directly (87).

Many D₂R interactions have been identified by standard biochemical methods. A yeast two-hybrid screen of the long third intracellular (IC3) loop of D₂R yielded a specific interaction with Par-4, a leucine zipper (88). Par-4 was shown to compete for a previously characterized calmodulin binding site in the IC3, and the authors detected behavioral abnormalities in a mouse with a mutated Par-4. Interestingly, the authors verified the D₂R/Par-4 interaction and believed that the mobility of D₂R on a gel from a Par-4 immunoprecipitation “may suggest a functionally selective interaction of Par-4 with a subspecies of D₂DR [*sic*] *in vivo*” presumably because of glycosylation, phosphorylation, and dimerization among other posttranslational modifications such as ubiquitination (all factors that contribute to gel mobility shift subspecies of GPCRs).

Similarly, a yeast two-hybrid screen of D₂R's IC3 also revealed a functional interaction with ZIP, a PKC ζ interacting protein (89) that inhibited G_{oi} signaling in HEK cells.

Many D₂R interactions have also been identified *in vivo*. For instance, the D₂R knockout mice revealed interactions with striatal-enriched protein tyrosine phosphatase (STEP) (90) and Nurr1, a nuclear receptor (91). Both of these interactions appear to be involved in MAP kinase/ERK signaling in D₂R mediated neuronal development. Cbl-interacting protein of 85 kDa (CIN85) mutant mice (92) showed subcellular localization with D₂R. Colocalization using immunolabeling of D₂R and neuronal calcium sensor-1 (NCS-1) (93) showed a direct interaction. The data presented in this section is by no means a comprehensive list of all of the D₂R interacting proteins. However, it illustrates another facet of functional selectivity that can be leveraged for therapeutic ligand development. At this stage such development would be premature, while the work presented here has extensive characterization of the D₂R interactions, it pales in comparison to the decades of research on G protein and β -arrestin interactions with D₂R.

1.2.5 D₂R possesses a common allosteric modulator binding site, the extracellular vestibule

Facile manipulation of functional selectivity could be achieved through allosteric modulation. Allosteric modulation of GPCR signaling has been the focus of many studies because of the therapeutic potential of such a ligand. Recently, cocaine was shown to function as a positive allosteric modulator *in vivo* at D₂R using behavioral,

microdialysis, and GTP γ S binding experiments (94). It is not unreasonable to assume that an allosteric modulator could preferentially potentiate or inhibit a particular D₂R signaling pathway, for example, DA binding could be modulated by an allosteric ligand to favor G protein activation over β -arrestin signaling or G_{ai} over G_{ao}. This very assumption has been proven for the activation of the M1 DREADD, because an allosteric modulator behaved as a negative allosteric modulator for Ca²⁺ mobilization, while having a neutral effect on MAP kinase signaling (95). A negative allosteric modulator at D₂R was shown to inhibit both G protein and β -arrestin 2 recruitment (96) while this does not show functional selectivity at D₂R, it demonstrates that D₂R has the capacity to be allosterically modulated in a biased fashion.

The recently crystallized muscarinic 2 receptor (M₂R) proved the existence of the binding of allosteric modulators to the extracellular vestibule, a binding site 1.5 nm proximal to the orthosteric binding site (97). Furthermore, molecular dynamics studies have computationally modeled the mechanism of positive and negative allosteric modulation at M₂R (98). To illustrate the significance of this extracellular vestibule, a rigorous structure-activity relationship (SAR) study was done at D₂R with cariprazine on functional selectivity (cAMP and MAP kinase signaling) (99). The authors speculate that one mechanism of achieving functional selectivity is through bitopic ligand interactions (i.e. orthosteric and allosteric binding in one ligand).

Allosterism through the extracellular vestibule allosteric site is an exciting avenue for achieving therapeutically relevant functionally selective D₂R ligands, as structural studies allow for precise modulation of activity and SAR studies allow for precise ligand design (100). In fact, D₂R functionally selective ligands have been created and screened for preclinical efficacy (101, 102). The studies mentioned here are the beginning of an exciting era for D₂R functionally selective ligands.

1.2.6 Unexpected sites of allosteric modulation

The extracellular vestibule is proximal to the orthosteric site and allows for the creation of bitopic ligands, however GPCRs have been shown to possess other sites of allosteric modulation. The A_{2A}R was crystallized to 1.8 angstroms, which was a high enough resolution to solve the location of sodium binding (103). Sodium has long been known to be required for proper D₂R radioligand binding (104) and also important in opiate receptor (105) and alpha adrenergic receptor (106) radioligand binding. A crucial and highly conserved residue, Asp 80 (2.50) coordinates sodium binding and was shown in D₂R to abolish G protein signaling while maintaining ligand binding affinity for antagonists (107) when mutated to an Ala, a property that was also shown in the α -adrenergic 2A receptor (108) with sodium mimetic mutations at the same residue. Sodium has also been suggested to be crucial to D₂R dimer formation (109). Recent molecular dynamics simulations have shown that the sodium binds from the

extracellular space (110), where sodium concentrations are high. Recently sodium ingestion was studied in mice lacking sour and bitter receptors (which are GPCRs) and it was shown that sodium, which is normally aversive at high concentrations, is not aversive when the sour and bitter receptors are knocked out (111). This is a remarkable result because it demonstrates the direct molecular effect sodium has on GPCRs, as bitter and sour receptors normally activate aversive responses, and high concentrations of sodium are able to elicit the same response. Functional selectivity due to sodium regulation has been shown directly in the δ -opioid receptor: mutation of Asp 2.50 to an Ala caused a G protein biased ligand to become a β -arrestin biased ligand (112). Similar to sodium, many other uncommon allosteric modulators have been characterized for D₂R. L-prolyl-L-leucyl-glycinamide (PLG) was shown to enhance agonist and G protein coupling for D₂R (113) but have no effects on antagonists (114). While a molecule related to PLG, called POAPA, enhanced the β -arrestin expression and function at D₂R (115). Additionally, zinc has been shown to modulate antagonist binding to D₂R (116). Sodium and other allosteric modulators are another important contributor to the heterogeneous conformational landscape of D₂R and allow for a better understanding of functional selectivity.

1.3 D₂R functional selectivity is a function of cellular organization

Every molecular and mechanistic contribution to D₂R functional selectivity mentioned in this chapter is dependent upon the cell, the tissue, and the organism. Kenakin proposes that in signal transduction the ligand and the signaling proteins are signaling vectors (Figure 2A) that work upon a conduit, the receptor (117). The presence and concentration of these vectors depends on the cellular expression as well as ligand availability, and the efficiency of signaling depends on the expression of the receptor. For this reason, functional selectivity must always be considered in the context of an organism. The actions of D₂R in the central nervous system are the basis for many therapeutics, including treatments for attention deficit-hyperactivity disorder, Parkinson's disease, schizophrenia, bipolar disorder, and addiction among many other diseases.

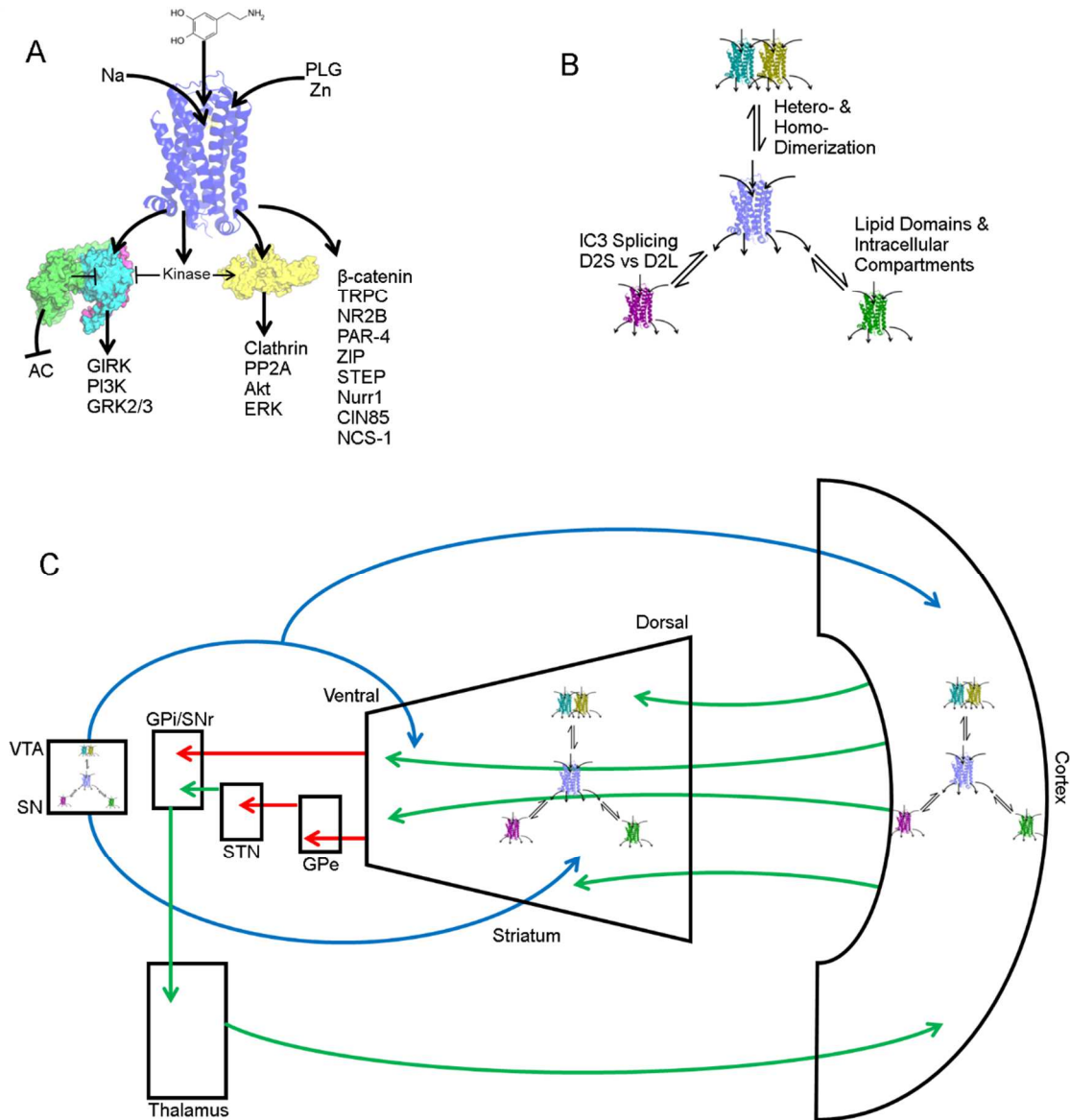


Figure 2: D₂R functional selectivity is dependent upon context. (A) D₂R interactions and downstream effectors leading to signaling events. (B) D₂R physical states are dynamic and determine extent of functional selectivity. (C) Central nervous system architecture of D₂R expression and connectivity. Dopaminergic projections (blue arrows) to cortex and striatum modulate excitatory (green arrows) and inhibitory (red arrows) neural circuits. D₂R is prominently expressed in dopaminergic, striatal and cortical cells. VTA: ventral tegmental area; SN: substantia nigra; GPI/SNr: internal globus

pallidus/substantia nigra reticulata; STN: subthalamic nucleus; GPe: external globus pallidus.

D₂R is expressed in the basal ganglia in a subpopulation of medium spiny neurons (MSNs) along with many other GPCRs. MSNs form the basis of the direct and indirect circuitry (where direct MSNs express D₁Rs and indirect MSNs express D₂Rs) and all drugs of abuse cause a robust increase in dopamine in the nucleus accumbens, a structure of the basal ganglia. In fact, the striatum (comprised of the ventral nucleus accumbens and the dorsal caudate putamen) receive 90% of their inputs, which are excitatory, from the cortex, the layer of the brain that has evolved the most in humans. The cortex is involved in information processing, and the striatum, through D₂R and D₁R expressing MSNs executes cortical commands to control locomotion, cognition and reward. MSNs release the inhibitory neurotransmitter GABA and connect to the midbrain. The midbrain in turn projects and releases dopamine (DA) to the dorsal striatum (through the substantia nigra, SN, a subset of cells that decay in Parkinson's disease) and the ventral striatum (through the ventral tegmental area, VTA). D₂R is highly expressed in the MSNs, the SN and VTA projection neurons, some cortical neurons, and interneurons in the striatum.

1.3.1 Dopamine and D₂R genetic mouse models reveal functional selectivity *in vivo*

The role of D₂R *in vivo* was most directly dissected with genetic models. The critical enzyme for tyrosine metabolism into DA is tyrosine hydroxylase (TH) and when TH was knocked out (and restored in adrenergic cells) DA could no longer be synthesized (118). These mice showed severe deficiencies in locomotor activity, feeding, and consuming water and all died within 30 days without treatment with L-DOPA, the enzymatic product of TH. Interestingly, rescue of TH to only the dorsolateral (119) or ventromedial (120) striatum rescued many of the feeding, cognitive, and locomotor deficits suggesting functional plasticity in the DA circuitry. In contrast, when the DA transporter (DAT) is knocked out, extracellular DA is increased and mice display increased locomotion (121) and D₂R is downregulated (122).

The function of D₂R signaling is most easily assessed in D₂R knockout mice, which have severe locomotion deficits (123) and are deficient in reward learning (124). D₂R knockout mice are also deficient in cocaine induced locomotion, and have an ablated MSN c-fos activation in response to cocaine (125). This result may seem unexpected, as c-fos is normally upregulated in D₁R expressing MSNs in response to cocaine (126). However, D₂R is able to exert control over D₁R MSNs because of its expression in presynaptic SN and VTA projection neurons. D₂R is alternatively spliced in the third intracellular loop into a long isoform, called D_{2L}R and a short isoform called

D_{2s}R (127) and D_{2s}R is more abundantly expressed presynaptically, while D_{2L}R is more abundantly expressed postsynaptically (128). The presynaptic D₂R directly inhibits the release of DA as well as the production of DA through TH phosphorylation (129) thus presynaptic D₂R can affect D₁R MSNs by controlling dopaminergic tone in the striatum. More recently, D₂R has been deleted specifically presynaptically (130) and postsynaptically (131) and it was shown that postsynaptic D₂R is necessary for cocaine induced locomotion, while loss of presynaptic D₂R resulted in supersensitivity to cocaine. The postsynaptic D₂R population was also shown to be sufficient for locomotion, as viral reexpression in the nucleus accumbens rescued the amphetamine response in D₂R knockout mice (132) and overexpression of D₂R in the nucleus accumbens caused an increase in basal locomotion (133). The cellular organization and splicing of D₂R is yet another layer of functional selectivity that affords D₂R the ability to transduce multiple, complex, and sometimes contradictory signaling events in response to a single stimulus. Cocaine and amphetamine are used to probe the behavioral responses in these genetically modified mice because they act to increase synaptic DA and have relevance to human disease (134). While behavioral outcomes are not as easily interpreted as biochemical assays, the relevance of D₂R splicing yielding functional selectivity has been shown biochemically (135). D₂R functions within a complex circuit

in the CNS, and the therapeutic implications of D₂R functional selectivity is that D₂R's control over that circuit can be manipulated specifically

1.3.2 Functional selectivity in D₂R circuitry

The most important property of D₂R in CNS circuitry is that it does not signal in a vacuum. As discussed earlier, presynaptic D₂R's inhibition of DA release directly affects D₁R expressing MSNs. However, activation of both D₁R and D₂R expressing MSNs (referred to as the direct and indirect pathway, respectively) is necessary for normal D₂R circuit modulation (136) and behavioral outcomes (137). In addition to the well-established direct and indirect pathway relationship, endocannabinoids induce long-term depression (eCB-LTD) in D₂R expressing MSNs selectively (138) and the induction of this eCB-LTD requires D₂R activation and induces parkinsonian motor deficits. Additionally, A_{2A}R signaling modulates this circuit, along with RGS4, a regulator of G_α subunits in MSNs (139). The limbic circuit, from the midbrain to the striatum and the cortex is modulated by D₂R, and D₂R itself is modulated by long term changes in circuitry. For instance, chronic haloperidol (an antipsychotic and potent D₂R antagonist) causes an upregulation of striatal D₂R but not cortical D₂R (140) while the atypical antipsychotic (and D₂R antagonist) sulpiride did not increase striatal D₂R expression (141) suggesting that the modulation of D₂R circuitry is a consequence of haloperidol's more dramatic antipsychotic efficacy and higher capacity for extra

pyramidal side effects. Behavioral changes can also alter D₂R circuitry directly, for example enhanced DA synaptic strength has been shown in response to cue-reward learning (142).

The role of D₂R MSNs was dissected directly using optogenetic activation and DREADD inactivation of the neurons which showed that they induce freezing behavior in the dorsal striatum (143) and restrain addictive behavior (cocaine self-administration) in the ventral striatum (144). In addition to the important role of D₂R in MSNs, D₂R is also expressed in the small population of cholinergic interneurons in the striatum, cells which have been shown to cause DA release themselves (145) and override the normal nucleus accumbens response to cocaine to block cocaine conditioning (146). The VTA projects to the striatum and cortex and individual projections have been shown to control aversion and also reward (147). The firing rate of the VTA projections is important for DA transmission, as tonic DA firing maintains dopaminergic tone, while phasic burst firing can cause a rapid increase in DA and the differences between these circuits has been shown to be anatomical and genetic (some projections do not express the autoinhibitory D₂R) (148). The phasic firing of the VTA neurons was shown to be sufficient for some behavioral adaptations implicated in addiction (149) while the precise anatomical circuitry of the VTA has only begun to be mapped and manipulated (150). The role of the projection neuron circuitry firing was also implicated in depression

phenotypes (151) and susceptibility to depression (152). While it is more difficult to directly assess the role of D₂R functional selectivity when the circuitry is assessed, it is obvious that DA and D₂R expressing cells play fundamental roles in many behaviors and human diseases.

1.4 The therapeutic implications of D₂R functional selectivity

D₂R functional selectivity has long been observed, and D₂R is a central target for many psychiatric disorders. The molecular mechanisms underlying D₂R functional selectivity, including dimerization, G protein and β -arrestin selectivity, and more recent hypotheses such as intracellular receptor signaling provide a unique opportunity to isolate D₂R signaling pathways. New classes of antipsychotics and antidepressants could be developed that manipulate these molecular properties. D₂R has long been a protein target with enormous therapeutic potential, and understanding its signal transduction properties only increases the capacity for the development of more effective pharmaceuticals with less occurrences of side effects.

The work presented in the next chapters represents elucidation of the functional selectivity of D₂R in a systematic and robust manner. Novel mutant D₂R were generated using the Evolutionary Trace (ET) approach (Chapter 2) and these mutants were extensively characterized (Chapter 3). Two mutants displayed extreme bias between G protein and β -arrestin pathways and these mutants retained the major functions of D₂R.

The two biased mutants were then used to unravel MAP kinase signaling *in vitro* and amphetamine induced locomotion *in vivo* (Chapter 4). Finally, the mutagenesis approach was applied to diverse GPCRs as well as more complex *in vivo* systems (Chapter 5). This work provides a clear impetus for more detailed functional selectivity studies of D₂R for the development of therapies with predictable outcomes.

2. Functional separation of D₂R using Evolutionary Trace

Understanding the contributions of functional selectivity at D₂R in intact biological systems is a challenge that cannot be elucidated in heterologous systems alone. In order to develop tools where this challenge can begin to be addressed, the *Evolutionary Trace* (ET) approach (153) was used to engineer D₂R mutants that selectively interact with either G proteins or β -arrestins, designated ^[Gprot]D₂R and ^[β arr]D₂R, respectively.

2.1 Evolutionary Trace guided mutagenesis of D₂R

The ET method identifies amino acids that determine the function of a protein and map its functional sites when a structure is available (154, 155). ET algorithms exploit protein orthologs and paralogs to correlate sequence variations with phylogenetic divergences and determine whether substitutions at a particular residue are likely to produce a functional change in the protein (156). The predictive power of ET is further enhanced when specific crystal structures (157) and more sophisticated models of the evolution of structure and function can be applied (155, 158). Here, a combination of these approaches (co-crystals of receptors and signaling molecules as well as novel algorithms, Figure 3) was used to identify residues in D₂R that could be mutated to achieve functional selectivity. The residues that were identified as being potentially critical for functional selectivity are mapped onto the crystal structure of D₃R

(Figure 3B; PDB ID: 3PBL) (159), which shows the physical proximity of each residue to each other as well as to the cytosolic side of the receptor.

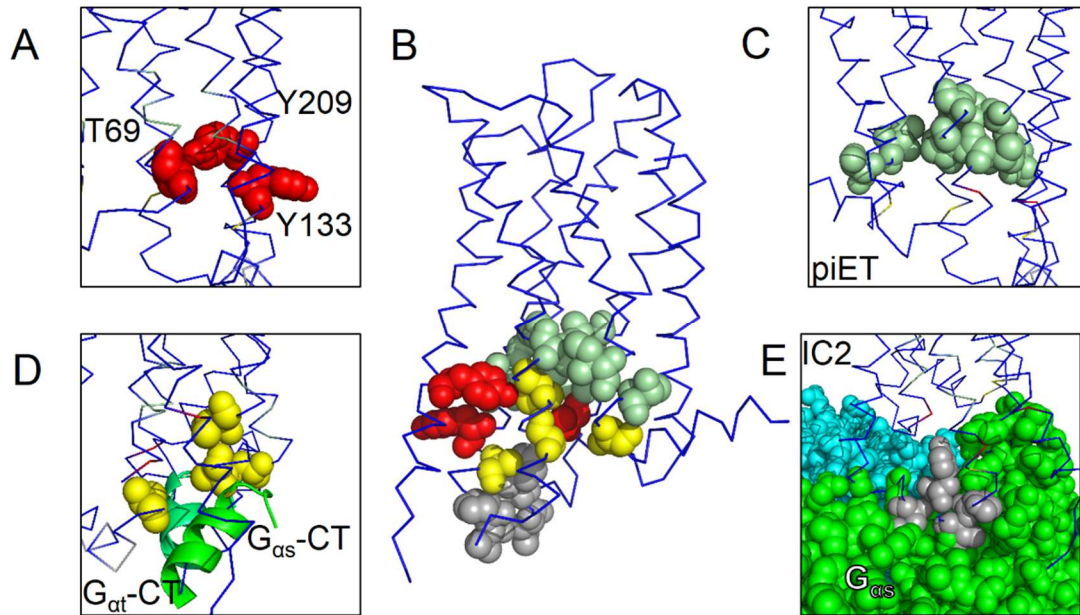


Figure 3: Evolutionary Trace of D₂R facilitated by advances in crystallography and algorithm design. (A) TYY mapped onto D₃R (159) (PDB ID: 3PBL in red). (B) Four rounds of ET predicted residues for mutagenesis mapped onto D₃R. (C) piET (green residues depicted as spheres). (D) G α -CT proximity (160) (PDB ID: 3DQB residues in yellow, G α -CT is represented as a green α -helix cartoon), and (E) G $\alpha\beta\gamma$ (161) (PDB ID: 3SN6 α is green and β is blue) interaction with IC2 of D₃R (grey spheres).

The β 2 adrenergic receptor (β 2AR) was originally mutated based on the crystal structure of rhodopsin (162) to yield a β -arrestin biased β 2AR termed β 2AR-TYY. These residues were mutated in D₂R (Figure 3A) however, robust separation between G

protein and β -arrestin pathways was not achieved. Therefore, four rounds of ET-guided residue determination (mapped to D₃R) (159); in Figure 3B) were carried out with the development of the more complex ET algorithm piET (Figure 3C) and as more detailed crystal structures were solved including the C-terminus of G_{at} in complex with rhodopsin (Figure 3D) (160) and β 2AR in complex with G _{$\alpha\beta\gamma$} (Figure 3E) (161).

2.2 Evolutionary Action at D₂R yields a robust landscape of functional selectivity

In order to achieve specific and robust separation of G protein- and β -arrestin-dependent interactions, *Evolutionary Action* (EA) (163) was used to predict residue changes. EA models the evolutionary relationship between genotype and phenotype as a smooth process upon which a mutation causes a small perturbation. Explicitly, if γ is the genotype sequence and φ the fitness phenotype, EA postulates an evolutionary function f between them exists, such that:

$$f(\gamma) = \varphi \quad (1)$$

and f is differentiable so that the Evolutionary Action point mutation $\Delta\gamma$ on fitness as:

$$f'(\gamma) \cdot \Delta\gamma = \Delta\varphi \quad (2)$$

In practice, f remains unknown but its derivative (or gradient) f' is given by ET, and $\Delta\gamma$ is given by substitution odds. The Evolutionary Action equation (2) is thus generally solvable for coding mutation of proteins and quantifies the effect of mutations over multiple scales, spanning molecular, clinical and population genetics effects (163-

166). Here, for each residue identified in Figure 3A-B, mutations were predicted and scored by EA according to how likely they would produce a phenotype (Table I). Each point mutation was tested for G protein activity by cAMP inhibition and β -arrestin 2 recruitment by Bioluminescent Resonance Energy Transfer (BRET) (75), fidelity of plasma membrane trafficking as well as lack of constitutive activity. These mutants were binned into four categories: 1) β -arrestin biased, 2) G protein biased, 3) deficient at both pathways, or 4) unaffected at either pathway (Figure 4A). Residues that retained the desired phenotype were further combined into double (Figure 4B), triple (Figure 4C), quadruple, and quintuple (Figure 4D) point mutations. This initial characterization yielded a robust landscape of unique functionally selective mutants.

Table I: Evolutionary Action guided mutagenesis. Each residue predicted from ET is color coded the same in Figure 3 and Figure 4 in the first column. The second column shows the predicted residues in increasing ET harshness (amino acid conservation and side chain chemistry) from left to right. Each single point mutation was generated and tested for G protein and β -arrestin activity. Note that A135 was found to be a critical residue for G protein activation, but not β -arrestin activation and all 19 mutations were made in order to titrate the most β -arrestin biased mutant.

T69	G	V	F	
Y133	L	A	G	
Y209	N	S	F	A
A135	C	S	G	V
	T	M	P	I
	L	F	Y	N
	W	Q	H	R
	E	K	D	
A372	S	Y	W	
L376	G	M		
N431	A	M	L	T
L72	V	N	D	
I73	T	Q	D	
L76	V	N	D	
L125	V	N	D	
I128	T	S	D	
S129	G	Y	I	
V379	L	D	K	
I426	F	Q	G	
T428	N	L	W	
P139	A	S	W	
M140	L	V	D	
Y142	F	H	E	
T144	A	N	W	

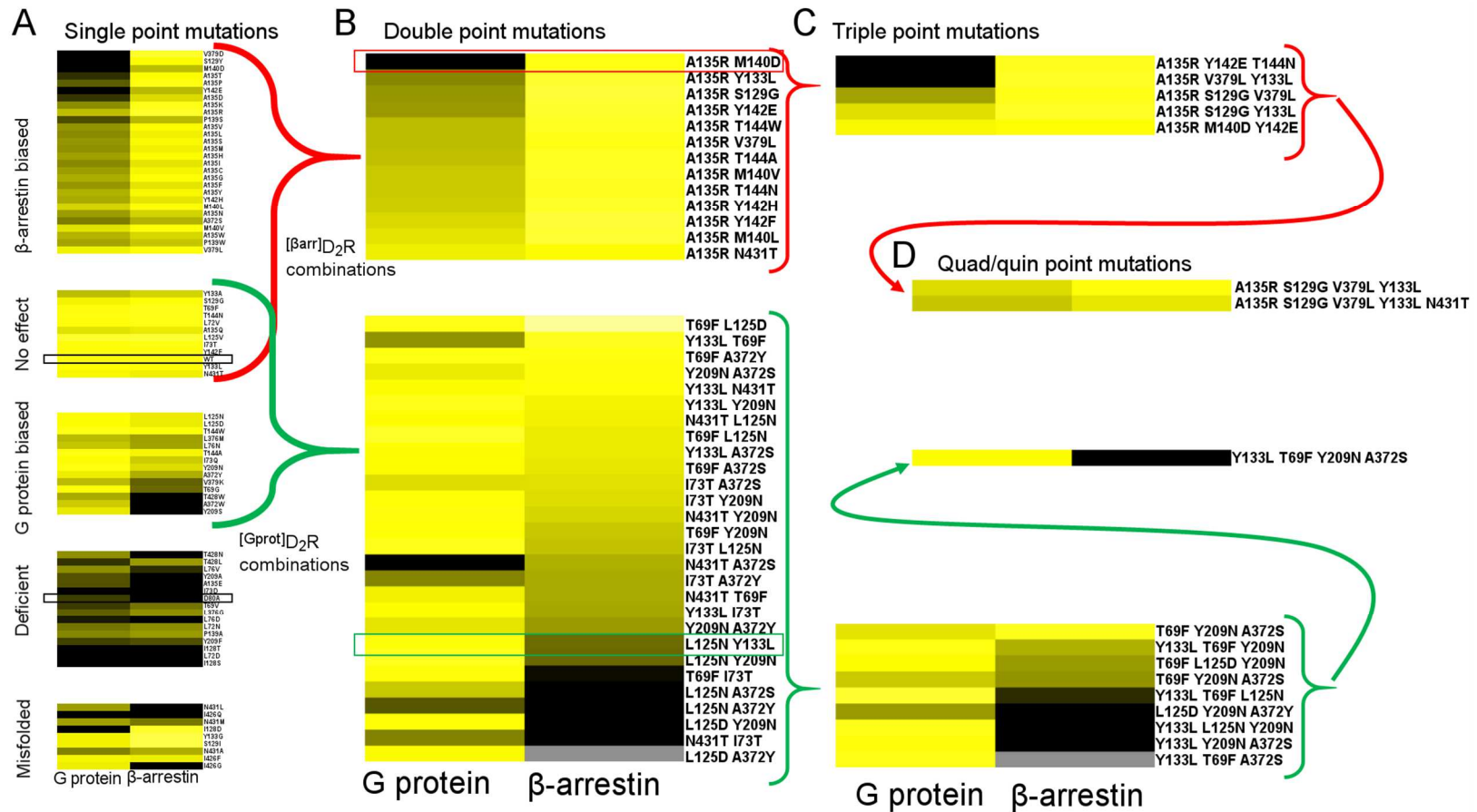


Figure 4: G protein and β -arrestin activity of ET predicted mutants. Dose response curves for each mutant were normalized to a WT control that was performed the same day and the $\log(\tau/K_A)$ was calculated. Since all values were

normalized to WT, $\tau=1$ and $K_A=1$ for WT, thus 0 is depicted as yellow, and -3 (100 log fold shift in τ/K_A) is depicted as black in the heat maps. **(A)** G protein and β -arrestin activity of single point mutations generated mutants that were misfolded, mutants that were biased toward G protein or β -arrestin, or mutants that had little to no effect on any tested function. **(B)** Mutations that had no effect on the desired pathway (red lines for β -arrestin and green for G protein) were combined into double point mutations and **(C)** triple and **(D)** quadruple and one quintuple. The mutations that were further characterized in Figure 6 are highlighted in boxes.

The four rounds of ET guided mutagenesis are depicted in a traditional snake-like plot of D₂R in Figure 5A with residues highlighted with the same color scheme as Figure 3 and Table I. The two mutants that showed the greatest functional separation are designated ^[Gprot]D₂R (L125N Y133L) and ^[βarr]D₂R (A135R M140D). Each of these mutations occurs within 20 amino acids of the DRY motif of TM3 (Figure 5C). Interestingly, ^[Gprot]D₂R mutations are more distal from the recently resolved co-crystals of receptors and G proteins or arrestin fragments, while ^[βarr]D₂R mutations are more proximal (Figure 5D). The ^[Gprot]D₂R mutant is derived from the more sophisticated ET algorithms (TYY and piET, Figure 3A and 3C), while ^[βarr]D₂R arose from residues identified in the more specific crystal structures of receptors and G proteins (Figure 3D and 3E)(160, 161).

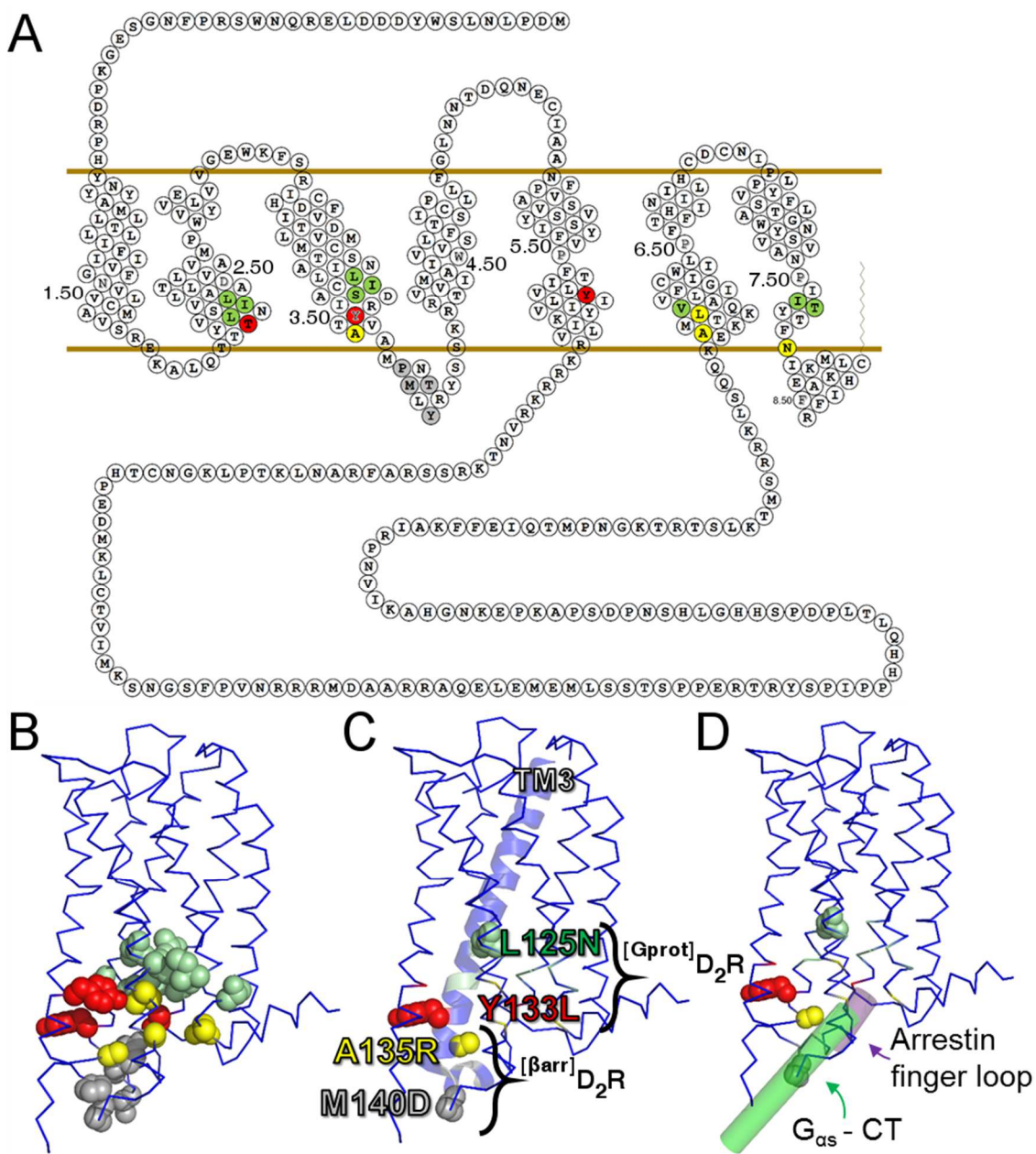


Figure 5: Generation of functionally selective D₂R mutants. (A) Snake-like plot of D₂R with each round of mutagenesis color-coded according to Table I and Figure 3. Red spheres: residues derived from TYY, green spheres: predicted from piET algorithm, yellow spheres: predicted from proximity to rhodopsin/transducin α subunit C-terminal fragment co-crystal; grey spheres: identified residues from β 2AR/G $\alpha\beta\gamma$ co-crystal in intracellular loop two.

Ballesteros-Weinstein numbering identified for each transmembrane domain. The same color scheme was used to highlight the residues on the structure of D₃R (159) because D₃R is the most closely related GPCR to D₂R with an available crystal structure (81% sequence identity for transmembrane domains). **(B)**, D₃R structure represented as a blue ribbon, and ET-identified residues are spheres. **(C)** The biased mutants all occur within 20 amino acids of the DRY motif on transmembrane domain three (TM3). **(D)** D₃R aligned to β 2AR in complex with G $_{\alpha\beta\gamma}$, green cylinder PDB ID: 3SN6 (161) as well as rhodopsin in complex with the finger-loop domain of visual arrestin (167) (purple cylinder PDB ID: 4PXF). D₃R to β 2AR alignment yielded an RMSD = 1.8 and D₃R alignment to rhodopsin RMSD = 2.7 using pymol MatchAlign command.

3. Ligand, receptor and transducer contributions to D₂R functional selectivity

While molecular and conformational theories have framed the development of biased agonist based therapies, the molecular details of functional selectivity remain elusive. D₂R's prominence as a pharmaceutical target for many disorders makes it a good receptor candidate for precise and robust dissection of functional selectivity.

Here, the contributions of ligand, receptor and transducer to functional selectivity are rigorously assessed. Novel mutants are characterized and assessed for their unique functional selectivity properties that provide insight into the quality of D₂R functional selectivity. These data demonstrate that functional selectivity is dynamic and malleable, and that leveraging specific D₂R pathways is possible.

3.1 *[G^{prot}]D₂R and [β^{arr}]D₂R display distinct but expected properties*

Each receptor mutant (Table I) was profiled for G protein and β-arrestin activity. In addition, a negative control point mutation, [D^{80A}]D₂R (107) was included in all experiments because this mutant has been shown to bind ligands and traffic to the plasma membrane but is deficient in signaling. As shown in Figure 6A, [G^{prot}]D₂R retained full efficacy and potency at cAMP inhibition compared to [WT]D₂R, while [β^{arr}]D₂R and [D^{80A}]D₂R are severely deficient. In contrast, β-arrestin 2 recruitment is retained and even enhanced in [β^{arr}]D₂R while both efficacy and potency are either lost or markedly reduced in [D^{80A}]D₂R and [G^{prot}]D₂R as determined by BRET (Figure 6B).

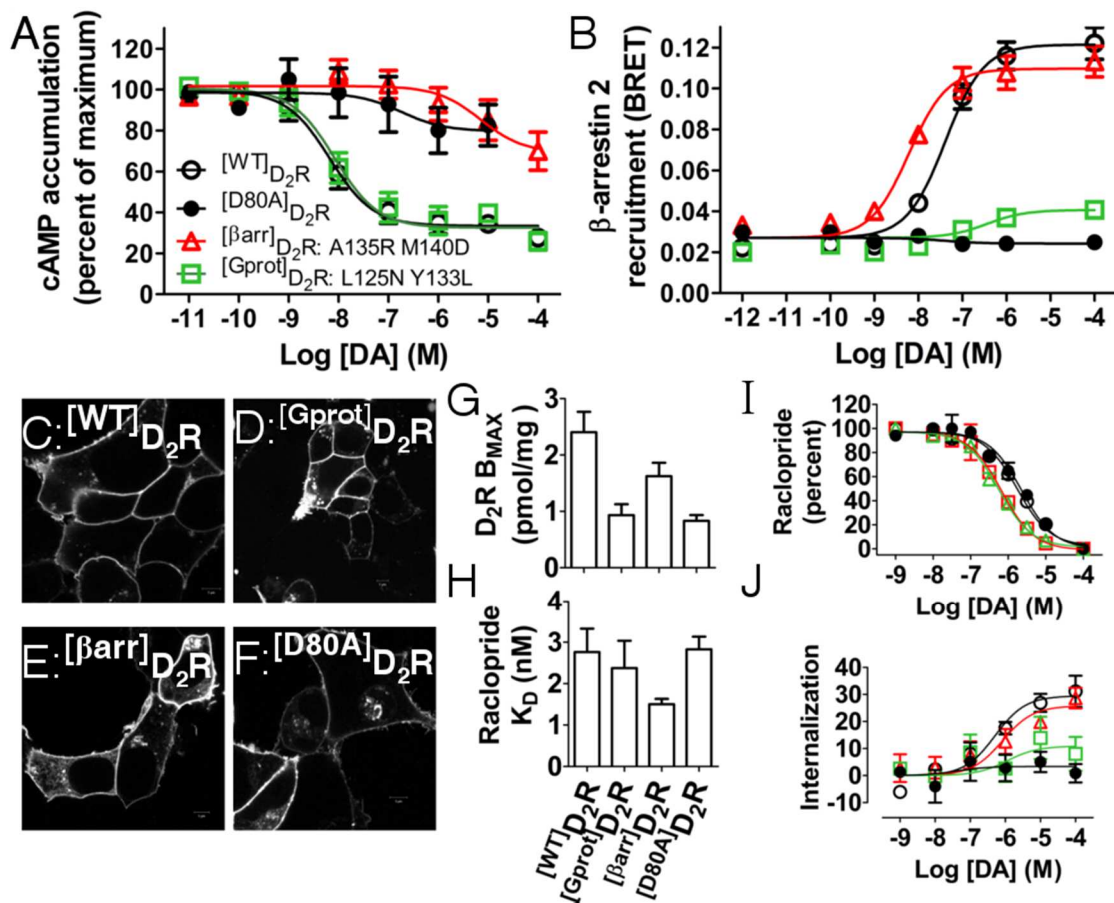


Figure 6: Biased D₂R mutants derived from Evolutionary Trace. (A) Inhibition of cAMP as determined by GloSensor compared to ^[WT]D₂R positive control and ^[D80A]D₂R negative control. (B) β -arrestin 2 recruitment determined by BRET for the same receptors as in (A). All points are SEM of n=3-7 done in duplicate. Confocal images of (C) ^[WT]D₂R, (D) ^[Gprot]D₂R, (E) ^[β arr]D₂R, and (F) ^[D80A]D₂R expressed in live cells. (G) B_{MAX} (with SEM) determined from n=3 radioligand binding experiments. (H) K_D from B_{MAX} determination experiments. (I) DA competition binding experiments to determine K_I. (J) D₂R internalization assessed by live cell HA antibody staining of D₂R (SEM, n=5 done in triplicate).

Point mutations in GPCRs, especially ones that affect signaling, are notorious for inducing unstable proteins (168). To address this concern, the membrane localization of ^[WT]D₂R (Figure 6C) in live cells was compared to ^[Gprot]D₂R (Figure 6D), ^[β arr]D₂R (Figure 6E), and ^[D80A]D₂R (Figure 6F). None of the receptors studied showed major trafficking

deficits. However, in order to quantitatively assess the expression of these mutants, traditional radioligand determinations of B_{MAX} (Figure 6G) and K_D (Figure 6H) were performed. When transiently transfected into HEK 293T cells all mutated receptors expressed between 1-1.5 pmol/mg protein and their levels were 30-50% lower than the $^{[WT]}D_2R$ under the same conditions (Figure 6G). However, the K_D for the antagonist raclopride was virtually identical (Figure 6H) and the K_I for DA was also unchanged (Figure 6I). Receptor internalization, as assessed by cell surface ELISA on live cells (169) demonstrates predictable internalization patterns: $^{[\beta arr]}D_2R$ and $^{[WT]}D_2R$ internalize to the same degree (30%) as previously reported (62) while $^{[Gprot]}D_2R$ and $^{[D80A]}D_2R$ are severely deficient (Figure 6J).

The separation in apparent affinity for the endogenous ligand dopamine for cAMP inhibition, β -arrestin 2 recruitment and internalization is 100-1000 fold between the two engineered receptors while the K_D of raclopride and K_I of DA remains unchanged. Similarly, the response of each receptor mutant would be greater than 90% distinct even at the highest physiological levels of dopamine (100 μ M in Figure 6A, 6B, and 6J). Additionally, the slight differences in expression levels of the various D_2R mutants does not seem to affect their coupling potencies as increasing the amounts of transfected D_2Rs has the same effects for $^{[WT]}D_2R$ and $^{[Gprot]}D_2R$. Thus, these ET-derived mutants display a robust but selective disruption in D_2R function.

3.2 Operationally defined, receptor dictated functional selectivity

The bias of a receptor can be simply viewed as being dependent upon its propensity to engage one signaling mechanism over the other. A well characterized biased D₂R was previously engineered (71, 170) by mutating a motif unique to D₂-like receptors (IYIV) to four alanines (^[IYIV]D₂R). As seen in Figure 7A, ^[IYIV]D₂R induces a complete loss of β-arrestin 2 recruitment, along with the previously observed (170) ~50% loss of G protein activity. Thus, ^[IYIV]D₂R is a G protein-biased mutant D₂R under these conditions. However, when GRK2 is overexpressed (Figure 7B), β-arrestin 2 recruitment potency is enhanced at ^[WT]D₂R and ^[IYIV]D₂R, and only slightly potentiated for the previously characterized ^[Gprot]D₂R and ^[βarr]D₂R when compared to endogenous levels of GRK2 (Figure 6B). Quantifying the bias between ^[Gprot]D₂R and ^[IYIV]D₂R using a statistical formalism (171) (Figure 7C), a bias plot (172) (Figure 7D) and $\Delta\Delta\log(\tau/K_A)$ calculations (Table IV) reveal the quality of G protein bias. ^[Gprot]D₂R and ^[IYIV]D₂R display similar degrees of bias using each method because while G protein activity is slightly perturbed at ^[IYIV]D₂R, at ^[Gprot]D₂R the G protein activity is completely intact, while a small amount of β-arrestin activity remains. However, when GRK2 is overexpressed ^[Gprot]D₂R does not shift appreciably whereas ^[IYIV]D₂R gains significantly in both efficacy and potency, this is revealed by the greater shift observed using the bias statistical formalism (Figure 7C). In contrast, the bias plot reveals that ^[IYIV]D₂R is inefficiently biased toward G protein activity, and $\Delta\Delta\log(\tau/K_A)$ values reveal that ^[IYIV]D₂R bias is dependent on GRK2 levels.

The GRK2 overexpression assay demonstrates the receptor capacity for β -arrestin recruitment under the most favorable conditions, and shows that $^{[YIV]}D_2R$ displays partial agonism at *both* G protein and β -arrestin activities. In contrast, $^{[Gprot]}D_2R$ retains its original biased signaling profile: full agonism at the G protein pathway and weak partial agonism at the β -arrestin pathway.

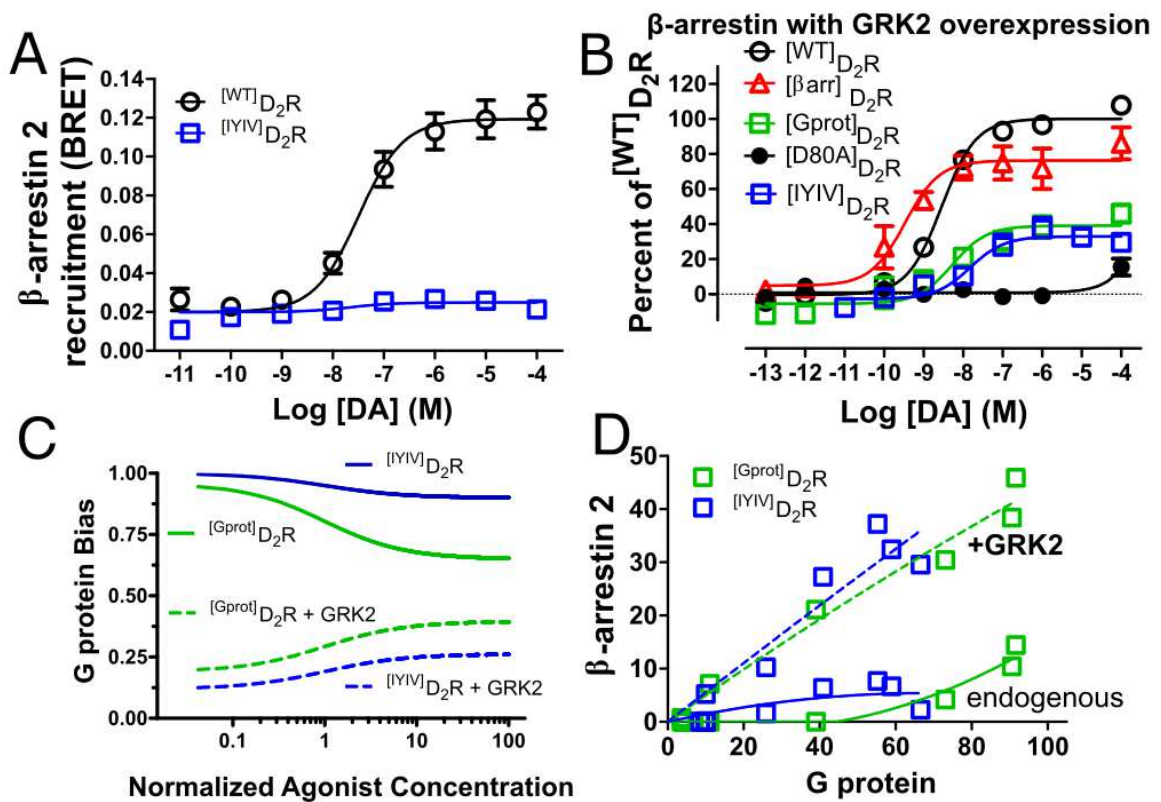


Figure 7: Functional selectivity is operationally defined. (A) β -arrestin 2 recruitment comparing $^{[WT]}D_2R$ and $^{[YIV]}D_2R$ as determined by bioluminescent resonance energy transfer (BRET). (B) GRK2 overexpression enhances β -arrestin 2 recruitment by BRET for $^{[YIV]}D_2R$ and $^{[WT]}D_2R$, but only slightly for $^{[Gprot]}D_2R$, $^{[\beta arr]}D_2R$, and $^{[D80A]}D_2R$ when compared to Figure 6B. All data are presented with SEM from $n=3-4$ independent experiments, with statistical significance calculated in Table IV. Quantification of bias between G protein activity and β -arrestin 2 recruitment using (C) a statistical formalism (171) or (D) bias plot mapping under normal (solid lines) and GRK2 overexpression enhanced (broken lines) conditions.

The controlled perturbation of G protein and β -arrestin pathways allows for a more detailed examination of partial biased agonism. Partial biased agonism is an important property displayed by many GPCR ligands, and mutants that avoid the operational inconsistency displayed between $^{[YIV]}D_2R$ and $^{[Gprot]}D_2R$ would prove valuable for further understanding of functional selectivity. The conserved residue A3.53 (A135) was mutated into all 19 possible amino acids (Table I, Figure 4) because it conferred remarkable functional selectivity properties. Basic residues lost ~50% of their G protein activity, while still retaining complete, and slightly more potent β -arrestin activity (Figures 8A and 8B, respectively). In contrast, acidic substitutions ablated activity at both pathways. Furthermore, substitution with a bulky polar residue (tyrosine) yielded a balanced reduction in both G protein and β -arrestin 2 activity to roughly 75% (Figure 8C and 8D, $^{[\tau/1.5]}D_2R$) and substitution with a bulky nonpolar residue (phenylalanine) yielded a balanced 50% reduction (Figure 8E and 8F, $^{[\tau/2]}D_2R$). These unique partial agonist mutants were combined with one residue substitution from $^{[Gprot]}D_2R$ (L125N) or $^{[\betaarr]}D_2R$ (M140D) to confer partial biased agonism for each pathway.

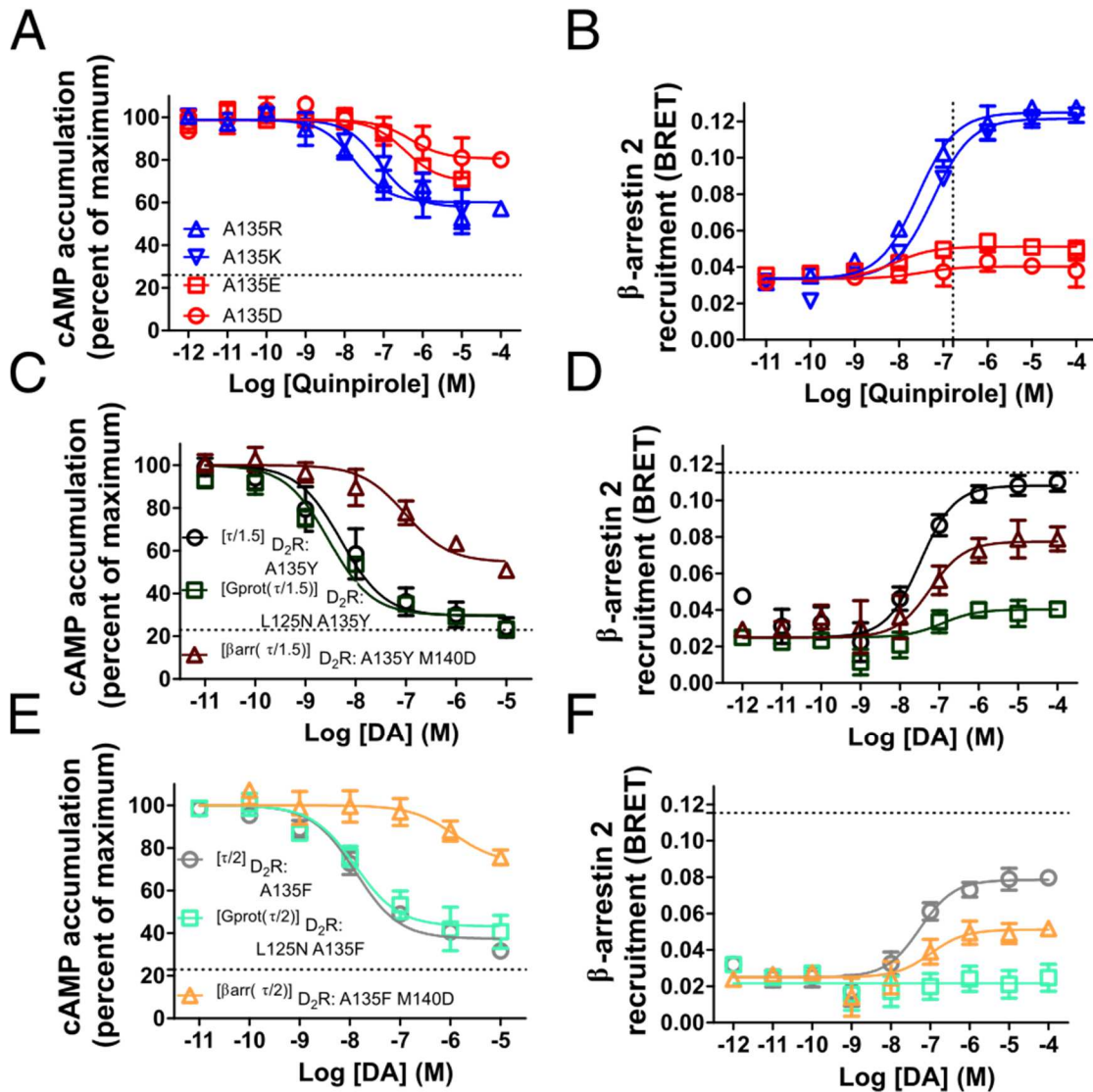


Figure 8: Receptor control of partial agonism at D_2R . (A) G protein activity as determined by inhibition of isoproterenol-induced cAMP accumulation of basic and acidic residue substitutions at A135 (A3.53) and (B) β -arrestin 2 recruitment. (C) G protein activity of bulky polar substitution (tyrosine) is roughly 75% ($\tau/1.5$) of $^{[WT]}$ D_2R (dotted line) and (D) β -arrestin 2 recruitment is similarly reduced. When combined with one residue from $^{[Gprot]}$ D_2R (L125N) or $^{[\beta arr]}$ D_2R (M140D) these mutants display partial biased agonism for their respective retained pathways. (E) G protein and (F) β -arrestin 2 recruitment of an even more reduced (50%; $\tau/2$) partial agonism induced by substitution of A135 for a bulky nonpolar residue (phenylalanine). Similarly combined with L125N or M140D to generate weak partial biased agonism in response to full agonists. All data presented with SEM from $n=3-5$ independent experiments.

3.3 Agonist texture reveals novel modes of functional selectivity

A unique G protein-biased mutant (termed ^[Gprot4PM]D₂R) displayed remarkable retention of G protein activity and loss of β -arrestin 2 recruitment when the reference agonist quinpirole was used to probe activity (Figure 9A and 9B, respectively). In contrast, when the endogenous ligand DA was used, the G protein activity was unchanged, but the β -arrestin activity was ~50% of ^[WT]D₂R (Figure 9A and 9B, Table V). To again assess the β -arrestin recruitment capacity, GRK2 overexpression rescued ^[Gprot4PM]D₂R for both DA and quinpirole to almost the same extent of ^[WT]D₂R (Figure 9C, Table V). However, the recruitment of GRK2 by ^[Gprot4PM]D₂R showed the same agonist selectivity between DA and quinpirole (Figure 9D) as observed with β -arrestin 2. These data demonstrate the concept of *agonist texture* (173), which is the concept that full agonists induce distinct receptor activation states and conformations.

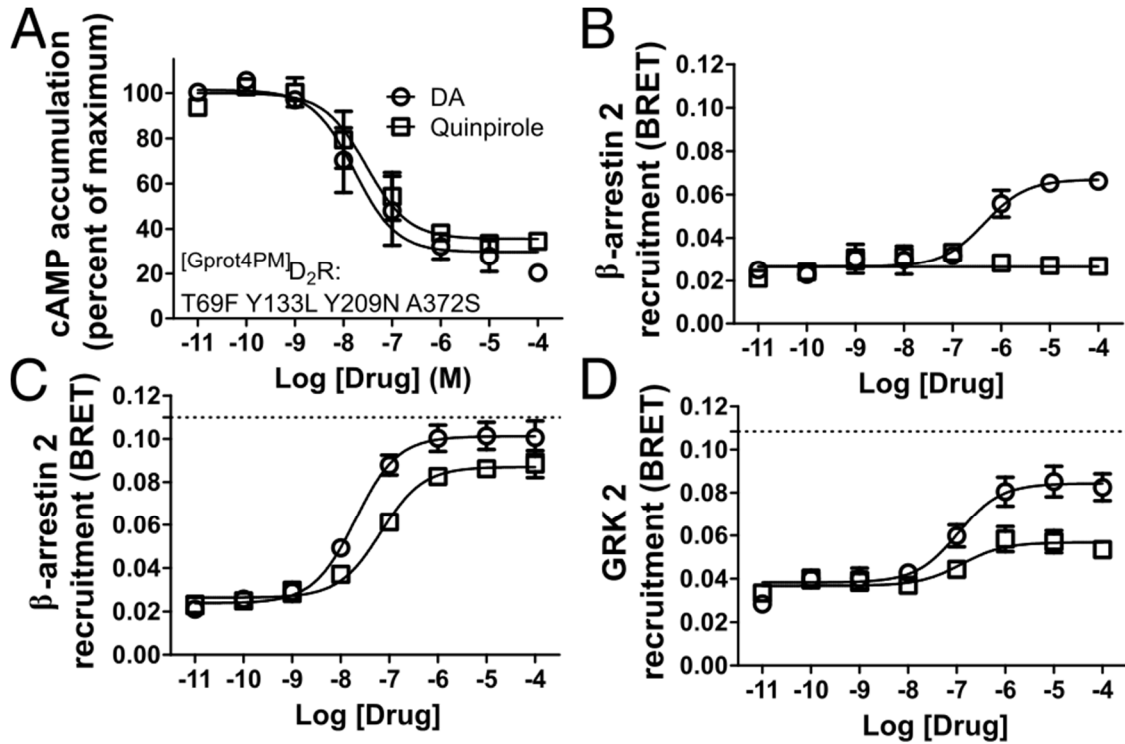


Figure 9: A unique G protein biased mutant demonstrates agonist texture. (A) Dopamine (DA) and quinpirole equivalently inhibit cAMP production, which is equivalent to $^{[WT]}D_2R$ for $^{[Gprot4PM]}D_2R$ (T69F Y133L Y209N A372S). (B) $^{[Gprot4PM]}D_2R$ has roughly 50% efficacy in response to DA but not quinpirole for β -arrestin 2 recruitment. (C) GRK2 overexpression rescues both DA and quinpirole β -arrestin 2 recruitment activity nearly to $^{[WT]}D_2R$ levels (dotted line, from Figure 7B). (D) GRK2 recruitment as determined by BRET (where GRK2 is tagged with YFP) shows the same ligand discrepancy as β -arrestin 2. All data are presented with SEM from $n=3$ independent experiments, with statistical significance calculated in Table V.

$^{[Gprot]}D_2R$ and $^{[\betaarr]}D_2R$ display unprecedented separation of signal in response to DA (Figure 6) and diverse D_2R agonists and antagonists were used to probe the extent of agonist texture between the mutants at G protein and β -arrestin 2 activation. Each agonist tested at cAMP inhibition was effectively equivalent for $^{[WT]}D_2R$ and $^{[Gprot]}D_2R$ while being severely disrupted for $^{[\betaarr]}D_2R$ and $^{[D80A]}D_2R$ (Figure 10A, 10C

and 10E, Table V). In contrast, $^{[\beta\text{arr}]}\text{D}_2\text{R}$ and $^{[\text{WT}]}\text{D}_2\text{R}$ were active at β -arrestin 2 recruitment and deficient with $^{[\text{Gprot}]}\text{D}_2\text{R}$ and $^{[\text{D80A}]}\text{D}_2\text{R}$ (Figure 10B, 10D and 10F, Table V). Similarly, the well characterized antagonist raclopride, typical antipsychotic haloperidol, and atypical antipsychotic aripiprazole inhibited DA-induced cAMP reduction for $^{[\text{Gprot}]}\text{D}_2\text{R}$ and $^{[\text{WT}]}\text{D}_2\text{R}$ (Figure 10G, 10I, and 10K, Table V), and β -arrestin 2 recruitment for $^{[\beta\text{arr}]}\text{D}_2\text{R}$ and $^{[\text{WT}]}\text{D}_2\text{R}$ (Figure 10H, 10J and 10L, Table V). These diverse D_2R ligands behave as expected for each assay and provide evidence that the complex activation states of $^{[\text{Gprot}]}\text{D}_2\text{R}$ and $^{[\beta\text{arr}]}\text{D}_2\text{R}$ remain intact, as opposed to $^{[\text{Gprot4PM}]}\text{D}_2\text{R}$, which has lost responsiveness to quinpirole at β -arrestin 2 recruitment selectively.

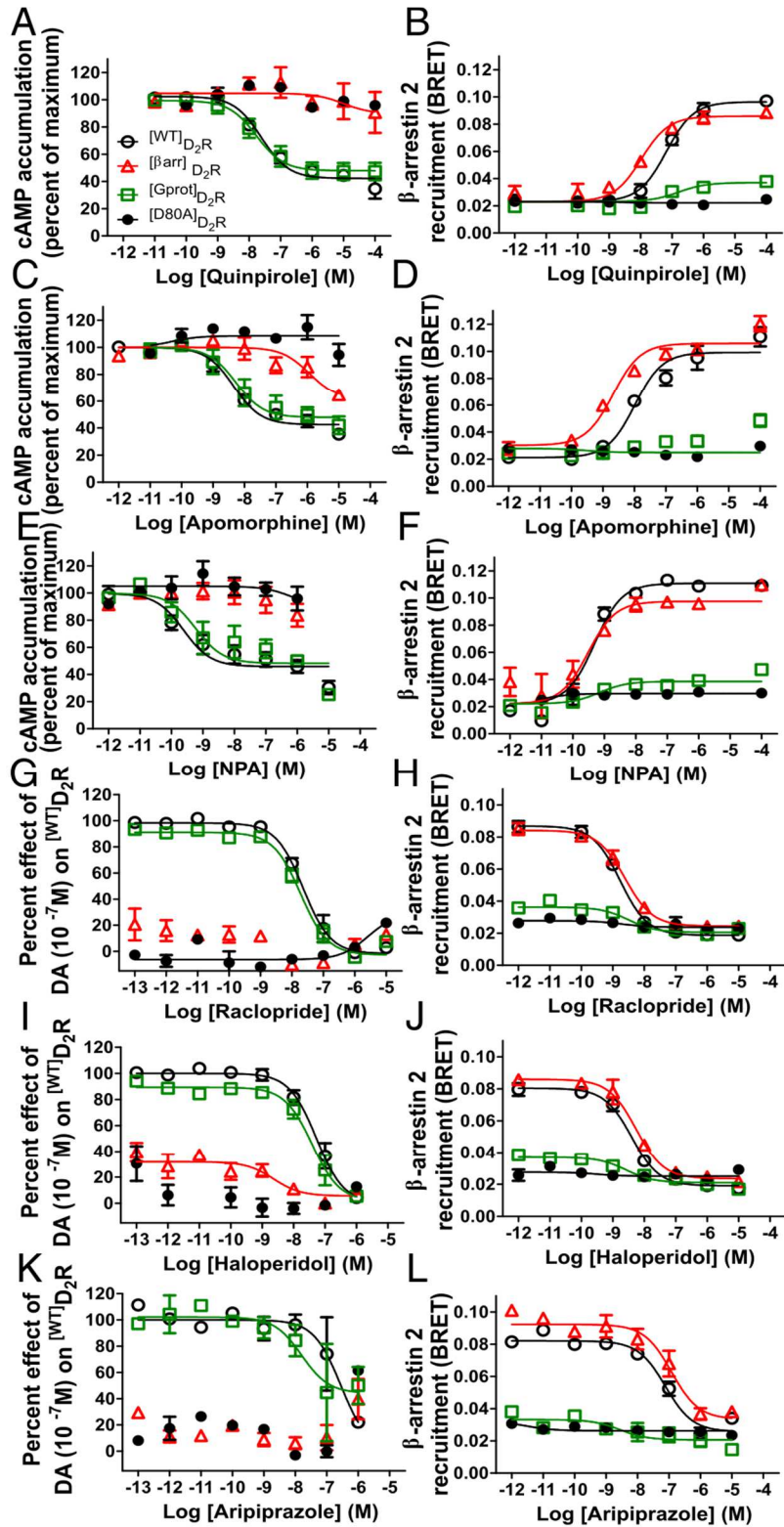


Figure 10: Agonists and antagonists with diverse pharmacophores elicit predictable responses at ^[Gprot]D₂R and ^[βarr]D₂R. The D₂R agonists quinpirole, apomorphine, and NPA were tested for G protein activity (**A,C,E**, respectively) and β-arrestin 2 recruitment (**B,D,F**, respectively). For each agonist, ^[Gprot]D₂R showed a response similar to ^[WT]D₂R at G protein activation and more similar to ^[D80A]D₂R for β-arrestin recruitment, while ^[βarr]D₂R was not active at the G protein pathway but retained activity at the β-arrestin pathway. The antagonists raclopride (**G,H**) haloperidol (**I,J**) and partial antagonist aripiprazole (**K,L**) were able to block DA elicited D₂R activation at the G protein pathway (**G,I,K**, respectively) for ^[Gprot]D₂R and ^[WT]D₂R to the same extent, while ^[D80A]D₂R and ^[βarr]D₂R had no effect to inhibit. In contrast, these antagonists block DA elicited β-arrestin 2 recruitment (**H,J,L**, respectively) for ^[βarr]D₂R and ^[WT]D₂R. All data are presented with SEM from n=3-4 independent experiments, with statistical significance calculated in Table V.

3.4 The status of receptor interacting partners in extremely biased mutant D₂Rs

The final determinant of functional selectivity: receptor interacting proteins and allosteric modulators, were assessed at ^[Gprot]D₂R and ^[βarr]D₂R while being compared to positive and negative controls (^[WT]D₂R and ^[D80A]D₂R, respectively). The interaction of each receptor with other components of the desensitization machinery mirrored the recruitment of β-arrestin 2. GRK2 (Figure 11A) and β-arrestin 1 (Figure 11B) showed a similar slight potentiation and loss of efficacy at ^[βarr]D₂R when compared to ^[WT]D₂R, while ^[Gprot]D₂R was severely deficient (Table VI). To test whether the mutagenesis induced loss of function at G protein and β-arrestin achieved with ^[Gprot]D₂R and ^[βarr]D₂R could potentially have induced aberrant activation of normally inactive receptor interacting proteins, major GPCR signaling avenues (G_{αs} and G_{αq}) were assessed and neither were activated by any D₂R mutant (Figure 11C and 11D, respectively, Table VI).

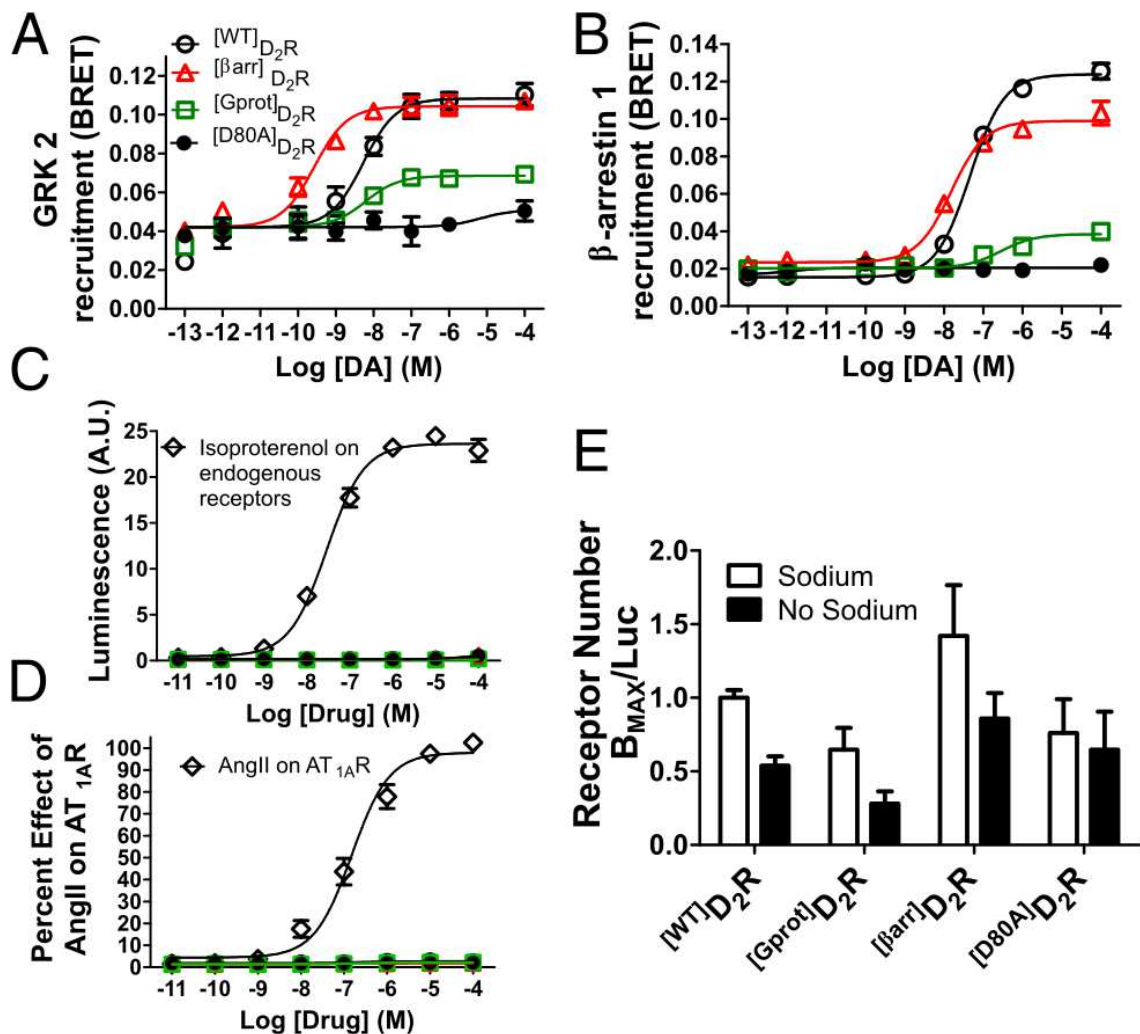


Figure 11: Interacting partners and allosteric D₂R determinants of functional selectivity. (A) GRK2 and (B) β-arrestin 1 recruitment as assessed by BRET show a similar profile as β-arrestin 2: [βarr]_{D2R} recruits normally, while [Gprot]_{D2R} is severely deficient. (C) Each D₂R construct was expressed in HEK 293T cells and assessed for its ability to stimulate cAMP in response to DA. Stimulation of endogenous receptor by isoproterenol was used as a control response. (D) G_{αq} mediated Ca²⁺ flux, as measured by the aequorin luminescence assay, is not stimulated by [WT]_{D2R}, [Gprot]_{D2R}, [βarr]_{D2R} or [D80A]_{D2R}, compared to AngII induced Ca²⁺ flux induced by transient expression of AT_{1A}R. (E) B_{MAX} was determined by binding, while luciferase-tagged receptors provided a B_{MAX}-independent measure of receptor number. In this assay, the responsiveness to salt is retained for all mutants (except [D80A]_{D2R}). All data are presented with SEM from n=3-4 independent experiments, with statistical significance calculated in Table VI.

The effect of the GPCR allosteric modulator sodium has been previously shown to inhibit dopamine binding to D₂R (107) and has been proposed to function as an efficacy switch for receptor bias (174). When sodium is removed from binding buffer this results in a 50% reduction in B_{MAX}. To assess sodium dynamics in D₂R, radioligand binding was used to determine B_{MAX} with and without sodium on the *Renilla luciferase* tagged D₂R constructs (75). The relative receptor amounts were normalized to luminescence output to provide an independent readout of receptor number. This assay yielded a 50% reduction in ^[WT]D₂R and ^[βarr]D₂R apparent B_{MAX} (Figure 11E) and ^[Gprot]D₂R also showed a sodium dependent reduction, although ^[Gprot]D₂R expresses lower than ^[WT]D₂R as previously described (Figure 6). ^[D80A]D₂R B_{MAX} did not change with sodium, validating the experiment as ^[D80A]D₂R is mutated at the presumed site of sodium interaction and has been previously shown to not bind sodium (107).

4. The physiological relevance of D₂R functional selectivity

The relationship between GPCR G protein- and β -arrestin-dependent signaling is complex. G protein-mediated signaling is rapid and transient and engagement of β -arrestin inhibits the G protein pathways. In addition, formation of the GPCR/ β -arrestin complex normally depends upon phosphorylation of the receptor (61). Moreover, G proteins and β -arrestins can engage the same pathway, but with distinct cellular consequences, as detailed in Chapter 1. As discussed, the physiological relevance of functional selectivity is profound for therapeutic applications, yet remains largely undefined. Thus, the ^[Gprot]D₂R and ^[\betaarr]D₂R mutants were applied to complex D₂R signaling systems to unravel functional selectivity.

4.1 MAP kinase signaling in ^[Gprot]D₂R and ^[\betaarr]D₂R

One well-documented example of G protein and β -arrestin control of a common signaling pathway in D₂R is the MAP kinase cascade (175). To address this relationship, two related transcriptional reporters for MAP kinase signaling were transfected along with the mutated D₂Rs in HEK 293T cells. As shown in Figure 12A and 12B a dose-dependent DA activation of MAP kinase transcription was observed in ^[WT]D₂R and ^[Gprot]D₂R but absent in ^[\betaarr]D₂R and ^[D80A]D₂R. Probing ERK phosphorylation through western blot analysis revealed activation by ^[\betaarr]D₂R when compared to ^[D80A]D₂R or untransfected cells only when β -arrestin 2 is overexpressed (Figure 12C and 12D). In contrast, ^[Gprot]D₂R activated ERK phosphorylation regardless of β -arrestin expression,

when compared to ^[D80A]D₂R. This indicates that D₂R activates canonical MAP kinase activity through G proteins, while β-arrestin may produce non-canonical ERK activity under conditions of enhanced β-arrestin or kinase expression, as observed in other GPCR systems (176).

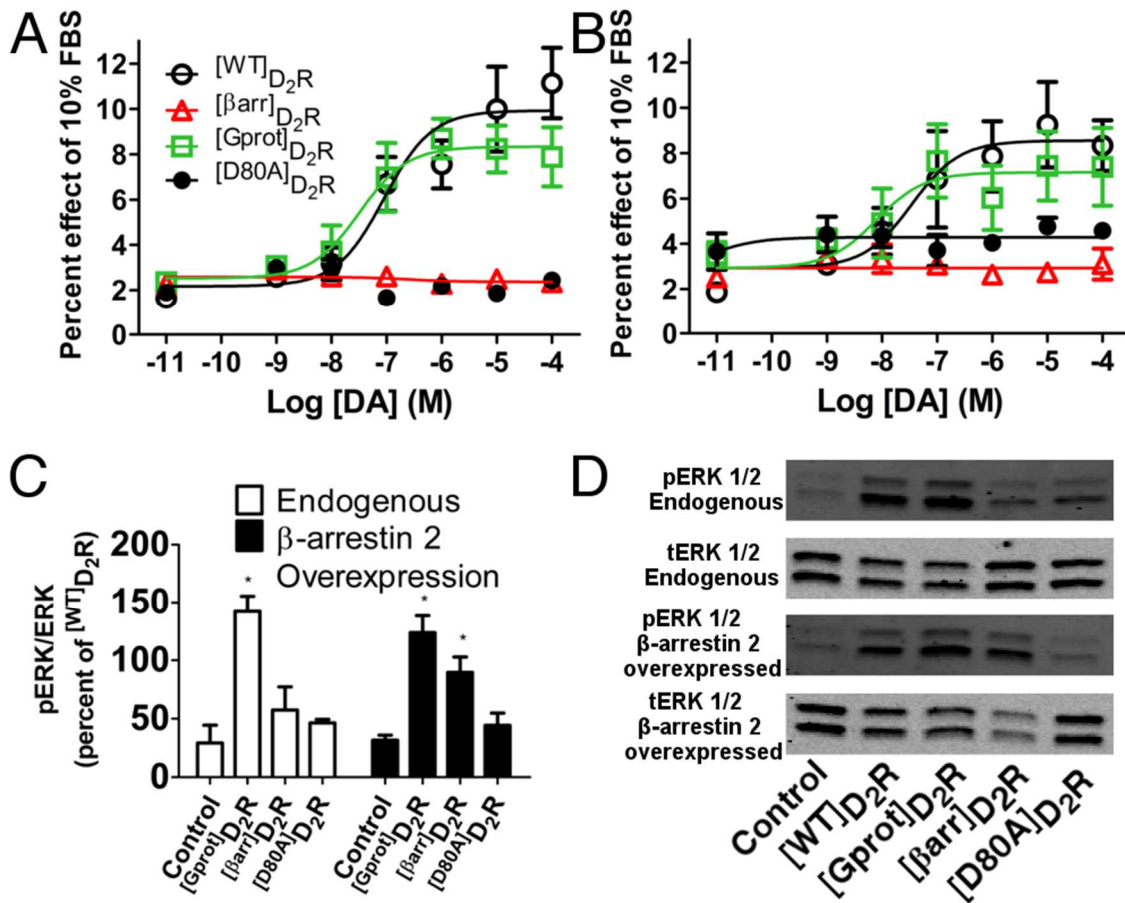


Figure 12: Assessment of MAP Kinase activity at D₂R. (A) SRF and (B) SRE MAP kinase transcriptional promoter mediated expression of luciferase (SEM, n=5-6 done in triplicate). (C) Traditional western blot analysis of ERK (*p<0.05 Newman-Keuls posthoc when compared to ^[D80A]D₂R or untransfected after one-way ANOVA p<0.05, SEM, n=3-6) with and without β-arrestin 2 overexpression. (D) Representative blot for the data presented in (C).

4.2 ^[Gprot]D₂R and ^[βarr]D₂R are biologically active and display functional differences

The biological activity and functional properties of ^[Gprot]D₂R and ^[βarr]D₂R were tested with a virally mediated *in vivo* overexpression approach. Adeno-associated viral (AAV) vectors containing a double-floxed inverted open reading frame (DIO) of each HA-tagged D₂R transgene driven by the housekeeping gene EF1α promoter (177) were synthesized (Figure 13A). Each D₂R construct was injected bilaterally into the dorsal striatum (caudate putamen) and the ventral striatum (nucleus accumbens) (Figure 13B). Extent of viral transduction was assessed by staining for the HA epitope tag on the N-terminus of D₂Rs (Figure 13C). Neuronal specificity of expression was achieved using the Adora2a-Cre mouse line, which selectively expresses Cre in D₂R-expressing medium spiny neurons (MSNs), but not presynaptic DA projection cells (178), and these Adora2a-Cre mice were also crossed to a mouse strain with β-arrestin 2 floxed to allow for specific deletion of β-arrestin 2 in indirect pathway MSNs. ^[WT]D₂R, ^[Gprot]D₂R, ^[βarr]D₂R or ^[D80A]D₂R yielded a two- to four- fold increase in striatal D₂R expression as measured by radioligand binding (Figure 13D, expression in Adora2a-Cre and Figure 13E, expression when β-arrestin 2 is genetically deleted). Overexpression of the ^[WT]D₂R lead to a ~1.5 fold potentiation in the amphetamine induced locomotor response (Figure 13F). ^[βarr]D₂R overexpression lead to a similar potentiation while the ^[Gprot]D₂R overexpression was much less effective. However, in order to demonstrate construct validity, the same experimental design was carried out in Adora2a-Cre::β-arrestin 2^{FLOX/FLOX} mice. As

shown in Figure 13G, while overexpression of ^[G^{prot}]D₂R produced a slight increase in the amphetamine response, the robust increase previously observed with both ^[WT]D₂R and ^[β^{arr}]D₂R was completely absent. Note the differences in baseline responses to amphetamine between Figure 13F and 13G as these mice are on a different background. This suggests that the enhanced amphetamine response of ^[β^{arr}]D₂R is dependent upon β-arrestin 2. These findings demonstrate that the functionally selective engineered D₂R mutants are biologically active *in vivo* and mediate distinct functions.

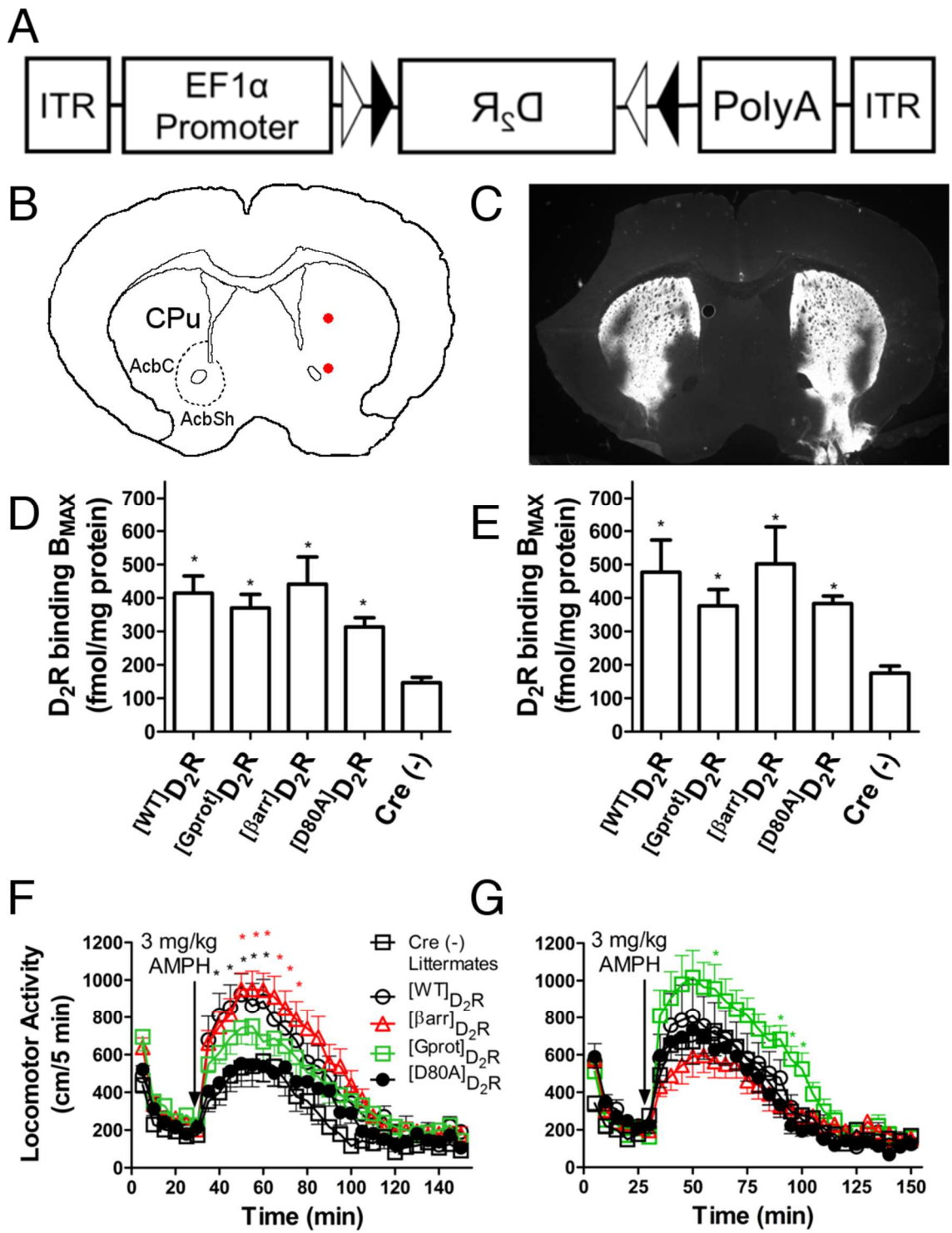


Figure 13: The physiological relevance of D₂R functional selectivity. (A) Viral transgene packaged into AAV, which allowed for Cre-dependent expression of D₂R through a double-floxed inverted open reading frame (DIO). (B) 0.75 μ L of virus was injected bilaterally into the dorsal and ventral striatum with each injection site indicated by the red dots, and a total of 3 μ L was injected into the striatum of each mouse. CPu: caudate putamen; AcbC: nucleus accumbens, core; AcbSh: nucleus accumbens, shell. (C) Representative staining pattern of the N-terminal HA tagged D₂R shows transduction of a majority of the dorsal striatum and at least 50% of the ventral striatum with variable transduction in the olfactory tubercle. Radioligand binding revealed a two- to four-fold overexpression of each receptor as determined from membranes prepared from striatal dissections from Adora2a-Cre (D) and Adora2a-Cre:: β -arrestin 2^{FLOX/FLOX} (E) mice (*p<0.05 Newman-Keuls posthoc when compared to Cre (-) controls after one-way ANOVA p<0.05, SEM, n=4-6). (F) Potentiation of amphetamine-induced locomotion in mice when D₂R is overexpressed (*p<0.05 bonferroni posthoc when compared to ^[D80A]D₂R after repeated measures two-way ANOVA p<0.05 for receptor expression type SEM, n=11-12, color coded for receptor type). (G) The amphetamine response potentiation of ^[WT]D₂R and ^[β arr]D₂R is abolished when β -arrestin 2 is genetically deleted from D₂R-expressing medium spiny neurons (*p<0.05 bonferroni posthoc when compared to ^[D80A]D₂R after repeated measures two-way ANOVA p<0.05 for receptor expression type SEM, n=8-13).

5. Application of functional selectivity principles to diverse receptor systems

Functional selectivity allows for the design of more effective therapeutics at previously identified receptor targets. D₂R serves as one of the prototypical GPCRs to exhibit functional selectivity. However, many principles of functional selectivity and D₂R contextual activation remain to be fully elucidated. The approaches presented in previous chapters will be applied here to begin to address functional selectivity in diverse receptors types and more complex D₂R neuronal systems.

5.1 Evolutionary Action at related but diverse GPCRs

Evolutionary Trace (ET) is a powerful method to predict residues that will generate phenotypes when guided by the robust predictive value of Evolutionary Action. ^[G_{prot}]D₂R and ^[β_{arr}]D₂R were generated through iterative rounds of mutagenesis screening for specific phenotypes (retention and loss of G protein or β-arrestin signaling). Therefore, the residues determined to confer functional selectivity to D₂R could be used to generate functionally selective mutants in other GPCRs, because ET predicted residues are conserved across all known sequences of Rhodopsin-like GPCRs. In order to test the feasibility of this approach, GPCRs with diverse genetic and signaling profiles were selected (Figure 14).

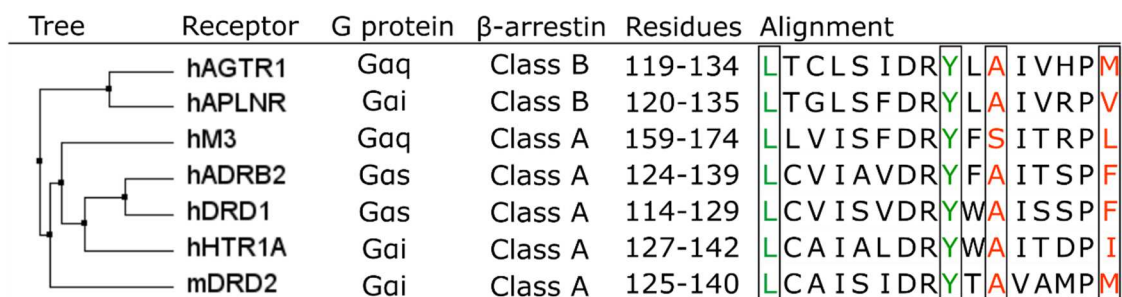


Figure 14: Evolutionary Trace at pharmacologically and genetically diverse GPCRs for the generation of functionally selective mutants. hAGTR1 (human angiotensin receptor), hAPLNR (human apelin receptor), hM3 (human muscarinic type 3 receptor), hADRB2 (human β -adrenergic receptor, type 2A), hDRD1 (human dopamine D1 receptor), hHTR1A (human serotonin type 1A receptor), and mDRD2 (mouse D₂R) GPCRs were chosen based on genetic diversity (Tree calculated from % identity), as well as G protein (Gaq, Gai or Gas) and β -arrestin coupling (Class A: transient β -arrestin interaction, Class B: robust β -arrestin interaction) profiles. The alignment of the twenty residues surrounding the DRY motif was the basis of the tree presented, and ^[G_{prot}]D₂R is color coded as green residues while ^[β arr]D₂R is red.

The analysis of these diverse receptors shows that L3.43 and Y3.51 do not vary, while A3.53 only varies with the M₃R (hM3) to serine while M3.58 varies greatly among these GPCRs. While each particular residue was chosen based on the residues identified from the generation of ^[G_{prot}]D₂R and ^[β arr]D₂R, the same substitutions would not necessarily result in the same profile of functional selectivity. This is due to two important features in the D₂R mutagenesis program: 1) the impact of mutations on phenotype (harshness) was predicted based on conservation relative to D₂R, and 2) the degree of harshness was determined by retention of G protein or β -arrestin activity at D₂R. Thus, Evolutionary Action was once again used to determine those residues that would most likely produce a phenotype, and different substitutions with varying

degrees of predicted harshness were calculated (Table II). The EA predictions yielded the same predicted substitutions for each receptor at L3.43 and Y3.51 because of the remarkable conservation of these residues across GPCRs.

Table II: Evolutionary Action predicted functional selectivity phenotype mutations in diverse GPCRs. Receptors presented in Figure 14 are predicted for mutations at the ^[G_{prot}]D₂R (L3.42 and Y3.51) and ^[β_{arr}]D₂R (A3.53 and M3.58) residues. Predicted harshness on phenotype is displayed from left to right.

Residue (WT)	Receptor	Mutation		
L3.43	hAGTR1	W	S	R
	hAPLNR	W	S	R
	hM3	W	S	R
	hADRB2	W	S	R
	hDRD1	W	S	R
	hHTR1A	W	S	R
Y3.51	hAGTR1	M	S	D
	hAPLNR	M	S	D
	hM3	M	S	D
	hADRB2	M	S	D
	hDRD1	M	S	D
	hHTR1A	M	S	D
A3.53	hAGTR1	S	L	E
	hAPLNR	S	L	E
(S)	hM3	A	L	E
	hADRB2	S	L	E
	hDRD1	S	L	E
	hHTR1A	S	L	E
M3.58	hAGTR1	V	K	G
	hAPLNR	M	Q	E
(V)	hM3	V	Q	E
(L)	hADRB2	L	S	E
(F)	hDRD1	M	T	E
(I)	hHTR1A	F	H	E

5.2 A roadmap to universal functional separation

Mutating the residues from ^[G_{prot}]D₂R and ^[β_{arr}]D₂R in other GPCRs represents a means by which functionally selective mutant receptors that retain most of the normal

functions of the wild type receptors might be generated. Some of the mutations presented in Table II were generated and tested for their G protein and β -arrestin activities (Figure 15).

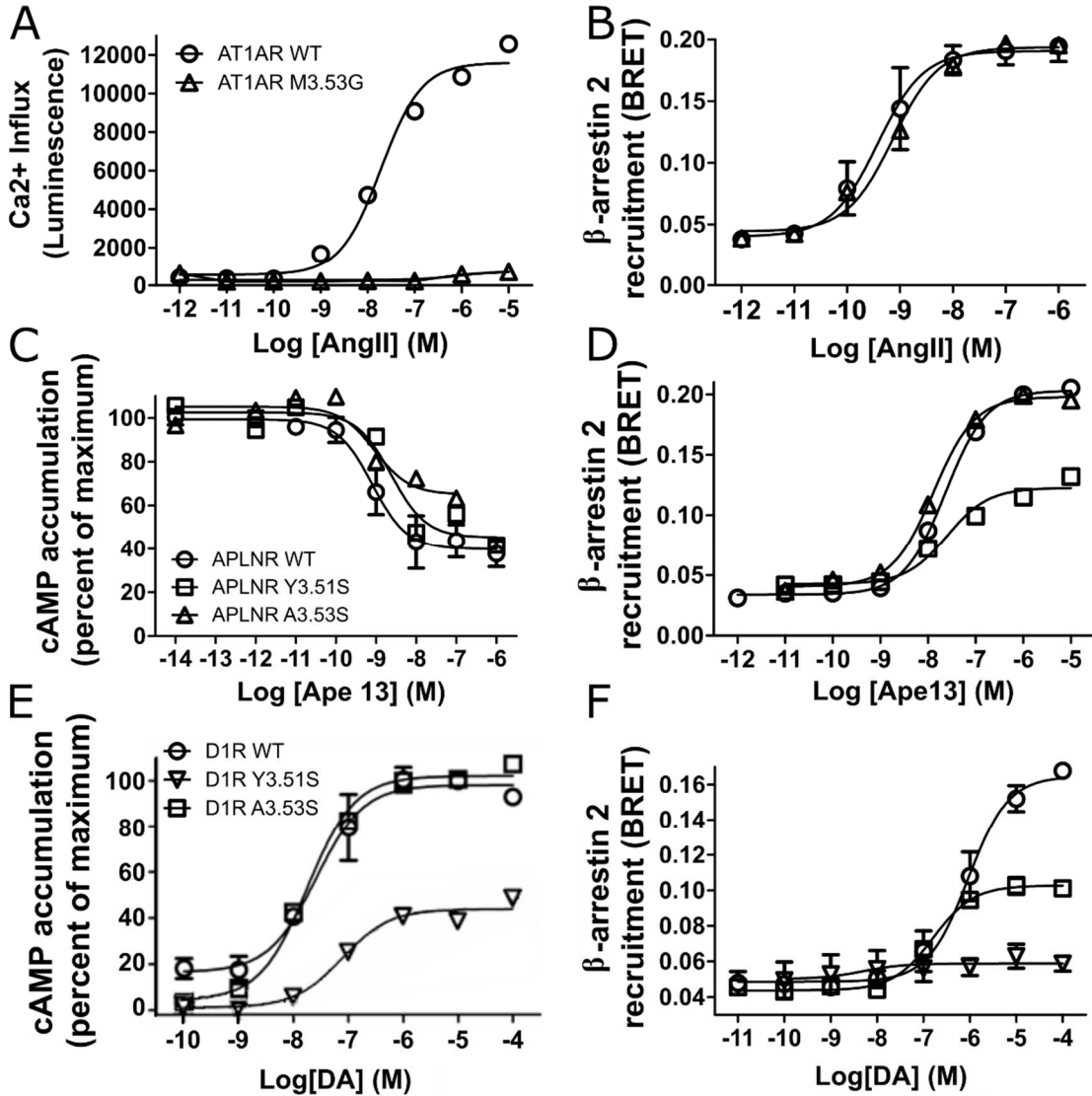


Figure 15: Achieving functional selectivity in GPCRs with diverse pharmacological and genetic profiles. (A) Cytosolic influx of Ca²⁺ as determined by the aequorin assay shows AT1AR M3.53G mutation completely abolishes G protein activity, while (B) β -arrestin 2 recruitment as determined by BRET remains intact. For the apelin

receptor (APLNR), $G_{\alpha i}$ activation as determined by inhibition of isoproterenol induced cAMP increase (**C**) is intact for Y3.51S but slightly decreased for A3.53S. In contrast, β -arrestin 2 recruitment (**D**) is intact for A3.53S but not Y3.51S. Finally, for D_1R , Y3.51S showed partial agonist activity at $G_{\alpha s}$ mediated cAMP accumulation as measured by GloSensor (**E**) and A3.53S showed full activity. While at β -arrestin 2 recruitment (**B**), Y3.51S had no activity while A3.53S showed partial activity, which means that both mutations display bias for the G protein pathway.

Many of the mutations proposed in Table II were generated and tested.

However, many of these mutations did not produce relevant signaling profiles (loss of activity at both pathways) or were not profiled at each signaling pathway. Nevertheless, the data presented in Figure 15 shows striking patterns of bias achieved. First, β -arrestin bias was achieved at AT1AR with high pharmacological fidelity from only a single harsh point mutation (M3.58G, Figure 15A and 15B). As shown in Table I, the residue change in $^{[\beta arr]}D_2R$ (M3.58D) was also predicted to produce a harsh phenotype. However, this single point mutation did not completely abolish G protein signaling (Figure 4).

Surprisingly, this same residue change was used to generate a biased ghrelin receptor (179). For the apelin receptor, some residues that produced bias at D_2R produced the same quality of bias, albeit with different changes. The mutation at Y3.51 to the mild predicted phenotype Ser (as opposed to Lys in $^{[G prot]}D_2R$) caused a ~50% reduction in β -arrestin recruitment (Figure 15D) and no appreciable shift in G protein activity (Figure 15C). In contrast, A3.53 when mutated to the weak predicted phenotype Ser (as opposed to Arg in $^{[\beta arr]}D_2R$) yielded a slight decrease in G protein activity (Figure 15C) and no change in β -arrestin 2 recruitment (Figure 15D). Thus, these mutations produce weak G

protein and β -arrestin bias at the apelin receptor, respectively. Finally, at D₁R bias was achieved in unexpected ways. The Y3.51S mutation generated a ~50% decrease at G protein activity (Figure 15E) and an almost complete ablation of β -arrestin activity (Figure 15F). In contrast, A3.53S (a critical residue in generating both [β arr]D₂R and [$\tau/2$]D₂R) yielded no change in G protein activity (Figure 15E) and a ~50% reduction in β -arrestin activity (Figure 15F), which surprisingly indicates that this mutation is also G protein biased. However, the quality of the G protein bias is very different, a phenomenon that is explored in Chapter 3 with the comparison of [Y^{14}]D₂R and [G^{prot}]D₂R in Figure 7 as well as the generation of partial biased D₂R mutants in Figure 8.

Figure 15 demonstrates the feasibility of generating biased GPCRs in diverse systems, and Table II presents a starting point that is likely to generate fruitful data without expending vast resources. In order to achieve robust separation of signal at other GPCRs more complex experimental manipulations would be necessary. This could include strategies such as generating all 19 permutations at a particular likely candidate residue or combining mutations in unexpected combinations (such as D₁R A3.53S with Y3.51S, a combination that should produce G protein bias but could not be predicted from ET/EA or the D₂R data sets). More complete data sets produced for even more diverse GPCRs will allow for deciphering universal patterns of functional activity and be incredibly powerful in understanding and manipulating GPCR signal transduction.

5.3 D₂R neuronal subtype expression dictates functional selectivity

The overexpression strategy presented in Chapter 5 yielded direct evidence that the activities of both [Gprot]D₂R and [βarr]D₂R are physiologically relevant in indirect pathway medium spiny neurons. However, as presented in Figure 2, the pleiotropic actions of D₂R can be attributed to both the biochemical diversity and heterogeneous neuronal expression in the central nervous system. Therefore, the actions of D₂R were assessed using the D₂R^{FLOX/FLOX} mouse which allows for cell-type specific deletion of D₂R and viral reexpression of biased D₂R mutants.

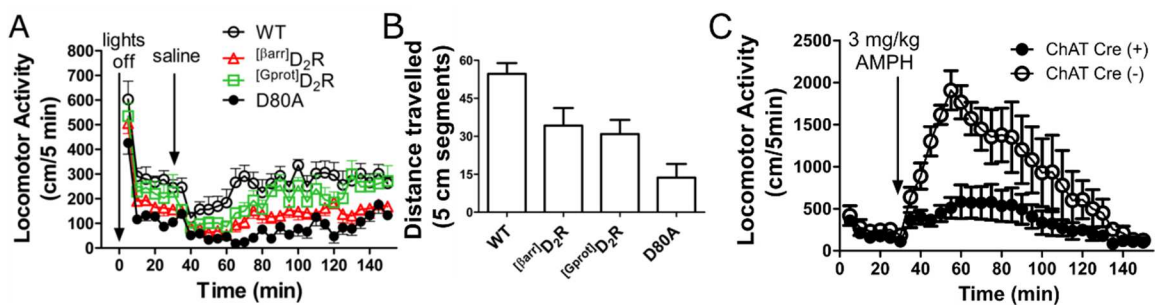


Figure 16: Dissection of diverse D₂R-expressing neuronal subpopulations. D₂R^{FLOX/FLOX}::Adora2A-Cre induces genetic deletion of D₂R and reexpression (using the same injection scheme in Figure 13) of each mutant D₂R. Assessment of (A) basal locomotor activity at the beginning of the night cycle (lights off) and (B) motor coordination with the beam walking assay. (C) D₂R^{FLOX/FLOX}::ChAT-Cre has D₂R deleted only from cholinergic interneurons which causes a major deficiency in the amphetamine locomotor response but not the basal/habituation locomotor phase.

The D₂R^{FLOX/FLOX} mouse was crossed to the same Adora2A-Cre presented in Chapter 4, and underwent the same viral injection surgery in order to achieve D₂R genetic replacement (deletion since birth and reexpression in adulthood in indirect

pathway MSNs). Deletion of D₂R from these indirect pathway neurons has previously been shown to cause loss of basal locomotion and motor coordination (131). The reexpression of ^[WT]D₂R rescued both basal locomotor activity (Figure 16A) as well as motor coordination (Figure 16B) when compared to ^[D80A]D₂R. Surprisingly, the biased mutants showed striking separation of function, especially when compared to the amphetamine response seen in the overexpression strategy (Figure 13). In contrast to those observations, ^[Gprot]D₂R mirrored the ^[WT]D₂R for basal locomotion, while ^[βarr]D₂R was not different from ^[D80A]D₂R (Figure 16A). Additionally, neither receptor fully rescued motor coordination but neither receptor was completely inactive at rescuing motor coordination (Figure 16B). Taken together, these data demonstrate an unpredicted role for G proteins in D₂R's control of locomotion in the indirect pathway and point toward a component effect for G proteins and β-arrestins in the control of coordination in these same neurons.

Finally, as discussed previously, D₂R functions as a postsynaptic receptor in GABAergic MSNs, cholinergic interneurons as well as cortical pyramidal and interneurons (180). Therefore, the D₂R^{FLOX/FLOX::ChAT-Cre} mouse was generated to delete D₂R from the population of cholinergic interneurons (which are predominantly in the striatum). This deletion caused a remarkable effect that is unique from any other D₂R genetic model: a reduction in the amphetamine response (Figure 16C) without an appreciable effect on basal locomotion. This is a distinct and unappreciated role for D₂R-

expressing interneurons that has profound implications for functional selectivity based D₂R pharmacotherapies.

6. Discussion

DA is an important regulator of both CNS and peripheral physiological homeostasis. Disruptions in the function of DA have been associated with schizophrenia, depression, mania, attention deficit disorders, drug abuse and Parkinson's disease in the CNS and hypertension and prolactinemia in the periphery (181). DA exerts its function through two major GPCRs: D₂R and D₁R (as well as the D₁R-like D₅R and D₂R-like D₃R and D₄R receptors which are expressed at lower levels). The results described here provide a functional template to begin to investigate the pharmacological, biochemical and neuronally selective actions of D₂R and how to apply these principals to other receptors. Precise molecular control was achieved by engineering D₂Rs specifically designed to interact with either G proteins or β -arrestins and these receptors can be reconstituted in cell culture or in specific neuronal populations *in vivo*.

Over the last several years, state of the art optogenetic (182) and pharmacogenetic (183) approaches have been developed to map brain pathways and cellular functions of neuronal populations. However, these approaches are not amenable to the elucidation of molecular mechanisms because they are not designed to manipulate the specific biochemical mechanisms of an endogenous ligand through its cognate receptor. Additionally, optogenetic or pharmacogenetic control of intracellular signaling cascades, such as G proteins (184) or ERK (185), do not allow for the interrogation of

endogenous ligand dynamic changes or the impact of therapeutics to the system.

Understanding the biology of D₂R will require determinants such as the contextual influence of phasic and tonic DA release (149) and the monitoring of therapeutics, such as antipsychotics. Although less widely applicable, functionally selective mutant GPCRs are a desirable alternative as they resolve many of the limitations of the more general approaches.

Previously, biochemical studies in mice carrying complete deletion of β -arrestin 2 (67) or cell type specific genetic deletion of GSK3 β (68) have provided evidence for the importance of the β -arrestin 2-mediated D₂R signaling pathway in the actions of DA. However, evidence from such studies is limited by the fact that β -arrestin 2 interacts with multiple GPCRs and GSK3 β is a signaling hub downstream of multiple signaling networks, including both G proteins (186) and β -arrestin 2 (67). The current *in vivo* approach more specifically targets D₂R and these pathway specific mutant D₂R were developed to begin to elucidate the contribution of individual pathways to physiological and pharmacological DA responses. Biased mutants in other GPCRs like the β 2-adrenergic (T69F Y133G Y209A) and angiotensin 1A (DRY 131-133 AAY) receptors (162, 187) generated unstable proteins when engineered into D₂R. Additionally, several D₂R mutants have also been generated and shown to affect β -arrestin and GPCR kinase interactions (64, 71), post-endocytic trafficking (62), desensitization (63), and resensitization (188). While these various D₂R mutants have informed various aspects of

function and regulation of D₂Rs, consideration of some of these mutants for the work described here did not fulfill all necessary inclusion criteria.

GPCR bias is operationally defined by the degree of engagement of a given signaling pathway. It is clear that ^[Y1V]D₂R and ^[Gprot]D₂R both share G protein bias, however the quality of bias differs, depending on their operational definition. For example, in some cases it may be beneficial to retain all of the G protein activity, while in others it may be crucial to abolish all β -arrestin recruitment at the sacrifice of some G protein activity. In fact, ^[Y1V]D₂R was mutated to contain fewer alanine substitutions which resulted in full G protein activity and partial β -arrestin activity (170). Nevertheless, ^[Y1V]D₂R and ^[Gprot]D₂R were used to dissect D₂R-mediated ERK phosphorylation (Figure 12) and (71) and both mutants yielded a similar conclusion: that D₂R-mediated ERK phosphorylation is largely G protein mediated.

Operational consistency allows for meaningful conclusions about D₂R signaling pathways to be drawn. The partial agonist activity of aripiprazole has raised the possibility that complete blockade of D₂R is not necessary to impart antipsychotic efficacy (189). This partial agonism allows for effective targeting of G protein or β -arrestin pathways (102). However, the causal relationship of partial agonism and biased partial agonism (as opposed to partial antagonism) has not been explored. The ^[τ /2]D₂R mutants described here are tools that allow for operationally defined agonism that is consistent, robust and specific. Coupled with viral expression technologies and

neuronal-specific Cre expressing lines, it will now be possible to test various hypotheses of D₂R partial agonism in intact biological systems and preclinical disease models.

While receptor manipulation is desirable to demonstrate causal relationships, biased ligands provide valuable insight and are a more reasonable avenue toward therapy development. However, precise details and principles governing ligand action remain elusive. Here, the phenomenon of agonist texture (173) is demonstrated with [Gprot4PM]D₂R. As previously observed, full agonists can stabilize different receptor activation states that have functional consequences (173). Therefore, functional selectivity could occur from the loss of function at one pathway or it could be thought of as a gain of new receptor activity. This phenomenon represents a valuable conceptual framework for a fundamental property of receptor activation that is relevant to functional selectivity.

Intracellular signal transduction proteins are key elements in dictating bias. Their interactions with receptors dictate agonist efficacy (117) and targeting their activation with biased agonists is an avenue by which already validated receptor targets can be leveraged for improved therapies. Here, the related desensitization allosteric modulators (β -arrestin 1, β -arrestin 2, and GRK2, Figures 6B, 11A and 11B) were shown to fall into a common activation family using [β arr]D₂R. This indicates that more detailed (but less well characterized) elements of D₂R's β -arrestin signaling arm remain intact for [β arr]D₂R, such as barcoded phosphorylation patterns (61) and other posttranslational modifications

(190). Additionally, related allosteric modulators (different G proteins, Figure 11C and 11D) remained inactive at each mutant receptor, which indicates that none of the mutants have a gross abnormal gain of function.

Interactions with small molecule allosteric modulators are also exciting avenues by which functional selectivity can be modulated. Sodium, an intracellular GPCR allosteric modulator, remains intact in both $^{[G^{prot}]D_2R}$ and $^{[\beta^{arr}]D_2R}$, indicating that both G protein and β -arrestin activation require dynamic sodium regulation. However, allosteric biased ligands may confer functional selectivity by exploiting the recently solved extracellular vestibule (97) to generate noncompetitive negative or positive allosteric modulators (191) or bitopic ligands (192).

The pharmacological fidelity (trafficking, ligand binding and signal transduction) of $^{[G^{prot}]D_2R}$ and $^{[\beta^{arr}]D_2R}$ revealed robust and specific engagement of each pathway. Through sequential iterations (Figure 4) each mutation converged on transmembrane domain three (TM3), an alpha helix critical for the transmission of conformational changes from ligand binding to signaling molecules (193). These changes in signal transduction allowed for the elucidation of complex signaling paradigms. MAP kinase cascades have previously been shown to be activated downstream of G proteins and β -arrestins (25, 26) but as shown here, $^{[G^{prot}]D_2R}$ is responsible for a major component of the ERK signaling cascade with the normal complement of kinases and β -arrestins present in HEK 293T cells. However, overexpression of β -arrestin 2 revealed the ability

of $^{[\beta\text{arr}]}$ D₂R to couple to ERK. It is interesting to note that while $^{[\text{Gprot}]}$ D₂R did not significantly enhance the transcriptional activity, there was a small potentiation in pERK observed when compared to $^{[\text{WT}]}$ D₂R. Taken together, these data indicate that receptor transducer elements, such as MAP kinases, may also exhibit functional selectivity (in this case the activating phosphorylation induced by β -arrestin is functionally distinct from the G protein mediated transcriptional activity).

Finally, to assess the *in vivo* function of the engineered receptors a neuronally selective overexpression approach was used, which admittedly carries the caveat of assessing function in the presence of the normal signaling of endogenous receptors. Despite this limitation, expression of mutant D₂Rs in D₂R+MSNs (indirect pathway, Adora2A+) was able to reveal marked differences in their ability to affect responses to the psychotropic drug amphetamine. Interestingly, $^{[\beta\text{arr}]}$ D₂R was more effective at enhancing the amphetamine response than $^{[\text{Gprot}]}$ D₂R. Although the extent of the separation was surprising, it is consistent with previous genetic manipulation studies, which have predicted an important role for the D₂R/ β -arrestin 2 pathway *in vivo* as genetic deletion of β -arrestin 2 has been shown to decrease the locomotor response to amphetamine (67, 123). Interestingly, $^{[\text{Gprot}]}$ D₂R only slightly potentiated the amphetamine response and this trend was enhanced by genetic deletion of β -arrestin 2 in D₂R expressing MSNs. In contrast, $^{[\text{WT}]}$ D₂R and $^{[\beta\text{arr}]}$ D₂R lost their potentiation of the amphetamine response when β -arrestin 2 was deleted. These data demonstrate the

complexity of even basic GPCR signaling events, and should allow for insights into the pleiotropic actions of the endogenous neurotransmitter.

In summary, functionally selective or biased signaling engineered GPCRs can display *in vivo* biological activity and mediate distinct pharmacological responses. The robust separation of signal achieved with ^[Gprot]D₂R and ^[βarr]D₂R will allow for direct elucidation of more complex functional selectivity principles when applied to diverse D₂R systems. These mutants differ from ^[WT]D₂R by only two amino acids and yet have specific D₂R functions disrupted. Functional selectivity has considerable therapeutic potential but the molecular details have been obscured by the complexity of receptor activation. Furthermore, some signaling events can only be understood in the context of the *in vivo* architecture (131). ^[Gprot]D₂R and ^[βarr]D₂R are unique tools that should allow for a better understanding of the molecular, cellular and physiological actions of dopamine, as well as provide a template for the development of small molecules with therapeutic predictive value.

6.1 Future Directions

The overall goal of this dissertation was to disassemble and reassemble D₂R's pleiotropic functions. This goal was necessitated by the unique challenges presented by GPCR signal transduction: a small molecule can permeate an entire organism yet still have specific actions. Thus, the concept of functional selectivity is a framework by which the nature of receptors can begin to be understood. While the present work

demonstrates how D₂R signals as a pleiotropic conduit of extracellular messages, there are many challenges that remain. Undertaking these challenges is crucial in developing a better understanding of the mechanisms of D₂R biology which allows for the design of more effective therapies.

GPCRs are the target of a majority of pharmaceuticals (194) therefore, the understanding of their unique capacity for pleiotropic signaling pathways through G proteins and β -arrestins represents an avenue by which novel pharmaceuticals could be developed for existing targets. Evolutionary Trace is an algorithm that is dependent upon sequence conservation and because GPCRs comprise 5% of the human genome (and more for other mammals) there is a rich set of sequences and now structures available to build precise predictions. In Chapters 3 and 5 the data set developed in Figure 4 was used to predict defined signaling mutants in D₂R and other GPCRs. These data show that more robust and specific mutants can be generated for virtually any GPCR, depending on the biological question. Furthermore, because these sequences are related by ET predictions they are comprised of only minor variations. For example ^[Gprot4PM]D₂R is comprised of mutations of residues that were used to generate the β 2AR-TYY mutant, and ^[Gprot]D₂R, ^[\betaarr]D₂R, ^[\tau/1.5]D₂R and ^[\tau/2]D₂R are all variations of the same four amino acids (L3.43, Y4.51, A3.53, and M3.58). This feature of the mutations is important for disrupting specific actions in complex systems. For instance, if the effect of the strength of partial agonism at D₂R was tested by knocking in the ^[\tau/1.5]D₂R and ^[\tau/2]D₂R,

any phenotype could be attributed to the difference of a single hydroxyl group, the difference between Tyr ($[\tau/1.5]D_2R$) and Phe ($[\tau/2]D_2R$).

Such rich translations from *in silico* and *in vitro* predictions to complex physiological systems warrant a more rigorous mechanistic analysis of how these residue changes induce bias. Some of the pioneering structural work in GPCRs have allowed for incredible detail for G protein (161) and β -arrestin (167) coupling. While D_2R has yet to be crystallized, the biased mutants are excellent candidates for understanding how the receptor transmits G protein and β -arrestin activities. An alternative approach would be to translate D_2R mutations to β_2AR or rhodopsin and utilize the robust crystallography protocols already developed for these mutants. This structural insight could lead to more specific molecular dynamics simulations (98, 195) which in turn could yield better predictions for more specific mutations, as the impact of changes could be simulated.

Preclinical models of psychiatric and neurological disorders have offered predictive and causal relationships for treatments in humans. The dopaminergic system has provided a rich translation because the fundamental architecture of the basal ganglia is similar between mice and humans, and the movement phenotypes are robust and easily assessed. The viral overexpression (Chapter 4.2) and reexpression (Chapter 5.3) strategies was designed to be iterative to adapt to any unforeseen caveats (such as unexpected signaling profiles of the mutants in neurons as opposed to HEK cells).

However, this versatility is cumbersome when applied to more complex behavioral assays of the dopaminergic system, such as social interaction, anxiety, or assessment of positive and negative responses to stimuli. The complexity of D₂R's genetic and neuronal architecture make any simple solution difficult to reconcile. For instance, ectopic, Cre-dependent expression of D₂R cDNA would lose splicing and receptor levels would be inherently inaccurate because of the use of exogenous promoters, while a knock-in approach would lose cell type specificity.

A knock-in would provide a top-down approach for studying these complex behavioral states. However, as demonstrated with the D₂R^{FLOX/FLOX}::ChAT-Cre data (Figure 16C) a unique response is generated that is distinct from the D₂R-KO mice (131) as well as models of D₂R deletion from indirect pathway neurons (123). Deletion of D₂R from the interneurons only affects amphetamine-induced locomotion and not basal locomotion (whereas D₂R-KO affects both responses). It should be noted that a viral reexpression strategy was not feasible with these mice, as ChAT-Cre is expressed in all cholinergic interneurons, but all cholinergic interneurons do not express D₂R. This strategy produced ectopic D₂R expression and generated uninterpretable data, most likely due to D₂R expression in the caudal areas of the striatum and adjacent structures such as the amygdala. Therefore, an intersectional approach (such as D₂R-Flp::ChAT-Cre::D₂R^{FLOX/FLOX} injected with a Flp and Cre dependent viral construct expressing mutant D₂R) would be necessary to dissect functional selectivity in interneuron control

of amphetamine induced locomotion. This approach is feasible, albeit cumbersome and time consuming.

All of these considerations have led to the development of a complex knock-in strategy in which multiple recombination events are used to knock-in the mutant D₂R exons into the endogenous locus. Such an approach would ideally provide: 1) cell type specific activation using previously characterized BAC-driven Cre lines (178) 2) retention of D₂R splicing because the endogenous locus and introns are intact, and 3) time regulated activation using DOX/tTA transcriptional control (196) of expression of a Flp recombinase (197). A strategy that satisfies all of these considerations is presented in Figure 17. While it could be argued that this particular strategy is overly complex, the approach is designed to allow for facile generation of mice (only two transgenes and one injection of DOX is required) as well as the design of experiments that utilize pairwise comparisons (before and after DOX treatment in one individual mouse). This important feature allows for powerful conclusions to be drawn, for instance a test could be designed in which the mouse is trained to receive a reward or interact with a social partner and the effect of the β -arrestin signaling pathway could then be examined after DOX treatment. However, with the complex design there are many points of failure, such as inappropriate/inefficient splicing. To address this, differential fluorophores monitor which receptor isoform is present, and radioligand binding experiments

performed on a mouse crossed to a ubiquitous Cre would ensure normal D₂R expression.

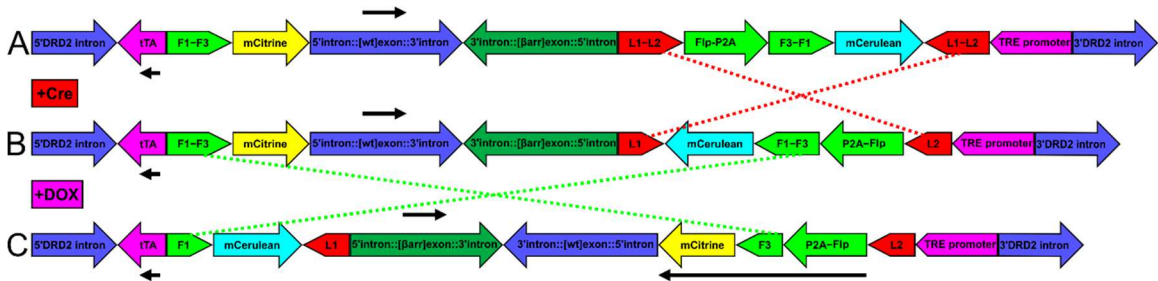


Figure 17: Potential inducible mouse knock-in construct design. This design relies upon expression of the DOX inducible tTA transcription factor and Flp recombinase from the introns of the endogenous DRD2 gene (polyadenylation and promoters abridged for simplicity). (A) tTA and the ^[WT]D₂R exon are expressed in normal cells (restricted by the endogenous DRD2 expression pattern). (B) Mouse crossed to Cre expressing lines orients Flp recombinase Cerulean expression cassette that is not active until (B) addition of DOX drives Flp::P2A::GFP (cerulean or citrine), and Flp recombinates ^[WT]D₂R exon to ^[βarr]D₂R exon (with cerulean or citrine serving as reporters of recombination).

6.2 Outlook and Impact

Functional selectivity is a complex process derived from the receptor's function as a conduit of extracellular messages to redistribute the intracellular signaling components through the law of mass action. Here, this redistribution was manipulated, rigorously assessed, and applied to diverse functional systems. While many questions remain regarding the physiological impact of functional selectivity, many of the previous conundrums have been solved with this work. When this project began, it was not clear that any GPCR could retain full agonist activity at G protein activation while losing all of its β-arrestin activity (and of course, vice versa) through mutagenesis, biased ligands, or cellular manipulations. In preliminary experiments, the

administration of pertussis toxin completely abolished G protein activity, while also reducing β -arrestin activity by close to 50% (presumably due to inactivity of GRK2/3). The work presented here was a tremendous effort to generate clear evidence and demonstrate causal relationships for functional selectivity at D₂R. While much work remains to be done before these data can be applied to the design of novel therapeutics, it is clear that biased ligands based on functional selectivity principles have the potential to yield a more effective standard of care for dopamine related disorders.

7. Materials and Methods

7.1 Evolutionary Trace

Multiple rounds of ET-guided mutagenesis were conducted on D₂R. Each round took advantage of enhancements to the Evolutionary Trace method and GPCR crystallography. The previously reported (162) β -adrenergic 2A receptor “TYY” served as a starting point for D₂R mutagenesis. β 2AR-TYY was previously shown to signal through β -arrestins but not G proteins. The first round targeted these homologous positions in D₂R (T69, Y133, and Y209). Based on the initial results of “TYY” mutations, new targets were added based on ET importance and structural location. Substitutions for targeted positions were based on homology in the multiple sequence alignment. In order for D₂R to be functional, mutations to cognate amino acids found in other GPCRs at the equivalent sequence position were selected.

Due to the variation in the GPCR loop regions, the transmembrane domains and loops were analyzed separately. The multiple sequence alignment of the transmembrane region was made up of 2512 Class A GPCRs. These sequences were gathered from GPCRDB, aligned, and filtered for the 195 gapless seven transmembrane helix residues. We used the updated pair interaction ET algorithm (piET) (155), which achieves greater accuracy by taking into account the residue contacts seen in a structure; here, the crystal structure of rhodopsin in complex with the C-terminus peptide of the endogenous G protein (160). The residues targeted for mutation were selected based on their

evolutionarily importance (top 5%) and proximity to the C-terminus peptide (within 12 Angstroms, the residues in DRY and NPXXY motifs being ignored). The Evolutionary Action algorithm (163) was used to identify substitutions with varying harshness.

An analysis specific to D₂R was used to identify the key ET residues in the second intracellular loop region. The crystal structure of β 2AR in complex with G α s (161) was also used to narrow down to the crucial residues for G protein activation. The multiple sequence alignment for D₂R entire sequence (including loops) was made of 66 homologues extracted from a BLAST analysis of the NCBI Reference Sequence database where we filtered based on protein length (90% of the query protein) and sequence identity (>60%). This was to ensure we use the most relevant information for ET analysis. Substitutions for targeted positions were also identified with the Evolutionary Action algorithm.

7.2 Molecular Pharmacology

7.2.1 Mutagenesis PCR

The Agilent Technologies (Santa Clara, CA) QuikChange mutagenesis kit was used to carry out all mutagenesis according to manufacturer's instructions. Primers were designed as instructed, with the minimum amount of nucleotide changes required to achieve a mutation. Multiple point mutations were created by using the same primers for single point mutations on already mutated constructs. All constructs were confirmed to have no coding errors by sequencing.

7.2.2 Cell culture and transfections

HEK-293T (ATCC, Manassas, VA) cells were cultured and transfected as previously reported (75).

7.2.3 G protein activity

D₂R's ability to inhibit cAMP production was carried out as previously described (102) using the Promega (Madison, WI) GloSensor assay with minor modifications. D₂R was expressed at a mass of 1 µg of DNA (except where indicated) and the GloSensor construct was transiently transfected along with D₂R at a mass of 5 µg of DNA. The luminescence was quantified with the Mithras LB940 instrument with no wavelength filter between the cells and the photomultiplier.

7.2.4 Bioluminescent Resonance Energy Transfer

BRET was performed as previously described (75) with some minor modifications. GRK2-YFP or β-arrestin 1-YFP replaced β-arrestin 2-YFP, where indicated. Untagged GRK2 was overexpressed at a ratio of 2-fold higher than receptor, while β-arrestin 2-YFP was always kept at the maximum allowable expression.

7.2.5 Radioligand binding

[³H]-raclopride (Promega, Waltman, MA) binding was carried out as previously described (68). When sodium was removed, the salt was not replaced with any other ion in the buffer. Rluc counts were conducted on the same membrane preparations, the

same day that the ligand binding was carried out, using the same RLuc counting protocol as (75).

7.2.6 Confocal microscopy

HEK 293T cells were transiently transfected with YFP C-terminally tagged to D₂R and plated onto 5% fibronectin treated glass bottom culture dishes. The cells were cultured and imaged as previously described (198) with minor modifications. Cells were cultured for 24 hours post transfection and images were captured on live cells.

7.2.7 Receptor internalization assay

All D₂R constructs have an N-terminal triple HA-tag, and internalization was performed as previously described (169). Percent internalization was determined from unstimulated receptor expressing cells.

7.2.8 MAP kinase transcriptional activity reporter

The SRF and SRE transcriptional reporter was assessed as previously described (179) with minor modifications. The cells were transfected using the calcium phosphate method described here, with 1 µg of D₂R DNA and 5 µg of SRF or SRE reporter DNA. Finally, the cells were incubated in serum-free DMEM overnight rather than using serum replacement medium.

7.2.9 ERK phosphorylation by western blot

HEK 293T cells were transiently co-transfected with 2.5 µg of mutant D₂Rs or pcDNA (for untransfected control) and 1 µg of either pcDNA or β-arrestin 2-YFP (the

same BRET construct). After 24 hrs, cells were starved in serum-free DMEM, and 24 hrs later, cells were stimulated with 1 μ M quinpirole for 10 minutes. Then cells were lysed in ice-cold RIPA buffer containing protease and phosphatase inhibitor cocktails (Sigma). Lysates were blotted for p-ERK (Cell Signaling Technology, #9106) and total ERK (Cell Signaling Technology, #9102).

7.2.10 Alternative G protein signaling

$G_{\alpha s}$ activation was determined using the GloSensor assay described above. However, cAMP production was not induced by stimulation of endogenous $\beta 2AR$. $G_{\alpha q}$ was measured using the aequorin assay, as previously described (179).

7.3 Neuropsychopharmacology

7.3.1 Adeno-associated viral expression vectors

The triple HA-D₂R constructs had NheI and AscI sites cloned onto the 5' and 3' end of D₂R (respectively). This construct was ligated into the NheI and AscI sites of the pAAV-EF1a-DIO EYFP construct provided by the laboratory of Dr. Karl Deisseroth. The YFP was replaced with D₂R.

7.3.2 Adeno-associated virus production

The constructs were packaged into pseudotyped AAV 2/10 using the triple-transfection technique, as previously described (199), which produces helper free virus. The titer was determined to be approximately 1×10^{13} vector genome copies/ml for each virus.

7.3.3 Mouse lines

All mouse studies were conducted in accordance with the National Institutes of Health Guidelines for Animal Care and Use and with an approved animal protocol from the Duke University Animal Care and Use Committee.

7.3.4 Mouse stereotaxic injection for viral delivery

Mice were anesthetized under 1-2% isoflurane and the coordinates from bregma for striatal viral delivery were AP = +1.1 mm; ML = +/- 1.7 mm; and DV = -2.9 mm for dorsal and -4.0 mm for ventral striatum. 0.75 μ L of virus was injected into each site, for a total volume of 3 μ L/mouse. The mice were allowed to recover for 2-4 weeks and then behavioral experiments were performed.

7.3.5 Locomotor activity

The Accuscan activity monitor (Omnitech Electronics, Inc. Columbus, OH) was used to assess locomotor activity, as previously described (68).

7.3.6 Motor coordination

Motor coordination was assessed via the beam walking assay. Briefly, a 3 cm circumference wooden dowel is suspended approximately 1 meter from the ground with open sides but closed edges and roof. The mice were video recorded for 3 minutes and scored for crossings on 5 cm hashes on the beam. The mice were allowed to fall onto a cushioning below and were quickly reinstated to the beam. Number of falls were also recorded but not significant as it did not frequently occur. The data presented were for

mice assayed after basal locomotor and amphetamine locomotor assays in the same room.

7.3.7 HA-staining of virally transduced brains

Transduced brains were fixed by perfusion of the mouse and left overnight in 4% PFA in PBS. 30 μ M sections were collected by vibratome sectioning and stained by free-floating in 0.3% triton-X in PBS supplemented with 2% NGS and 3% BSA. The HA-antibody (3724, Cell Signaling) was diluted 1:1,000 and allowed to incubate overnight.

7.4 Data Analysis

Dose response curves were fit to the nonlinear regression curve $y = \text{Bottom} + (\text{Top} - \text{Bottom}) / (1 + 10^{-(\text{LogEC}_{50} - X)})$ for agonist curves and $y = \text{Bottom} + (\text{Top} - \text{Bottom}) / (1 + 10^{(X - \text{LogIC}_{50})})$ for antagonists in Graphpad Prism 5. Statistical tests were performed (described in Figure and Table legends) in Graphpad Prism 5. Binding curves were fit to $Y = B_{\text{max}} * X / (K_d + X)$. Bias quantification was carried out as previously described in (171) and (172). For bias plots (Figures 8D) the points were calculated from normalized (to ^[WT]D₂R) responses to the two assays and fit to a quadratic equation with the constraint that $B_0 = 0$. Each bias quantification used the same G protein activity when compared to endogenous and GRK2 overexpression data sets at β -arrestin. All values calculated in Tables III, IV, V, and VI were normalized to ^[WT]D₂R (or control receptors in Table VI) for each individual assay for efficacy but not potency. Tables III-VI presented

below present all of the calculations from dose response curves as well as statistical analyses performed.

Table III: Calculated values from Figure 6 and 12

	WT _{D2R}	[Gprot] _{D2R}	[βarr] _{D2R}	D80A _{D2R}
cAMP E _{MAX} (% of WT)	100 +/- 6.9	103 +/- 7.1	49 +/- 15	28 +/- 16
cAMP EC ₅₀ (nM)	6.6 +/- 1.6	8.4 +/- 1.5	7,000 +/- 3,000	18,000 +/- 12,000
β-arrestin E _{MAX} (% of WT)	104 +/- 4.0	15 +/- 7.0	88 +/- 3.3	-3.0 +/- 5.4
β-arrestin EC ₅₀ (nM)	41 +/- 1.0	360 +/- 92	6.2 +/- 0.1	39 +/- 32
K _i of DA (nM)	810 +/- 10	260 +/- 10	310 +/- 10	1,100 +/- 100
Internalization % of surface D _{2R}	29 +/- 2.5	8.4 +/- 3.1	26 +/- 3.1	3.4 +/- 2.7
Internalization EC ₅₀ (nM)	510 +/- 10	47 +/- 16	830 +/- 10	410 +/- 40
SRF E _{MAX} (% of FBS)	7.8 +/- 1.0	5.8 +/- 0.9	-0.2 +/- 0.2	Not Converged
SRF EC ₅₀ (nM)	90 +/- 2.0	32 +/- 2.0	250 +/- 200	Not Converged
SRE E _{MAX} (% of FBS)	5.6 +/- 1.8	4.2 +/- 1.4	Not Converged	1.3 +/- 0.8
SRE EC ₅₀ (nM)	35 +/- 5.0	8.0 +/- 12	Not Converged	0.09 +/- 0.03

Table IV: Receptor manipulations yield operationally defined functional selectivity. Values derived from Figures 7 and 8 to demonstrate the receptor's contributions to functional selectivity. *p<0.05 when compared to ^[WT]D₂R for efficacy and potency as determined by Bonferroni post-hoc test after p<0.05 for one-way ANOVA. B_{INF} and $\Delta\Delta\log(\tau/K_A)$ were calculated according to references in the table.

Mutant	Assay (ligand)	EC ₅₀ (nM)	E _{MAX} (% ^[WT] D ₂ R)	Figure
^[Y1V] D ₂ R	β-arrestin 2 (DA)	0.2 +/- 0.3*	13 +/- 3*	1A
	β-arrestin 2+GRK2 (DA)	15 +/- 2*	36 +/- 3*	1B
^[Gprot] D ₂ R	β-arrestin 2+GRK2 (DA)	5.3 +/- 1.8	44 +/- 5*	1B
	Calculation Method	Bias Factor	Bias Factor with GRK2	
^[Y1V] D ₂ R	Barak and Peterson, 2012	0.9 (B _{INF})	0.3 (B _{INF})	1C
^[Gprot] D ₂ R		0.7 (B _{INF})	0.4 (B _{INF})	1C
^[Y1V] D ₂ R	Kenakin and Christopoulos, 2013	4.2 ($\Delta\Delta\log(\tau/K_A)$)	0.5 ($\Delta\Delta\log(\tau/K_A)$)	1D
^[Gprot] D ₂ R		1.3 ($\Delta\Delta\log(\tau/K_A)$)	0.5 ($\Delta\Delta\log(\tau/K_A)$)	1D
	Assay (ligand)	EC ₅₀ (nM)	E _{MAX} (% ^[WT] D ₂ R)	
^[τ/1.5] D ₂ R	cAMP (DA)	7 +/- 2	85 +/- 8	2A
	β-arrestin 2 (DA)	33 +/- 1	79 +/- 4	2B
^[Gprot(τ/1.5)] D ₂ R	cAMP (DA)	6 +/- 1	81 +/- 4	2A
	β-arrestin 2 (DA)	120 +/- 10*	15 +/- 5*	2B
^[βarr(τ/1.5)] D ₂ R	cAMP (DA)	110 +/- 2*	57 +/- 6*	2A
	β-arrestin 2 (DA)	59 +/- 2*	50 +/- 5*	2B
^[τ/2] D ₂ R	cAMP (DA)	18 +/- 1*	75 +/- 4	2C
	β-arrestin 2 (DA)	55 +/- 2*	51 +/- 4*	2D
^[Gprot(τ/2)] D ₂ R	cAMP (DA)	16 +/- 2*	69 +/- 6	2C
	β-arrestin 2 (DA)	440 +/- 2500*	3.1 +/- 5.9*	2D
^[βarr(τ/2)] D ₂ R	cAMP (DA)	580 +/- 3*	38 +/- 10*	2C
	β-arrestin 2 (DA)	69 +/- 3*	29 +/- 5*	2D

Table V: Ligand contributions to functional selectivity. Calculated from Figures 9 and 10. *p<0.05 when compared to ^[WT]D₂R for efficacy and potency at each ligand as determined by Bonferroni post-hoc test after p<0.05 by one-way ANOVA.

Mutant	Ligand (Assay)	EC ₅₀ /IC ₅₀ (nM)	E _{MAX} /IC _{MAX} (% [^{WT}]D ₂ R)	Figure
[Gprot4PM]D ₂ R	DA (cAMP)	17 +/- 2*	100 +/- 11	3A
	Quinpirole (cAMP)	29 +/- 2	89 +/- 7	3A
	DA (β-arrestin 2)	450 +/- 20*	48 +/- 4*	3B
	Quinpirole (β-arrestin 2)		Ambiguous Fit	3B
	DA (β-arrestin 2 + GRK2)	20 +/- 1*	89 +/- 4	3C
	Quinpirole (β-arrestin2+GRK2)	68 +/- 1*	69 +/- 3*	3C
	DA (GRK2)	110 +/- 2*	63 +/- 6*	3D
	Quinpirole (GRK2)	130 +/- 2*	27 +/- 4*	3D
[^{WT}]D ₂ R	Quinpirole (cAMP)	25 +/- 1	100 +/- 6	4A
	Apomorphine (cAMP)	4.6 +/- 1	100 +/- 6	4C
	NPA (cAMP)	0.2 +/- 0.1	98 +/- 11	4E
[Gprot]D ₂ R	Quinpirole (cAMP)	17 +/- 2*	86 +/- 8	4A
	Apomorphine (cAMP)	5.6 +/- 2	91 +/- 11	4C
	NPA (cAMP)	0.6 +/- 0.1	94 +/- 14	4E
[βarr]D ₂ R	Quinpirole (cAMP)	10,000 +/- 2,500*	25 +/- 20*	4A
	Apomorphine (cAMP)	1,300 +/- 229*	67 +/- 15	4C
	NPA (cAMP)		Not Converged	4E
[D80A]D ₂ R	Quinpirole (cAMP)	510 +/- 400*	14 +/- 10*	4A
	Apomorphine (cAMP)		Ambiguous Fit	4C
	NPA (cAMP)	650 +/- 320*	27 +/- 90	4E
[^{WT}]D ₂ R	Quinpirole (β-arrestin 2)	66 +/- 1	100 +/- 4	4B
	Apomorphine (β-arrestin 2)	10 +/- 1	100 +/- 7	4D
	NPA (β-arrestin 2)	0.5 +/- 0.1	100 +/- 4	4F
[Gprot]D ₂ R	Quinpirole (β-arrestin 2)	160 +/- 28	19 +/- 4*	4B
	Apomorphine (β-arrestin 2)	1,700 +/- 200*	29 +/- 5*	4D
	NPA (β-arrestin 2)	0.7 +/- 0.4	19 +/- 4*	4F
[βarr]D ₂ R	Quinpirole (β-arrestin 2)	11 +/- 1	86 +/- 3	4B
	Apomorphine (β-arrestin 2)	2.0 +/- 0.2	97 +/- 6	4D
	NPA (β-arrestin 2)	0.3 +/- 0.1	86 +/- 4	4F
[D80A]D ₂ R	Quinpirole (β-arrestin 2)		Ambiguous Fit	4B
	Apomorphine (β-arrestin 2)		Ambiguous Fit	4D
	NPA (β-arrestin 2)	0.1 +/- 0.8	9 +/- 4*	4F
[^{WT}]D ₂ R	Raclopride (cAMP)	23 +/- 1	100 +/- 4	4G
	Haloperidol (cAMP)	54 +/- 1	100 +/- 6	4I
	Aripiprazole (cAMP)	280 +/- 23	100 +/- 25	4K
[Gprot]D ₂ R	Raclopride (cAMP)	19 +/- 1	94 +/- 4	4G
	Haloperidol (cAMP)	39 +/- 1	89 +/- 6	4I
	Aripiprazole (cAMP)	16 +/- 3*	58 +/- 16	4K
[βarr]D ₂ R	Raclopride (cAMP)		Not Converged	4G
	Haloperidol (cAMP)	2.3 +/- 2.6*	26 +/- 5*	4I
	Aripiprazole (cAMP)		Not Converged	4K
[D80A]D ₂ R	Raclopride (cAMP)		Ambiguous Fit	4G
	Haloperidol (cAMP)		Not Converged	4I
	Aripiprazole (cAMP)		Not Converged	4K
[^{WT}]D ₂ R	Raclopride (β-arrestin 2)	1.7 +/- 1.2	100 +/- 3	4H
	Haloperidol (β-arrestin 2)	4.0 +/- 1.2	100 +/- 4	4J
	Aripiprazole (β-arrestin 2)	77 +/- 2	99 +/- 7	4L

Table VI: Transducer contributions to functional selectivity. Calculated from Figure 11. *p<0.05 when compared to ^[WT]D₂R or control receptors (β_{2A} R for G_{as} or AT_{1A}R for G_{aq}) for efficacy and potency as determined by Bonferroni post-hoc test after p<0.05 for one-way ANOVA.

Receptor	Assay (Ligand)	EC ₅₀ (nM)	E _{MAX} (% Control)	Figure
^[WT] D ₂ R	GRK2 recruitment (DA)	4.6 +/- 1.5	100 +/- 4	5A
[Gprot]D ₂ R		6 +/- 2	40 +/- 4*	5A
[β arr]D ₂ R		0.3 +/- 0.2	94 +/- 4	5A
[D80A]D ₂ R		6,600 +/- 250*	14 +/- 10*	5A
^[WT] D ₂ R	β -arrestin 1 recruitment (DA)	46 +/- 1	100 +/- 2	5B
[Gprot]D ₂ R		280 +/- 10*	17 +/- 2*	5B
[β arr]D ₂ R		15 +/- 1*	70 +/- 2*	5B
[D80A]D ₂ R		0.1 +/- 1.5*	3 +/- 3*	5B
Endogenous β_{2A} R	G _{as} (isoproterenol)	29 +/- 1	100 +/- 2	5C
^[WT] D ₂ R		(DA)	8,800 +/- 950*	1 +/- 1*
[Gprot]D ₂ R			Ambiguous Fit	5C
[β arr]D ₂ R		1.8e8 +/- 1.5e7*	5 +/- 7*	5C
[D80A]D ₂ R		1.4e8 +/- 8.9e7*	4 +/- 6*	5C
AT _{1A} R	G _{aq} (ANGII) (DA)	150 +/- 12	94 +/- 3	5D
^[WT] D ₂ R		210 +/- 40	1 +/- 1*	5D
[Gprot]D ₂ R		270 +/- 34	1 +/- 1*	5D
[β arr]D ₂ R		77 +/- 52	1 +/- 1*	5D
[D80A]D ₂ R			Not Converged	5D

References

1. Urban JD, *et al.* (2007) Functional selectivity and classical concepts of quantitative pharmacology. *The Journal of pharmacology and experimental therapeutics* 320(1):1-13.
2. Roth BL & Chuang DM (1987) Multiple mechanisms of serotonergic signal transduction. *Life sciences* 41(9):1051-1064.
3. Galandrin S & Bouvier M (2006) Distinct signaling profiles of beta1 and beta2 adrenergic receptor ligands toward adenylyl cyclase and mitogen-activated protein kinase reveals the pluridimensionality of efficacy. *Molecular pharmacology* 70(5):1575-1584.
4. Zhang J, *et al.* (1998) Role for G protein-coupled receptor kinase in agonist-specific regulation of mu-opioid receptor responsiveness. *Proceedings of the National Academy of Sciences of the United States of America* 95(12):7157-7162.
5. Kilts JD, *et al.* (2002) Functional selectivity of dopamine receptor agonists. II. Actions of dihydrexidine in D2L receptor-transfected MN9D cells and pituitary lactotrophs. *The Journal of pharmacology and experimental therapeutics* 301(3):1179-1189.
6. Mottola DM, *et al.* (2002) Functional selectivity of dopamine receptor agonists. I. Selective activation of postsynaptic dopamine D2 receptors linked to adenylate cyclase. *The Journal of pharmacology and experimental therapeutics* 301(3):1166-1178.
7. Wacker D, *et al.* (2013) Structural features for functional selectivity at serotonin receptors. *Science* 340(6132):615-619.
8. Kenakin T (1995) Pharmacological proteus? *Trends in pharmacological sciences* 16(8):256-258.
9. Violin JD & Lefkowitz RJ (2007) Beta-arrestin-biased ligands at seven-transmembrane receptors. *Trends in pharmacological sciences* 28(8):416-422.
10. Sotnikova TD, *et al.* (2010) The dopamine metabolite 3-methoxytyramine is a neuromodulator. *PloS one* 5(10):e13452.

11. Ahlquist RP (1948) A study of the adrenotropic receptors. *The American journal of physiology* 153(3):586-600.
12. Mosharov EV, *et al.* (2009) Interplay between cytosolic dopamine, calcium, and alpha-synuclein causes selective death of substantia nigra neurons. *Neuron* 62(2):218-229.
13. Guatteo E, *et al.* (2013) Dual effects of L-DOPA on nigral dopaminergic neurons. *Experimental neurology* 247:582-594.
14. Jodko-Piorecka K & Litwinienko G (2013) First experimental evidence of dopamine interactions with negatively charged model biomembranes. *ACS chemical neuroscience* 4(7):1114-1122.
15. Sharma M, Celver J, Oceau JC, & Koovor A (2013) Plasma membrane compartmentalization of D2 dopamine receptors. *The Journal of biological chemistry* 288(18):12554-12568.
16. Cho DI, *et al.* (2012) The N-terminal region of the dopamine D2 receptor, a rhodopsin-like GPCR, regulates correct integration into the plasma membrane and endocytic routes. *British journal of pharmacology* 166(2):659-675.
17. Paspalas CD, Rakic P, & Goldman-Rakic PS (2006) Internalization of D2 dopamine receptors is clathrin-dependent and select to dendro-axonic appositions in primate prefrontal cortex. *The European journal of neuroscience* 24(5):1395-1403.
18. Irannejad R, *et al.* (2013) Conformational biosensors reveal GPCR signalling from endosomes. *Nature* 495(7442):534-538.
19. Ferre S, *et al.* (2009) Building a new conceptual framework for receptor heteromers. *Nature chemical biology* 5(3):131-134.
20. Bouvier M & Hebert TE (2014) CrossTalk proposal: Weighing the evidence for Class A GPCR dimers, the evidence favours dimers. *The Journal of physiology* 592(Pt 12):2439-2441.
21. Lambert NA & Javitch JA (2014) CrossTalk opposing view: Weighing the evidence for class A GPCR dimers, the jury is still out. *The Journal of physiology* 592(Pt 12):2443-2445.

22. Frederick AL, *et al.* (2015) Evidence against dopamine D1/D2 receptor heteromers. *Molecular psychiatry*.
23. Guo W, Shi L, & Javitch JA (2003) The fourth transmembrane segment forms the interface of the dopamine D2 receptor homodimer. *The Journal of biological chemistry* 278(7):4385-4388.
24. Han Y, Moreira IS, Urizar E, Weinstein H, & Javitch JA (2009) Allosteric communication between protomers of dopamine class A GPCR dimers modulates activation. *Nature chemical biology* 5(9):688-695.
25. Wang M, *et al.* (2010) Schizophrenia, amphetamine-induced sensitized state and acute amphetamine exposure all show a common alteration: increased dopamine D2 receptor dimerization. *Molecular brain* 3:25.
26. Lane JR, *et al.* (2014) A new mechanism of allostery in a G protein-coupled receptor dimer. *Nature chemical biology* 10(9):745-752.
27. Urizar E, *et al.* (2011) CODA-RET reveals functional selectivity as a result of GPCR heteromerization. *Nature chemical biology* 7(9):624-630.
28. Rashid AJ, *et al.* (2007) D1-D2 dopamine receptor heterooligomers with unique pharmacology are coupled to rapid activation of Gq/11 in the striatum. *Proceedings of the National Academy of Sciences of the United States of America* 104(2):654-659.
29. Verma V, Hasbi A, O'Dowd BF, & George SR (2010) Dopamine D1-D2 receptor Heteromer-mediated calcium release is desensitized by D1 receptor occupancy with or without signal activation: dual functional regulation by G protein-coupled receptor kinase 2. *The Journal of biological chemistry* 285(45):35092-35103.
30. Chun LS, *et al.* (2013) D1-D2 dopamine receptor synergy promotes calcium signaling via multiple mechanisms. *Molecular pharmacology* 84(2):190-200.
31. So CH, *et al.* (2009) Calcium signaling by dopamine D5 receptor and D5-D2 receptor hetero-oligomers occurs by a mechanism distinct from that for dopamine D1-D2 receptor hetero-oligomers. *Molecular pharmacology* 75(4):843-854.

32. Pou C, Mannoury la Cour C, Stoddart LA, Millan MJ, & Milligan G (2012) Functional homomers and heteromers of dopamine D2L and D3 receptors co-exist at the cell surface. *The Journal of biological chemistry* 287(12):8864-8878.
33. Gonzalez S, *et al.* (2012) Dopamine D4 receptor, but not the ADHD-associated D4.7 variant, forms functional heteromers with the dopamine D2S receptor in the brain. *Molecular psychiatry* 17(6):650-662.
34. Navarro G, *et al.* (2009) Interactions between calmodulin, adenosine A2A, and dopamine D2 receptors. *The Journal of biological chemistry* 284(41):28058-28068.
35. Fernandez-Duenas V, *et al.* (2012) Molecular determinants of A2AR-D2R allostereism: role of the intracellular loop 3 of the D2R. *Journal of neurochemistry* 123(3):373-384.
36. Azdad K, *et al.* (2009) Dopamine D2 and adenosine A2A receptors regulate NMDA-mediated excitation in accumbens neurons through A2A-D2 receptor heteromerization. *Neuropsychopharmacology : official publication of the American College of Neuropsychopharmacology* 34(4):972-986.
37. Trincavelli ML, *et al.* (2012) A new D(2) dopamine receptor agonist allosterically modulates A(2A) adenosine receptor signalling by interacting with the A(2A)/D(2) receptor heteromer. *Cellular signalling* 24(4):951-960.
38. Koschatzky S, Tschammer N, & Gmeiner P (2011) Cross-receptor interactions between dopamine D2L and neurotensin NTS1 receptors modulate binding affinities of dopaminergics. *ACS chemical neuroscience* 2(6):308-316.
39. Kern A, Albarran-Zeckler R, Walsh HE, & Smith RG (2012) Apo-ghrelin receptor forms heteromers with DRD2 in hypothalamic neurons and is essential for anorexigenic effects of DRD2 agonism. *Neuron* 73(2):317-332.
40. Wall MA, *et al.* (1995) The structure of the G protein heterotrimer Gi alpha 1 beta 1 gamma 2. *Cell* 83(6):1047-1058.
41. Lambright DG, Noel JP, Hamm HE, & Sigler PB (1994) Structural determinants for activation of the alpha-subunit of a heterotrimeric G protein. *Nature* 369(6482):621-628.

42. Nobles M, Benians A, & Tinker A (2005) Heterotrimeric G proteins precouple with G protein-coupled receptors in living cells. *Proceedings of the National Academy of Sciences of the United States of America* 102(51):18706-18711.
43. Montmayeur JP & Borrelli E (1994) Targeting of G alpha i2 to the Golgi by alternative spliced carboxyl-terminal region. *Science* 263(5143):95-98.
44. Bertran-Gonzalez J, *et al.* (2009) Histone H3 phosphorylation is under the opposite tonic control of dopamine D2 and adenosine A2A receptors in striatopallidal neurons. *Neuropsychopharmacology : official publication of the American College of Neuropsychopharmacology* 34(7):1710-1720.
45. Farrell MS, *et al.* (2013) A Galphas DREADD mouse for selective modulation of cAMP production in striatopallidal neurons. *Neuropsychopharmacology : official publication of the American College of Neuropsychopharmacology* 38(5):854-862.
46. Snyder SH (2011) What dopamine does in the brain. *Proceedings of the National Academy of Sciences of the United States of America* 108(47):18869-18871.
47. Tsukamoto T, *et al.* (1991) Structure of the human gene and two rat cDNAs encoding the alpha chain of GTP-binding regulatory protein Go: two different mRNAs are generated by alternative splicing. *Proceedings of the National Academy of Sciences of the United States of America* 88(8):2974-2978.
48. Conklin BR, Farfel Z, Lustig KD, Julius D, & Bourne HR (1993) Substitution of three amino acids switches receptor specificity of Gq alpha to that of Gi alpha. *Nature* 363(6426):274-276.
49. Sternweis PC & Robishaw JD (1984) Isolation of two proteins with high affinity for guanine nucleotides from membranes of bovine brain. *The Journal of biological chemistry* 259(22):13806-13813.
50. Jiang M, Spicher K, Boulay G, Wang Y, & Birnbaumer L (2001) Most central nervous system D2 dopamine receptors are coupled to their effectors by Go. *Proceedings of the National Academy of Sciences of the United States of America* 98(6):3577-3582.
51. Jiang M, *et al.* (1998) Multiple neurological abnormalities in mice deficient in the G protein Go. *Proceedings of the National Academy of Sciences of the United States of America* 95(6):3269-3274.

52. Nakamura K, *et al.* (2013) De Novo mutations in GNAO1, encoding a Galphao subunit of heterotrimeric G proteins, cause epileptic encephalopathy. *American journal of human genetics* 93(3):496-505.
53. Bardwell L, Cook JG, Inouye CJ, & Thorner J (1994) Signal propagation and regulation in the mating pheromone response pathway of the yeast *Saccharomyces cerevisiae*. *Developmental biology* 166(2):363-379.
54. Whorton MR & MacKinnon R (2013) X-ray structure of the mammalian GIRK2-beta gamma G-protein complex. *Nature* 498(7453):190-197.
55. Tang W, *et al.* (2006) Gbetagamma inhibits Galpha GTPase-activating proteins by inhibition of Galpha-GTP binding during stimulation by receptor. *The Journal of biological chemistry* 281(8):4746-4753.
56. Wang J, Sengupta P, Guo Y, Golebiewska U, & Scarlata S (2009) Evidence for a second, high affinity Gbetagamma binding site on Galphai1(GDP) subunits. *The Journal of biological chemistry* 284(25):16906-16913.
57. Garcia-Olivares J, *et al.* (2013) Inhibition of dopamine transporter activity by G protein betagamma subunits. *PloS one* 8(3):e59788.
58. Pitcher JA, *et al.* (1992) Role of beta gamma subunits of G proteins in targeting the beta-adrenergic receptor kinase to membrane-bound receptors. *Science* 257(5074):1264-1267.
59. Stoffel RH, Randall RR, Premont RT, Lefkowitz RJ, & Inglesse J (1994) Palmitoylation of G protein-coupled receptor kinase, GRK6. Lipid modification diversity in the GRK family. *The Journal of biological chemistry* 269(45):27791-27794.
60. Gainetdinov RR, *et al.* (2003) Dopaminergic supersensitivity in G protein-coupled receptor kinase 6-deficient mice. *Neuron* 38(2):291-303.
61. Nobles KN, *et al.* (2011) Distinct phosphorylation sites on the beta(2)-adrenergic receptor establish a barcode that encodes differential functions of beta-arrestin. *Science signaling* 4(185):ra51.

62. Namkung Y, Dipace C, Javitch JA, & Sibley DR (2009) G protein-coupled receptor kinase-mediated phosphorylation regulates post-endocytic trafficking of the D2 dopamine receptor. *The Journal of biological chemistry* 284(22):15038-15051.
63. Celver J, Sharma M, Thanawala V, Christopher Oceau J, & Koor A (2013) Arrestin-dependent but G-protein coupled receptor kinase-independent uncoupling of D2-dopamine receptors. *Journal of neurochemistry* 127(1):57-65.
64. Namkung Y, Dipace C, Urizar E, Javitch JA, & Sibley DR (2009) G protein-coupled receptor kinase-2 constitutively regulates D2 dopamine receptor expression and signaling independently of receptor phosphorylation. *The Journal of biological chemistry* 284(49):34103-34115.
65. Laporte SA, *et al.* (1999) The beta2-adrenergic receptor/betaarrestin complex recruits the clathrin adaptor AP-2 during endocytosis. *Proceedings of the National Academy of Sciences of the United States of America* 96(7):3712-3717.
66. Xiao K, *et al.* (2010) Global phosphorylation analysis of beta-arrestin-mediated signaling downstream of a seven transmembrane receptor (7TMR). *Proceedings of the National Academy of Sciences of the United States of America* 107(34):15299-15304.
67. Beaulieu JM, *et al.* (2005) An Akt/beta-arrestin 2/PP2A signaling complex mediates dopaminergic neurotransmission and behavior. *Cell* 122(2):261-273.
68. Urs NM, Snyder JC, Jacobsen JP, Peterson SM, & Caron MG (2012) Deletion of GSK3beta in D2R-expressing neurons reveals distinct roles for beta-arrestin signaling in antipsychotic and lithium action. *Proceedings of the National Academy of Sciences of the United States of America* 109(50):20732-20737.
69. Souza BR, Romano-Silva MA, & Tropepe V (2011) Dopamine D2 receptor activity modulates Akt signaling and alters GABAergic neuron development and motor behavior in zebrafish larvae. *The Journal of neuroscience : the official journal of the Society for Neuroscience* 31(14):5512-5525.
70. Speed N, *et al.* (2011) Impaired striatal Akt signaling disrupts dopamine homeostasis and increases feeding. *PLoS one* 6(9):e25169.
71. Lan H, Liu Y, Bell MI, Gurevich VV, & Neve KA (2009) A dopamine D2 receptor mutant capable of G protein-mediated signaling but deficient in arrestin binding. *Molecular pharmacology* 75(1):113-123.

72. Beaulieu JM, Sotnikova TD, Gainetdinov RR, & Caron MG (2006) Paradoxical striatal cellular signaling responses to psychostimulants in hyperactive mice. *The Journal of biological chemistry* 281(43):32072-32080.
73. Blasi G, et al. (2011) DRD2/AKT1 interaction on D2 c-AMP independent signaling, attentional processing, and response to olanzapine treatment in schizophrenia. *Proceedings of the National Academy of Sciences of the United States of America* 108(3):1158-1163.
74. Creese I, Burt DR, & Snyder SH (1976) Dopamine receptor binding predicts clinical and pharmacological potencies of antischizophrenic drugs. *Science* 192(4238):481-483.
75. Masri B, et al. (2008) Antagonism of dopamine D2 receptor/beta-arrestin 2 interaction is a common property of clinically effective antipsychotics. *Proceedings of the National Academy of Sciences of the United States of America* 105(36):13656-13661.
76. Bowling H, et al. (2014) Antipsychotics Activate mTORC1-Dependent Translation to Enhance Neuronal Morphological Complexity. *Science signaling* 7(308):ra4.
77. Chen HT, Ruan NY, Chen JC, & Lin TY (2012) Dopamine D2 receptor-mediated Akt/PKB signalling: initiation by the D2S receptor and role in quinpirole-induced behavioural activation. *ASN neuro* 4(6):371-382.
78. Pogorelov VM, et al. (2012) Mutant DISC1 affects methamphetamine-induced sensitization and conditioned place preference: a comorbidity model. *Neuropharmacology* 62(3):1242-1251.
79. Mines MA & Jope RS (2012) Brain region differences in regulation of Akt and GSK3 by chronic stimulant administration in mice. *Cellular signalling* 24(7):1398-1405.
80. Beaulieu JM, et al. (2008) A beta-arrestin 2 signaling complex mediates lithium action on behavior. *Cell* 132(1):125-136.
81. Sutton LP, Honardoust D, Mouyal J, Rajakumar N, & Rushlow WJ (2007) Activation of the canonical Wnt pathway by the antipsychotics haloperidol and clozapine involves dishevelled-3. *Journal of neurochemistry* 102(1):153-169.

82. Min C, *et al.* (2011) Novel regulatory mechanism of canonical Wnt signaling by dopamine D2 receptor through direct interaction with beta-catenin. *Molecular pharmacology* 80(1):68-78.
83. Harrison LM, Muller SH, & Spano D (2013) Effects of the Ras homolog Rhes on Akt/protein kinase B and glycogen synthase kinase 3 phosphorylation in striatum. *Neuroscience* 236:21-30.
84. Hannan MA, Kabbani N, Paspalas CD, & Levenson R (2008) Interaction with dopamine D2 receptor enhances expression of transient receptor potential channel 1 at the cell surface. *Biochimica et biophysica acta* 1778(4):974-982.
85. Shukla AK, *et al.* (2010) Arresting a transient receptor potential (TRP) channel: beta-arrestin 1 mediates ubiquitination and functional down-regulation of TRPV4. *The Journal of biological chemistry* 285(39):30115-30125.
86. Por ED, *et al.* (2012) beta-Arrestin-2 desensitizes the transient receptor potential vanilloid 1 (TRPV1) channel. *The Journal of biological chemistry* 287(44):37552-37563.
87. Liu XY, *et al.* (2006) Modulation of D2R-NR2B interactions in response to cocaine. *Neuron* 52(5):897-909.
88. Park SK, *et al.* (2005) Par-4 links dopamine signaling and depression. *Cell* 122(2):275-287.
89. Kim OJ, *et al.* (2008) D2 dopamine receptor expression and trafficking is regulated through direct interactions with ZIP. *Journal of neurochemistry* 106(1):83-95.
90. Kim SY, *et al.* (2008) Striatal-enriched protein tyrosine phosphatase regulates dopaminergic neuronal development via extracellular signal-regulated kinase signaling. *Experimental neurology* 214(1):69-77.
91. Kim SY, *et al.* (2006) The dopamine D2 receptor regulates the development of dopaminergic neurons via extracellular signal-regulated kinase and Nurr1 activation. *The Journal of neuroscience : the official journal of the Society for Neuroscience* 26(17):4567-4576.

92. Shimokawa N, *et al.* (2010) CIN85 regulates dopamine receptor endocytosis and governs behaviour in mice. *The EMBO journal* 29(14):2421-2432.
93. Negyessy L & Goldman-Rakic PS (2005) Subcellular localization of the dopamine D2 receptor and coexistence with the calcium-binding protein neuronal calcium sensor-1 in the primate prefrontal cortex. *The Journal of comparative neurology* 488(4):464-475.
94. Ferraro L, *et al.* (2012) A novel mechanism of cocaine to enhance dopamine d2-like receptor mediated neurochemical and behavioral effects. An in vivo and in vitro study. *Neuropsychopharmacology : official publication of the American College of Neuropsychopharmacology* 37(8):1856-1866.
95. Abdul-Ridha A, Lane JR, Sexton PM, Canals M, & Christopoulos A (2013) Allosteric modulation of a chemogenetically modified G protein-coupled receptor. *Molecular pharmacology* 83(2):521-530.
96. Silvano E, *et al.* (2010) The tetrahydroisoquinoline derivative SB269,652 is an allosteric antagonist at dopamine D3 and D2 receptors. *Molecular pharmacology* 78(5):925-934.
97. Kruse AC, *et al.* (2013) Activation and allosteric modulation of a muscarinic acetylcholine receptor. *Nature* 504(7478):101-106.
98. Dror RO, *et al.* (2013) Structural basis for modulation of a G-protein-coupled receptor by allosteric drugs. *Nature* 503(7475):295-299.
99. Shonberg J, *et al.* (2013) A structure-activity analysis of biased agonism at the dopamine D2 receptor. *Journal of medicinal chemistry* 56(22):9199-9221.
100. Lane JR, *et al.* (2013) Structure-based ligand discovery targeting orthosteric and allosteric pockets of dopamine receptors. *Molecular pharmacology* 84(6):794-807.
101. Chen X, *et al.* (2012) Structure-functional selectivity relationship studies of beta-arrestin-biased dopamine D(2) receptor agonists. *Journal of medicinal chemistry* 55(16):7141-7153.
102. Allen JA, *et al.* (2011) Discovery of beta-arrestin-biased dopamine D2 ligands for probing signal transduction pathways essential for antipsychotic efficacy.

Proceedings of the National Academy of Sciences of the United States of America
108(45):18488-18493.

103. Liu W, *et al.* (2012) Structural basis for allosteric regulation of GPCRs by sodium ions. *Science* 337(6091):232-236.
104. Theodorou AE, Jenner P, & Marsden CD (1983) Cation specificity of 3H-sulpiride binding involves alteration in the number of striatal binding sites. *Life sciences* 32(11):1243-1254.
105. Pert CB, Pasternak G, & Snyder SH (1973) Opiate agonists and antagonists discriminated by receptor binding in brain. *Science* 182(4119):1359-1361.
106. Tsai BS & Lefkowitz RJ (1978) Agonist-specific effects of monovalent and divalent cations on adenylate cyclase-coupled alpha adrenergic receptors in rabbit platelets. *Molecular pharmacology* 14(4):540-548.
107. Neve KA, Cox BA, Henningsen RA, Spanoyannis A, & Neve RL (1991) Pivotal role for aspartate-80 in the regulation of dopamine D2 receptor affinity for drugs and inhibition of adenylyl cyclase. *Molecular pharmacology* 39(6):733-739.
108. Ceresa BP & Limbird LE (1994) Mutation of an aspartate residue highly conserved among G-protein-coupled receptors results in nonreciprocal disruption of alpha 2-adrenergic receptor-G-protein interactions. A negative charge at amino acid residue 79 forecasts alpha 2A-adrenergic receptor sensitivity to allosteric modulation by monovalent cations and fully effective receptor/G-protein coupling. *The Journal of biological chemistry* 269(47):29557-29564.
109. Armstrong D & Strange PG (2001) Dopamine D2 receptor dimer formation: evidence from ligand binding. *The Journal of biological chemistry* 276(25):22621-22629.
110. Selent J, Sanz F, Pastor M, & De Fabritiis G (2010) Induced effects of sodium ions on dopaminergic G-protein coupled receptors. *PLoS computational biology* 6(8).
111. Oka Y, Butnaru M, von Buchholtz L, Ryba NJ, & Zuker CS (2013) High salt recruits aversive taste pathways. *Nature* 494(7438):472-475.

112. Fenalti G, *et al.* (2014) Molecular control of delta-opioid receptor signalling. *Nature*.
113. Verma V, *et al.* (2005) Modulation of agonist binding to human dopamine receptor subtypes by L-prolyl-L-leucyl-glycinamide and a peptidomimetic analog. *The Journal of pharmacology and experimental therapeutics* 315(3):1228-1236.
114. Bhargava HN (1983) The effect of melanotropin release inhibiting factor, its metabolites and analogs on [3H]spiroperidol and [3H]apomorphine binding sites. *General pharmacology* 14(6):609-614.
115. Basu D, *et al.* (2013) Effects of the dopamine D2 allosteric modulator, PAOPA, on the expression of GRK2, arrestin-3, ERK1/2, and on receptor internalization. *PLoS one* 8(8):e70736.
116. Schetz JA, Chu A, & Sibley DR (1999) Zinc modulates antagonist interactions with D2-like dopamine receptors through distinct molecular mechanisms. *The Journal of pharmacology and experimental therapeutics* 289(2):956-964.
117. Kenakin TP (2012) Biased signalling and allosteric machines: new vistas and challenges for drug discovery. *British journal of pharmacology* 165(6):1659-1669.
118. Zhou QY & Palmiter RD (1995) Dopamine-deficient mice are severely hypoactive, adipsic, and aphagic. *Cell* 83(7):1197-1209.
119. Darvas M & Palmiter RD (2009) Restriction of dopamine signaling to the dorsolateral striatum is sufficient for many cognitive behaviors. *Proceedings of the National Academy of Sciences of the United States of America* 106(34):14664-14669.
120. Darvas M & Palmiter RD (2010) Restricting dopaminergic signaling to either dorsolateral or medial striatum facilitates cognition. *The Journal of neuroscience : the official journal of the Society for Neuroscience* 30(3):1158-1165.
121. Giros B, Jaber M, Jones SR, Wightman RM, & Caron MG (1996) Hyperlocomotion and indifference to cocaine and amphetamine in mice lacking the dopamine transporter. *Nature* 379(6566):606-612.
122. Ghisi V, *et al.* (2009) Reduced D2-mediated signaling activity and trans-synaptic upregulation of D1 and D2 dopamine receptors in mice overexpressing the dopamine transporter. *Cellular signalling* 21(1):87-94.

123. Baik JH, *et al.* (1995) Parkinsonian-like locomotor impairment in mice lacking dopamine D2 receptors. *Nature* 377(6548):424-428.
124. Tran AH, *et al.* (2002) Altered accumbens neural response to prediction of reward associated with place in dopamine D2 receptor knockout mice. *Proceedings of the National Academy of Sciences of the United States of America* 99(13):8986-8991.
125. Welter M, *et al.* (2007) Absence of dopamine D2 receptors unmasks an inhibitory control over the brain circuitries activated by cocaine. *Proceedings of the National Academy of Sciences of the United States of America* 104(16):6840-6845.
126. Lobo MK, *et al.* (2013) DeltaFosB induction in striatal medium spiny neuron subtypes in response to chronic pharmacological, emotional, and optogenetic stimuli. *The Journal of neuroscience : the official journal of the Society for Neuroscience* 33(47):18381-18395.
127. Park E, *et al.* (2011) Regulatory roles of heterogeneous nuclear ribonucleoprotein M and Nova-1 protein in alternative splicing of dopamine D2 receptor pre-mRNA. *The Journal of biological chemistry* 286(28):25301-25308.
128. Usiello A, *et al.* (2000) Distinct functions of the two isoforms of dopamine D2 receptors. *Nature* 408(6809):199-203.
129. Lindgren N, *et al.* (2003) Distinct roles of dopamine D2L and D2S receptor isoforms in the regulation of protein phosphorylation at presynaptic and postsynaptic sites. *Proceedings of the National Academy of Sciences of the United States of America* 100(7):4305-4309.
130. Bello EP, *et al.* (2011) Cocaine supersensitivity and enhanced motivation for reward in mice lacking dopamine D2 autoreceptors. *Nature neuroscience* 14(8):1033-1038.
131. Anzalone A, *et al.* (2012) Dual control of dopamine synthesis and release by presynaptic and postsynaptic dopamine D2 receptors. *The Journal of neuroscience : the official journal of the Society for Neuroscience* 32(26):9023-9034.
132. Neve KA, *et al.* (2013) Normalizing dopamine D2 receptor-mediated responses in D2 null mutant mice by virus-mediated receptor restoration: Comparing D2 and D2. *Neuroscience* 248c:479-487.

133. Gallo EF, *et al.* (2015) Upregulation of dopamine d2 receptors in the nucleus accumbens indirect pathway increases locomotion but does not reduce alcohol consumption. *Neuropsychopharmacology : official publication of the American College of Neuropsychopharmacology* 40(7):1609-1618.
134. Di Chiara G & Imperato A (1988) Drugs abused by humans preferentially increase synaptic dopamine concentrations in the mesolimbic system of freely moving rats. *Proceedings of the National Academy of Sciences of the United States of America* 85(14):5274-5278.
135. Radl D, De Mei C, Chen E, Lee H, & Borrelli E (2013) Each individual isoform of the dopamine D2 receptor protects from lactotroph hyperplasia. *Molecular endocrinology (Baltimore, Md.)* 27(6):953-965.
136. Shen W, Flajolet M, Greengard P, & Surmeier DJ (2008) Dichotomous dopaminergic control of striatal synaptic plasticity. *Science* 321(5890):848-851.
137. Hikida T, *et al.* (2013) Pathway-specific modulation of nucleus accumbens in reward and aversive behavior via selective transmitter receptors. *Proceedings of the National Academy of Sciences of the United States of America* 110(1):342-347.
138. Kreitzer AC & Malenka RC (2007) Endocannabinoid-mediated rescue of striatal LTD and motor deficits in Parkinson's disease models. *Nature* 445(7128):643-647.
139. Lerner TN & Kreitzer AC (2012) RGS4 is required for dopaminergic control of striatal LTD and susceptibility to parkinsonian motor deficits. *Neuron* 73(2):347-359.
140. Liskowsky DR & Potter LT (1987) Dopamine D2 receptors in the striatum and frontal cortex following chronic administration of haloperidol. *Neuropharmacology* 26(5):481-483.
141. Rupniak NM, *et al.* (1984) Differential effects of continuous administration for 1 year of haloperidol or sulpiride on striatal dopamine function in the rat. *Psychopharmacology* 84(4):503-511.
142. Stuber GD, *et al.* (2008) Reward-predictive cues enhance excitatory synaptic strength onto midbrain dopamine neurons. *Science* 321(5896):1690-1692.

143. Kravitz AV, *et al.* (2010) Regulation of parkinsonian motor behaviours by optogenetic control of basal ganglia circuitry. *Nature* 466(7306):622-626.
144. Bock R, *et al.* (2013) Strengthening the accumbal indirect pathway promotes resilience to compulsive cocaine use. *Nature neuroscience* 16(5):632-638.
145. Threlfell S, *et al.* (2012) Striatal dopamine release is triggered by synchronized activity in cholinergic interneurons. *Neuron* 75(1):58-64.
146. Witten IB, *et al.* (2010) Cholinergic interneurons control local circuit activity and cocaine conditioning. *Science* 330(6011):1677-1681.
147. Lammel S, *et al.* (2012) Input-specific control of reward and aversion in the ventral tegmental area. *Nature* 491(7423):212-217.
148. Lammel S, *et al.* (2008) Unique properties of mesoprefrontal neurons within a dual mesocorticolimbic dopamine system. *Neuron* 57(5):760-773.
149. Tsai HC, *et al.* (2009) Phasic firing in dopaminergic neurons is sufficient for behavioral conditioning. *Science* 324(5930):1080-1084.
150. Lammel S, Ion DI, Roeper J, & Malenka RC (2011) Projection-specific modulation of dopamine neuron synapses by aversive and rewarding stimuli. *Neuron* 70(5):855-862.
151. Tye KM, *et al.* (2013) Dopamine neurons modulate neural encoding and expression of depression-related behaviour. *Nature* 493(7433):537-541.
152. Chaudhury D, *et al.* (2013) Rapid regulation of depression-related behaviours by control of midbrain dopamine neurons. *Nature* 493(7433):532-536.
153. Wilkins A, Erdin S, Lua R, & Lichtarge O (2012) Evolutionary trace for prediction and redesign of protein functional sites. *Methods Mol Biol* 819:29-42.
154. Lichtarge O, Bourne HR, & Cohen FE (1996) An evolutionary trace method defines binding surfaces common to protein families. *Journal of molecular biology* 257(2):342-358.
155. Wilkins AD, *et al.* (2013) Accounting for epistatic interactions improves the functional analysis of protein structures. *Bioinformatics* 29(21):2714-2721.

156. Rodriguez GJ, Yao R, Lichtarge O, & Wensel TG (2010) Evolution-guided discovery and recoding of allosteric pathway specificity determinants in psychoactive bioamine receptors. *Proceedings of the National Academy of Sciences of the United States of America* 107(17):7787-7792.
157. Granier S & Kobilka B (2012) A new era of GPCR structural and chemical biology. *Nature chemical biology* 8(8):670-673.
158. Katsonis P, *et al.* (2014) Single nucleotide variations: Biological impact and theoretical interpretation. *Protein science : a publication of the Protein Society* 23(12):1650-1666.
159. Chien EY, *et al.* (2010) Structure of the human dopamine D3 receptor in complex with a D2/D3 selective antagonist. *Science* 330(6007):1091-1095.
160. Scheerer P, *et al.* (2008) Crystal structure of opsin in its G-protein-interacting conformation. *Nature* 455(7212):497-502.
161. Rasmussen SG, *et al.* (2011) Crystal structure of the beta2 adrenergic receptor-Gs protein complex. *Nature* 477(7366):549-555.
162. Shenoy SK, *et al.* (2006) beta-arrestin-dependent, G protein-independent ERK1/2 activation by the beta2 adrenergic receptor. *The Journal of biological chemistry* 281(2):1261-1273.
163. Katsonis P & Lichtarge O (2014) A formal perturbation equation between genotype and phenotype determines the Evolutionary Action of protein-coding variations on fitness. *Genome research* 24(12):2050-2058.
164. Neskey DM, *et al.* (2015) Evolutionary Action score of TP53 (EAp53) identifies high risk mutations associated with decreased survival and increased distant metastases in head and neck cancer. *Cancer research*.
165. Osman AA, *et al.* (2015) Evolutionary Action Score of TP53 Coding Variants (EAp53) is Predictive of Platinum Response in Head and Neck Cancer Patients. *Cancer research*.
166. Osman AA, *et al.* (2015) Wee-1 Kinase Inhibition Overcomes Cisplatin Resistance Associated with High-Risk TP53 Mutations in Head and Neck Cancer through

- Mitotic Arrest Followed by Senescence. *Molecular cancer therapeutics* 14(2):608-619.
167. Szczepek M, *et al.* (2014) Crystal structure of a common GPCR-binding interface for G protein and arrestin. *Nature communications* 5:4801.
 168. Wilbanks AM, Laporte SA, Bohn LM, Barak LS, & Caron MG (2002) Apparent loss-of-function mutant GPCRs revealed as constitutively desensitized receptors. *Biochemistry* 41(40):11981-11989.
 169. Espinoza S, *et al.* (2011) Functional interaction between trace amine-associated receptor 1 and dopamine D2 receptor. *Molecular pharmacology* 80(3):416-425.
 170. Clayton CC, Donthamsetti P, Lambert NA, Javitch JA, & Neve KA (2014) Mutation of three residues in the third intracellular loop of the dopamine D2 receptor creates an internalization-defective receptor. *The Journal of biological chemistry* 289(48):33663-33675.
 171. Barak LS & Peterson S (2012) Modeling of bias for the analysis of receptor signaling in biochemical systems. *Biochemistry* 51(6):1114-1125.
 172. Kenakin T & Christopoulos A (2013) Signalling bias in new drug discovery: detection, quantification and therapeutic impact. *Nature reviews. Drug discovery* 12(3):205-216.
 173. Stallaert W, Dorn JF, van der Westhuizen E, Audet M, & Bouvier M (2012) Impedance responses reveal beta(2)-adrenergic receptor signaling pluridimensionality and allow classification of ligands with distinct signaling profiles. *PloS one* 7(1):e29420.
 174. Katritch V, *et al.* (2014) Allosteric sodium in class A GPCR signaling. *Trends in biochemical sciences* 39(5):233-244.
 175. Tohgo A, *et al.* (2003) The stability of the G protein-coupled receptor-beta-arrestin interaction determines the mechanism and functional consequence of ERK activation. *The Journal of biological chemistry* 278(8):6258-6267.
 176. Lee MH, El-Shewy HM, Luttrell DK, & Luttrell LM (2008) Role of beta-arrestin-mediated desensitization and signaling in the control of angiotensin AT1a

- receptor-stimulated transcription. *The Journal of biological chemistry* 283(4):2088-2097.
177. Cardin JA, *et al.* (2010) Targeted optogenetic stimulation and recording of neurons in vivo using cell-type-specific expression of Channelrhodopsin-2. *Nature protocols* 5(2):247-254.
 178. Gerfen CR, Paletzki R, & Heintz N (2013) GENSAT BAC cre-recombinase driver lines to study the functional organization of cerebral cortical and basal ganglia circuits. *Neuron* 80(6):1368-1383.
 179. Evron T, *et al.* (2014) G Protein and beta-Arrestin Signaling Bias at the Ghrelin Receptor. *The Journal of biological chemistry* 289(48):33442-33455.
 180. Tritsch NX & Sabatini BL (2012) Dopaminergic modulation of synaptic transmission in cortex and striatum. *Neuron* 76(1):33-50.
 181. Missale C, Nash SR, Robinson SW, Jaber M, & Caron MG (1998) Dopamine receptors: from structure to function. *Physiological reviews* 78(1):189-225.
 182. Boyden ES, Zhang F, Bamberg E, Nagel G, & Deisseroth K (2005) Millisecond-timescale, genetically targeted optical control of neural activity. *Nature neuroscience* 8(9):1263-1268.
 183. Armbruster BN, Li X, Pausch MH, Herlitze S, & Roth BL (2007) Evolving the lock to fit the key to create a family of G protein-coupled receptors potently activated by an inert ligand. *Proceedings of the National Academy of Sciences of the United States of America* 104(12):5163-5168.
 184. O'Neill PR & Gautam N (2014) Subcellular optogenetic inhibition of G proteins generates signaling gradients and cell migration. *Molecular biology of the cell* 25(15):2305-2314.
 185. Toettcher JE, Weiner OD, & Lim WA (2013) Using optogenetics to interrogate the dynamic control of signal transmission by the Ras/Erk module. *Cell* 155(6):1422-1434.
 186. Mannoury la Cour C, Salles MJ, Pasteau V, & Millan MJ (2011) Signaling pathways leading to phosphorylation of Akt and GSK-3beta by activation of

- cloned human and rat cerebral D(2)and D(3) receptors. *Molecular pharmacology* 79(1):91-105.
187. Wei H, *et al.* (2003) Independent beta-arrestin 2 and G protein-mediated pathways for angiotensin II activation of extracellular signal-regulated kinases 1 and 2. *Proceedings of the National Academy of Sciences of the United States of America* 100(19):10782-10787.
188. Cho D, *et al.* (2010) Agonist-induced endocytosis and receptor phosphorylation mediate resensitization of dopamine D(2) receptors. *Molecular endocrinology (Baltimore, Md.)* 24(3):574-586.
189. Strange PG (2008) Antipsychotic drug action: antagonism, inverse agonism or partial agonism. *Trends in pharmacological sciences* 29(6):314-321.
190. Kommaddi RP & Shenoy SK (2013) Arrestins and protein ubiquitination. *Progress in molecular biology and translational science* 118:175-204.
191. Wootten D, Christopoulos A, & Sexton PM (2013) Emerging paradigms in GPCR allostery: implications for drug discovery. *Nature reviews. Drug discovery* 12(8):630-644.
192. Lane JR, Sexton PM, & Christopoulos A (2013) Bridging the gap: bitopic ligands of G-protein-coupled receptors. *Trends in pharmacological sciences* 34(1):59-66.
193. Venkatakrisnan AJ, *et al.* (2013) Molecular signatures of G-protein-coupled receptors. *Nature* 494(7436):185-194.
194. Ma P & Zimmel R (2002) Value of novelty? *Nature reviews. Drug discovery* 1(8):571-572.
195. Dror RO, *et al.* (2015) SIGNAL TRANSDUCTION. Structural basis for nucleotide exchange in heterotrimeric G proteins. *Science* 348(6241):1361-1365.
196. Zhou X, Vink M, Klaver B, Berkhout B, & Das AT (2006) Optimization of the Tet-On system for regulated gene expression through viral evolution. *Gene therapy* 13(19):1382-1390.

197. Turan S, Kuehle J, Schambach A, Baum C, & Bode J (2010) Multiplexing RMCE: versatile extensions of the FLP-recombinase-mediated cassette-exchange technology. *Journal of molecular biology* 402(1):52-69.
198. Snyder JC, Rochelle LK, Lyerly HK, Caron MG, & Barak LS (2013) Constitutive internalization of the leucine-rich G protein-coupled receptor-5 (LGR5) to the trans-Golgi network. *The Journal of biological chemistry* 288(15):10286-10297.
199. Xiao X, Li J, & Samulski RJ (1998) Production of high-titer recombinant adeno-associated virus vectors in the absence of helper adenovirus. *Journal of virology* 72(3):2224-2232.

Biography

I was born on August 23, 1983 to John and Virginia Peterson in Seward, Alaska. I attended the University of South Florida in Tampa, Florida from 2002-2006 and received my Bachelor's of Science degree in Biology. I worked as a technician at the University of North Carolina, Chapel Hill in the laboratory of Dr. Bryan Roth from 2006-2008 where I was first exposed to GPCR and dopamine receptor research. I was accepted into the Cell and Molecular Biology training program at Duke in 2008 and joined the Cell Biology department under the mentorship of Dr. Marc Caron in the summer of 2009. In Dr. Caron's laboratory I published "Elucidation of G-protein and β -arrestin functional selectivity at the dopamine D2 receptor" in 2015 in PNAS and a chapter in the textbook "Primer on the Autonomic Nervous System" titled "Dopamine Receptors" in 2012. I will be pursuing a postdoctoral fellowship in Dr. John Kuriyan's laboratory at the University of California, Berkeley to study how the kinase domain of EGFR is activated by ligands using structural and molecular dynamics techniques, as well as the techniques presented in this dissertation.